The role of *Empodisma robustum* litter in CO_2 exchange at Kopuatai bog

A thesis submitted in partial fulfilment

of the requirements for the degree

of

Master of Science

in Earth Sciences

at

The University of Waikato

by

Alexandra Margaret Keyte Beattie

The University of Waikato
2014

THE UNIVERSITY OF
WAIKATO
Te Whare Wānanga o Waikato

Abstract

Respiration from the decomposition of standing dead litter in peatlands influences the ecosystem carbon balance through its contribution to total ecosystem respiration (ER). This research determined the proportion of ER estimated at Kopuatai bog that is sourced from the decomposition of *Empodisma robustum* litter in the canopy. Canopy harvests were carried out to measure the mass of standing litter in the canopy; laboratory litter incubations were used to measure respiration rates over a range of temperatures and moisture contents; and a simple model was developed to estimate annual litter respiration using inputs of canopy wetness duration and canopy temperature.

E. robustum litter comprised an average of 51% of the total canopy biomass, with 0.92 kg m^{-2} standing litter dry matter in 1.8 kg m^{-2} of total canopy dry matter. The majority of this litter is located in the lower part of the canopy. Very low respiration rates were measured for the *E. robustum* litter, although respiration was significantly higher in litter which was more physically decomposed (R_{10} = 0.44 (± 0.1) µmol kg^{-1} s^{-1}) than that which was freshly dead (R_{10} = 0.24 (± 0.05) µmol kg^{-1} s^{-1}). Litter respiration showed a strong temperature response, and was moisture-limited below approximately 50% moisture content. The model of litter respiration estimated that standing dead *E. robustum* litter contributed 59 g C m^{-2} yr^{-1} (8.8%) to annual total ER. This represents an estimated litter turnover time of 7 – 8 years. While the contribution of litter respiration to ER is relatively small, the resulting large mass of recalcitrant litter in the canopy may contribute to *E. robustum's* ability to engineer its environment.

Acknowledgements

My sincere thanks to:

My primary supervisor Dr Dave Campbell, for his patience, guidance and unwavering commitment to making this project work. Dave, your passion for Kopuatai (and life) is infectious and made it easy to stay engaged. I have really appreciated the opportunity to learn from such an astute and discerning scientist.

Louis Schipper, my secondary supervisor, for your input and interest throughout the year. Your insights have been really useful.

Dean Sandwell, who not only dedicated hours to the wetness sensors and incubation setup, but did so with real enthusiasm and interest. Mostly, thank you for teaching me the skills I needed to make these myself, so I could take ownership of all aspects of the project. Thanks also to Janine Ryburn for your enthusiastic help whenever it was needed.

Jordan Goodrich, for sharing so much knowledge, data and Matlab code, and to Anna Carter, Aaron Huesser and David Zweig for your help in the field.

Mark Riddell, for taking time during his summer holidays to help me make sense of the statistical side of my data.

This research was funded through the MSI 'Restoring wetland function' programme, with the University of Waikato subcontracted to Landcare Research. I gratefully acknowledge generous support from the University of Waikato Masters Research Scholarship, the Dr Stella Frances Memorial Scholarship and the National Wetland Trust's Golden Plover Scholarship.

I would also like to thank my family for developing such a genuine interest in Kopuatai, and a perhaps slightly more transient interest in the plant life and gas exchanges that occur there. Thanks Mum and Dad for your endless encouragement. Thank you Kay and Mike for so generously taking me in for these last few weeks when you have had so much else on your plates.

To my friends, Ultimate Frisbee teammates, the 2012-14 MSc students, and especially to Ben, Esther and my flatmates Anna, Sophie, Nikki and Carley – this would have been way less fun without you all. Anna – we've lived in each other's pockets for three years and I'd happily take three more. Here's to a friendship that will outreach the longest piece of string.

Table of Contents

Abstract iii

Acknowledgements v

Table of Contents vii

List of Figures xiii

List of Tables xv

Chapter One: Introduction 1

1.1 Peatlands and carbon at a global scale 1

1.2 Peatlands in New Zealand 1

1.3 Canopy structure and questions arising from it 2

1.4 Thesis objectives 3

1.5 Thesis outline 3

Chapter Two: Carbon and water exchange in peatlands: Review of the literature 5

2.1 Peatlands 5

2.1.1 The importance of peatlands, and their carbon and water processes 6

2.2 Contrasting bogs of the northern and southern hemispheres 7

2.3 H_2O and CO_2 exchange 8

2.3.1 Vegetation type as a control on CO_2 and H_2O exchange 10

2.3.1.1 *Sphagnum* species 10

2.3.1.2 *Empodisma robustum* 11

2.3.2 Abiotic control: Water table 14

2.4 Influence of canopy architecture on CO_2 and H_2O exchanges 15

2.4.1 Reduced CO_2 uptake 15

2.4.2 Mulching Effect 16

2.4.3 Decomposition of standing dead litter 17

2.4.4 Photodegradation 18

Chapter Three: Site Description 19

3.1 Background on Kopuatai bog 19

3.2 Vegetation 19
3.3 Research site 21
Chapter Four: Canopy Architecture 23
4.1 Methodology 23
4.1.1 Canopy harvest 23
4.1.2 Canopy sorting 25
4.2 Results 27
4.2.1 Spatial variation of canopy characteristics 27
4.2.1.1 Height 27
4.2.1.2 Standing mass 28
4.2.2 Relating canopy height to vegetation mass and density 29
4.2.3 Canopy structure 30
4.3 Discussion 34
4.3.1 Canopy architecture 34
4.3.2 Standing dead litter mass in other ecosystems 34
4.3.3 Ecosystem implications of canopy structure 35
4.3.4 Canopy height 37
4.3.5 Implications of harvesting methods 38
Chapter Five: Canopy Litter Respiration 41
5.1 Methodology 41
5.1.1 System design 41
5.1.2 Samples 42
5.1.3 Test for CO_2 pulse 42
5.1.4 Moisture 43
5.1.5 Experimental procedures 44
5.1.5.1 Respiration from dry litter 44
5.1.5.2 Temperature response 45
5.1.5.3 Respiration from different litter types 45

5.1.5.4 Effect of moisture content 45
5.1.5.5 Compiled data and model fitting 46
5.2 Results 47
5.2.1 Moisture contents of saturated litter 47
5.2.2 CO_2 pulse from moistened litter 47
5.2.3 Measuring respiration from litter 48
5.2.4 The effect of moisture content on respiration rates 50
5.2.5 Temperature response of litter respiration 52
5.3 Discussion points 55
5.3.1 Differences between litter qualities 55
5.3.2 Temperature response of litter respiration 56
5.3.3 Rates of respiration from different litter types 57
5.3.4 Moisture dependence 57
5.3.5 Implications for using these data for modelling respiration 58
Chapter Six: Modelling Canopy Respiration 61
6.1 Methodology 61
6.1.1 Wetness Sensors 61
6.1.1.1 Leaf wetness sensor construction 61
6.1.1.2 Wetness sensor deployment 63
6.1.1.3 Data logging 63
6.1.2 Antecedent Precipitation Index (API) 64
6.1.3 Model of litter respiration 64
6.1.3.1 Sensitivity testing the model 65
6.1.4 Ecosystem respiration 66
6.1.5 Recalcitrance of canopy litter 67
6.2 Results 68
6.2.1 Matching LW data with litter field moisture contents 68
6.2.2 Leaf wetness sensor data 68

6.2.3 Canopy wetness and energy flux 70
6.2.3.1 LW sensor data 70
6.2.3.2 Energy Balance 71
6.2.3.3 API 73
6.2.4 Litter respiration model outputs 75
6.2.4.1 Model settings 75
6.2.4.2 Seasonal change in litter respiration 75
6.2.4.3 Annual litter respiration 76
6.2.5 Model sensitivity testing 77
6.2.5.1 The estimated fraction of upper and lower litter 77
6.2.5.2 API threshold between wet and dry 78
6.2.5.3 Difference between using fitted E_0 and standard value 78
6.2.6 Recalcitrance of canopy litter 78
6.3 Discussion 79
6.3.1 Modelled canopy litter respiration 79
6.3.2 Litter recalcitrance 80
6.3.3 Implications of CO_2 pulse on wetting 80
6.3.4 Relationship between wetness and the energy balance 80
6.3.5 Methods of determining canopy wetness 81
6.3.5.1 Leaf wetness sensors 81
6.3.5.2 API 81
6.3.5.3 Comparison of API and LW data 81
Chapter Seven: Synthesis and conclusions 83
7.1 The contribution of E. robustum litter respiration to ER 83
7.2 The role of litter in ecosystem engineering 84
7.3 Further Research 84
References 87
Appendix 95

List of Figures

Figure 2.1 Estimated global distribution of peatlands from Vitt (2008). Light green areas have >10% peat cover. 7

Figure 2.2 Schematic diagram of the pathways of carbon movement through bog ecosystems. Adapted from Luyssaert et al. (2007) and Rutledge-Jonker (2010). 9

Figure 3.1 The location of Kopuatai bog in the North Island of New Zealand, with the location of the field site indicated. (Source: Sturgeon (2013)). 20

Figure 3.2 Four plant species common at Kopuatai bog 21

Figure 3.3 The site eddy covariance tower 22

Figure 4.1 Map of the eddy covariance (EC) tower area 25

Figure 4.2 (a) The plot harvest set up, showing the wooden frame used as a boundary for canopy harvests; (b) Cross section of canopy showing the typical structure, including the dense layer of standing dead litter. The vertical sections used for harvesting are labelled. 26

Figure 4.3 Histograms of (a) the distribution of 149 canopy height measurements from the preliminary survey; and (b) the distribution of heights of the 15 harvested plots. 28

Figure 4.4 Histogram showing the distribution of canopy mass in the 15 harvested plots 29

Figure 4.5 Regression analyses of plot height vs vegetation density (kg m^{-3}) and plot height vs vegetation mass (kg m^{-2}), with the R^2 values equations for each regression. 30

Figure 4.6 Boxplot showing the upper limit of canopy section boundaries in the 15 harvested sites.. 31

Figure 4.7 Average dry matter mass grouped by vegetation species and state in each vertical section of the harvested plots. S = Sedge (*B. teretifolia* and *S. pauciflorus*), E = *E. robustum*, G = live green material, BL = live brown material, D = dead material. 32

Figure 4.8 The two different qualities of E. robustum litter (a) from the upper portion of the standing dead litter layer; and (b) from the lower portion of the layer. 33

Figure 4.9 Aerial view of the Kopuatai research site under construction, with examples of wave crests circled, running parallel to the white lines. 35

Figure 4.10 Close up view of a canopy wave crest 35

Figure 4.11 Average mass of vegetation canopy at a plot divided by height increments rather than canopy structure (Data from J. Goodrich, personal communication, 12 February 2013) 39

Figure 5.1 A schematic diagram of the incubation system, showing both the top (experimental) and bottom (heating/cooling) layers of the polystyrene box 42

Figure 5.2 (a) The polystyrene box housing eight sealed chambers which held samples of litter; (b) photo of the incubation setup 43

Figure 5.3 Moisture contents of saturated upper (n = 8) and lower (n = 8) canopy litter samples. 47

Figure 5.4 CO_2 flux from moistened lower canopy litter (averaged over five chambers) over a 19 hour period at ambient temperature (18-19°C). 48

Figure 5.5 Litter respiration rates over a range of ascending and descending temperatures. 50

Figure 5.6 Respiration rates from upper and lower litter samples with different moisture contents over a range of temperatures. 52

Figure 5.7 Relationship between moisture content and respiration rate at 20°C for the upper and lower litter, with the hypothesised relationship shown. 53

Figure 5.8 Compiled respiration data from multiple experiments 55

Figure 6.1 Schematic diagram of the electronic circuit used in the leaf wetness sensors (Source: Campbell Scientific Inc., Leaf Wetness Sensor Model 237 Instruction Manual, revision 7/10, 2010) 62

Figure 6.2 LW sensors (a) showing the gold print of the sensor face; and (b) after coating the sensor with latex paint. The epoxy casting covers the R1 100K Ω resistor (Figure 6.1) and soldered joints 62

Figure 6.3 (a) A LW sensor deployed in the upper canopy; (b) the wet canopy on a winter morning after a heavy dewfall. 63

Figure 6.4 Flow chart describing the respiration model 66

Figure 6.5 Wetting and drying cycles recorded by leaf wetness sensors positioned in a tall stand of *E. robustum*.. 70

Figure 6.6 Example time series showing the relationships between (a) leaf wetness sensor data; (b) energy flux densities; (c) API; and (d) half hourly rainfall, over a five day period in June 2013 72

Figure 6.7 Equivalent to the example in Figure 6.6, but for a late-spring period, from 8 – 12 November 2013 73

Figure 6.8 Monthly sums of ecosystem and litter respiration for the period 8 February – 30 November 2013, calculated by the respiration model 77

List of Tables

Table 4.1 Number of samples required to achieve the stated confidence levels and accuracies 24

Table 4.2 Statistical properties of the preliminary height survey and 15 harvested plots..... 28

Table 4.3 Thickness (cm) of vertical sections within each profile 31

Table 4.4 Canopy height and litter mass data from studies looking at standing dead litter in different environments 36

Table 5.1 Results of the analysis of covariance, indicating the significance of the difference between the least squares means between each of the treatments. 50

Table 5.2 Average moisture contents (± standard deviation) of upper and lower litter used in experiments for data presented in Figure 5.6. 51

Table 5.3 A review of litter respiration rates reported in the literature for a variety of ecosystems 60

Table 6.1 Comparison of litter field moisture and LW data at the same time and location.. 68

Table 6.2 Variable inputs to the litter respiration model 76

Chapter One

Introduction

1.1 Peatlands and carbon at a global scale

The large volumes of carbon sequestered by peatlands over thousands of years render them globally important atmospheric carbon stores. Covering over 17 million hectares of land area (Petrone et al., 2001) and containing 10 – 35% of the total carbon estimated to be stored in soils (Lafleur, 2009), peatlands represent one of the major terrestrial carbon pools. Long term carbon sequestration and the ongoing carbon sink that peatlands represent have implications for global atmospheric CO_2 concentrations and related climatic conditions. Holden (2005) estimated that carbon storage in peat over the past 10,000 years has led to a 1.5 – 2°C reduction in global temperatures. Peatlands are also highly valued for the range of different ecosystem services they provide, including flood control, supporting biodiversity and catchment hydrology regulation, as well as carbon sequestration (Kimmel and Mander, 2010; Lafleur, 2008).

The accumulation of peat occurs because the system is unbalanced (more carbon is taken up by the ecosystem than released), and the direction of this balance is dependent on a range of environmental factors. Climate change, drainage, fires and poor management can change the carbon balance of peatland ecosystems, leading to reduced carbon uptake and potentially to a net loss of carbon from peat (Holden, 2005; Lafleur, 2009). The global importance of peatlands drives research into the movement of carbon within these ecosystems and between peatlands and the atmosphere, as understanding these fluxes is critical for predicting peatland responses to environmental changes (Roulet et al., 2007). The need for better understanding of peatland carbon fluxes has led to an increase in studies focused on measuring individual components of net ecosystem carbon balances (NECB) (Chapin et al., 2006; Limpens et al., 2008).

1.2 Peatlands in New Zealand

Prior to European settlement, wetlands covered around 1% of the New Zealand land area, with peatlands prominent in two main regions of the country: Southland and Waikato. Subsequently, extensive draining of wetlands for urban and agricultural development has diminished them to around 10% of the pre-European

coverage (McGlone, 2009). Fragments of peatlands remain in the Waikato, although many are considerably altered by the effects of drainage and invasive species. Extending over an area of more than 90 km^2 in the lower Hauraki Plains, Kopuatai bog is New Zealand's largest raised peat bog and, although the edges are influenced by the surrounding land uses (Myers et al., 2013), the centre of the bog is considered unmodified (Campbell and Williamson, 1997). Kopuatai is recognised as a site of international importance due to the range of indigenous biodiversity it supports, and has been listed as a Ramsar site (one of six in New Zealand) since 1989 (Myers et al., 2013).

The vast majority of peatland carbon balance research has been carried out in the northern hemisphere. New Zealand bogs are dominated by vascular vegetation, which makes them structurally and functionally different to their northern hemisphere counterparts, which are dominated by *Sphagnum* moss species. Whereas in the northern hemisphere *Sphagnum* mosses are the primary peat forming plants, this role is carried out by two members of the Restionaceae family in bogs in the Waikato region. *Empodisma robustum* (wire rush) is the primary peat former in these restiad bogs, and *Sporadanthus ferrugineus* is an indigenous species found in only three peatlands in New Zealand (Agnew et al., 1993; Clarkson et al., 2009; Wagstaff and Clarkson, 2012).

1.3 Canopy structure and questions arising from it

The *E. robustum* canopy at Kopuatai is around 40 – 100 cm high (Agnew et al., 1993), and contains a very dense layer of standing dead litter. This litter is highly recalcitrant, and observations suggest it remains in the canopy for long periods of time (Campbell and Williamson, 1997; Clarkson et al., 2014; Hodges and Rapson, 2010). The standing dead litter layer is thought to play an important role in the water balance at Kopuatai, intercepting rainfall and storing up to around 2 mm of water (Campbell and Williamson, 1997). This high water storage capacity, combined with a mulching effect caused by the density of the canopy, restricts evaporation from the lower canopy and peat surface (Campbell and Williamson, 1997; Thompson et al., 1999). This conservation of water in the canopy and peat likely contributes to the ability of bogs to form in the Waikato, which would otherwise be climatically unsuitable for bog development (Hodges and Rapson, 2010; McGlone, 2009).

The standing dead litter layer also influences the carbon balance of Kopuatai: the recalcitrance of the litter suggests that it emits only a small amount of carbon through microbial respiration as it decomposes. The overall contribution of standing litter to total ecosystem respiration has not previously been investigated. A complete understanding of the fluxes of carbon and water through an ecosystem contributes towards knowledge of ecosystem functioning. A number of studies have been carried out at Kopuatai and other Waikato bogs which contribute to the quantification of all elements of the NECB and water balance in these ecosystems (Campbell et al., in press; Campbell and Williamson, 1997; Hodge, 2002; Smith, 2003; Sturgeon, 2013; Thompson et al., 1999). The present study will contribute to this body of work.

1.4 Thesis objectives

The purpose of this thesis is to investigate the role that the *E. robustum* canopy plays in the CO_2 balance at Kopuatai bog. In particular, this study aims to determine the proportion of total ecosystem respiration measured at Kopuatai that is sourced from the decomposition of *E. robstum* litter in the canopy. This is achieved through three main objectives:

- Quantify the mass of litter in the standing dead layer of the canopy, and how this varies spatially;
- Measure the rate of CO_2 evolution from the microbial decomposition of standing dead litter, and how this is influenced by temperature and moisture;
- Develop a method of identifying when canopy moisture is sufficient for respiration to occur; and
- Develop a simple model of canopy litter respiration, in order to estimate the proportion of calculated ecosystem respiration this accounts for.

1.5 Thesis outline

Chapter two is a literature review which examines the exchange of carbon and water in peatland ecosystems, from a global scale to Kopuatai bog, and the biotic and abiotic drivers of these exchanges. The importance of canopy structure in regulating fluxes of carbon and water is also investigated.

Chapter three gives a brief description of Kopuatai bog and the research site established there. It also describes the development of the bog and the current vegetation.

The results of this research are presented in Chapters four to six, each of which contains the methodology used and a discussion of the results. Chapter four is an analysis of the canopy architecture within the Kopuatai research site's eddy covariance footprint, with a specific focus on properties of the standing dead litter layer. Chapter five describes an investigation into the respiration rate of canopy litter, and the influence of temperature and moisture on this rate. Chapter six describes two methods which were used to gauge canopy wetness, and also details the development of a simple model of litter respiration.

Chapter seven synthesises the results of the preceding three chapters and draws conclusions about how the information generated in this thesis may contribute to the growing body of literature and understanding of the role that the *E. robustum* canopy plays in the functioning of Kopuatai bog.

Chapter Two

Carbon and water exchange in peatland ecosystems: A review of the literature

2.1 Peatlands

Peat-forming wetlands are commonly known as peatlands or mires, and can be divided into two broad categories: bogs and fens. Bogs represent the endpoint of a continuum of wetland types which transition from swamps to fens and bogs (McGlone, 2009). Peatlands form when, for a long period of time, the net primary production of a wetland ecosystem exceeds the decomposition of organic material, resulting in the accumulation of incompletely decomposed organic matter which forms a deposit (peat) (Wieder et al., 2006). Peat can be defined as an accumulation of more than 30 cm of deposits which are primarily (>65% dry weight) organic, mostly constituted of incompletely decomposed organic material (McGlone, 2009). Peat largely forms under anaerobic conditions, which are necessary to inhibit the decomposition of the organic matter, and are usually achieved through water table levels which are close to the peat surface (Campbell and Jackson, 2004).

The continued accumulation of peat affects the major sources of water to a wetland, which determines the peatland type. Fens receive water and nutrients primarily from groundwater and adjacent mineral soils, and subsequently their nutrient statuses range from oligotrophic to mesotrophic (commonly referred to as 'poor' or 'rich' fens accordingly). Bogs are very poorly drained, with very little water movement and usually no groundwater or soil nutrient inputs (Devito et al., 1997; Fraser et al., 2001). Raised bogs are a highly developed form of bog, where highest rates of peat accumulation occur in the most poorly drained bog centre, resulting in a domed surface which is further isolated from nutrient inputs (Johnson and Gerbeaux, 2004). Meteoric water is very low in nutrients, and as this is the only source of water to raised bogs, these environments are generally oligotrophic (Campbell and Jackson, 2004).

2.1.1 The importance of peatlands, and their carbon and water processes

Wetlands are considered to be valuable ecosystems for a number of different reasons, including the unique biodiversity they support, their roles in flood control, erosion control and water storage, and also for their ability to act as sinks for atmospheric carbon (Lafleur, 2008; Lafleur, 2009). Globally, wetlands are estimated to contain 202 to 535 Gt of C; a significant portion (10 - 35%) of the estimated 1500 to 2000 Gt of C estimated to be stored in soils (Lafleur, 2009). Peatlands represent one of the largest terrestrial carbon pools, covering more than 17 million hectares of land (Petrone et al., 2001) and containing around one third of the terrestrial biosphere carbon stores. The long-term ability of bogs to store carbon means they have played a substantial part in moderating atmospheric CO_2 concentrations (Frolking and Roulet, 2007; Holden, 2005).

Plants take up carbon dioxide (CO_2) though photosynthesis and release it through plant (autotrophic) and microbial (heterotrophic) respiration when organic matter is decomposed. While plant stomata are open, which is necessary for the plant to assimilate carbon, water vapour is lost to the atmosphere as transpiration (Ponton et al., 2006). The exchanges of CO_2 and H_2O between a bog ecosystem and the atmosphere are affected by a range of different factors, both biological (plant functional types and physiology, availability of nutrients and types of microbes present in the soil) and physical (light, water availability and temperature). Lafleur (2009) described the ecosystem fluxes of carbon gases (CO_2, CH_4) and the influence of atmospheric turbulence on these exchanges. Chapin et al. (2006) outlined the common methods used to quantify carbon cycling in ecosystems, particularly the calculation of gross primary productivity (GPP), ecosystem respiration (ER), net ecosystem productivity (NEP) and net ecosystem carbon balance (NECB), which can be used to gauge the status of an ecosystem as a source or sink of carbon.

The water balance of peatland systems plays a key role in the ability of the systems to store carbon, as the accumulation of carbon as peat relies on anoxic conditions generated by a high water table. The properties of peat-forming plants, which tend to have litter which is more resistant to decay than the litter of other plants, also play an important role in peat growth. In order to understand the

development of peatlands and carbon processes in these ecosystems, it is necessary to understand the ways in which bog vegetation, decay processes and hydrology interact (Holden, 2005).

2.2 Contrasting bogs of the northern and southern hemispheres

The global distribution of peatlands, illustrated in Figure 2.1, shows that they form in a variety of climates. 80% of global peatland area is located in temperate to cold areas of the northern hemisphere, most notably in Russia, Scandinavia, Canada and the USA, and most of the remaining area is tropical or sub-tropical, predominantly in south-east Asia (Limpens et al., 2008). Temperate peatlands in the southern hemisphere are present in parts of South Africa (Thamm et al., 1996), South America (Benvenuto et al., 2013), southeast Australia and New Zealand (Wagstaff and Clarkson, 2012).

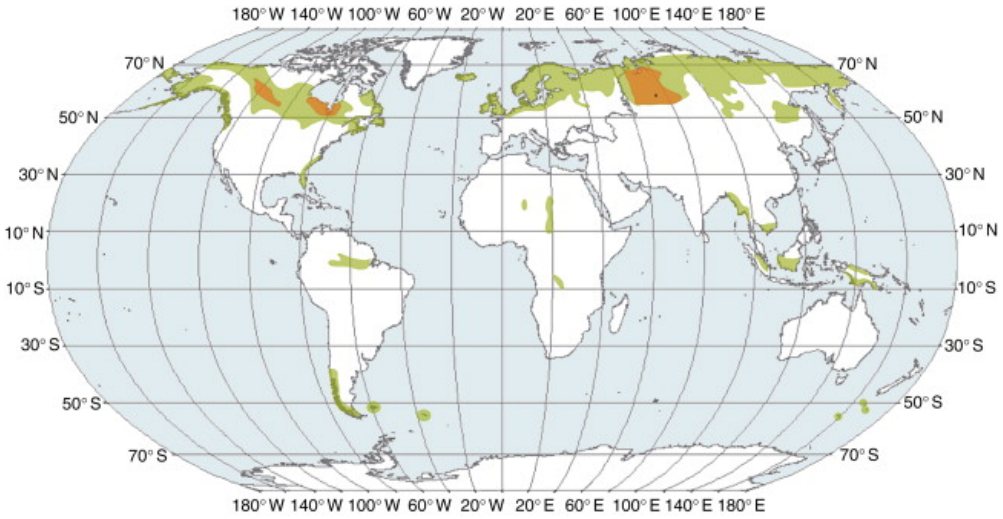

Figure 2.1 Estimated global distribution of peatlands from Vitt (2008). Light green areas have >10% peat cover. The orange areas are the world's largest peatland complexes.

The vast majority of existing peat bog literature is based on data from northern hemisphere bogs and fens, many of which are dominated or highly populated by moss species of the *Sphagnum* genus (Clarkson et al., 2004; Limpens et al., 2008). In contrast, New Zealand raised peat bogs are dominated by three vascular plant species of the Restionaceae family, and are therefore commonly referred to as 'restiad bogs'. The three dominant species in these New Zealand bogs are *Empodisma robustum, E. minus* and *Sporadanthus ferrugineus* (Wagstaff and Clarkson, 2012). *E. robustum* is the dominant peat-forming vegetation in northern New Zealand (north of 38°S) while *E. minus* occurs further south in New Zealand and also in south eastern Australia. *S. ferrugineus* is a threatened plant species

which is only found at limited sites in northern New Zealand (de Lange et al., 1999). The type of vegetation which dominates within bogs is important in the ecological functioning of these ecosystems (Laine et al., 2011). One of the most significant influences the vegetation has on the nature of a bog is in the formation of peat. The different ways in which the *Sphagnum* and *Empodisma* influence peat development as well as other functional aspects of bogs is discussed below.

2.3 H_2O and CO_2 exchange

The cycles of water and carbon through bogs are integral to the functioning of these systems. In ombrotrophic raised bogs such as Kopuatai, precipitation is the only input of water. This water is then either evaporated from the canopy or peat surface, taken up by plant roots and ultimately transpired, or it makes its way into the peat and becomes groundwater. In most bog systems, groundwater flows laterally and is discharged into streams or canals. Peat formation occurs in waterlogged environments when aerobic microbial degradation of plant biomass is prevented by anoxic conditions. The balance between water inputs and outputs determines the height and stability of the water table, which affects the oxygen content of the peat and the subsequent rate of peat accumulation or decomposition (Campbell and Jackson, 2004; Lafleur, 2008).

The pathways of carbon movement between the atmosphere and vegetated ecosystems such as bogs are described using a range of terms and equations. An overview of these processes and the corresponding terminology is given here. Carbon taken up as CO_2 through photosynthesis is referred to as gross primary production (GPP). Some of this carbon is lost as the plant respires (autotrophic respiration, AR), both above ground (AR_a) and below ground (AR_b). The remaining carbon is assimilated into the plant organic material, and is termed net primary production (NPP). Heterotrophic respiration (HR) is the loss of carbon through respiration of microbial and fungal organisms breaking down organic matter in the litter and peat. Net ecosystem production (NEP) is the carbon which is not lost through any of the respiration pathways and becomes stored in the peat. NEP can be calculated as NPP – HR, and also as GPP – ER, where ER is ecosystem respiration (the sum of all autotrophic and heterotrophic respiration). The overall flux of CO2 between the atmosphere and the ecosystem is known as the net ecosystem exchange (NEE). The sign convention of NEE is defined from an atmospheric perspective, with uptake of CO2 by an ecosystem being defined

by a negative flux, while losses from an ecosystem to the atmosphere are positive fluxes. The opposite definitions apply for NEP, which is defined from an ecosystem perspective, so ecosystem gains are defined as positive fluxes and vice versa. Abiotic degradation processes (AD), such as fire and photodegradation, can also contribute to the NEE balance, however, studies of carbon cycling in ecosystems do not always include these in their calculation of NEE (Chapin et al., 2006; Rutledge-Jonker, 2010).

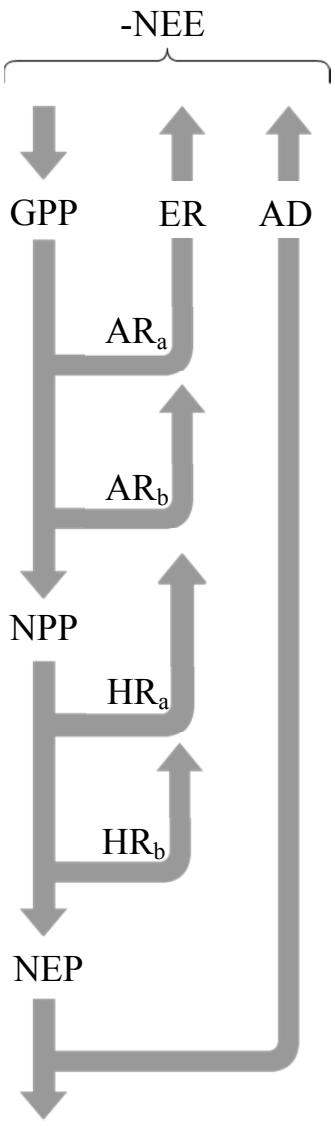

Abbreviations:

NEE	Net ecosystem exchange
GPP	Gross primary production
NPP	Net primary production
NEP	Net ecosystem production
ER	Ecosystem respiration
AR_a	Aboveground autotrophic respiration
AR_b	Belowground autotrophic respiration
HR_a	Aboveground heterotrophic respiration
HR_b	Belowground heterotrophic respiration
AD	Abiotic degradation (including photodegradation)

Figure 2.2 Schematic diagram of the pathways of carbon movement through bog ecosystems. Adapted from Luyssaert et al. (2007) and Rutledge-Jonker (2010).

When the rate of vegetation growth is greater than that of its decomposition, peat accumulates. Many microorganisms can quickly transform cellulose (the most

easily degraded polymer in plant biomass) to carbon dioxide and water through aerobic decomposition. In anoxic conditions, however, a range of microorganisms is required for each successive reaction in anaerobic decomposition, making this process much lengthier and promoting peat accumulation (Brown, 1998). Water and carbon processes are therefore strongly interlinked, and integral to the functioning of bog ecosystems.

2.3.1 Vegetation type as a control on CO_2 and H_2O exchange

Plant growth plays an important role in the ecosystem exchanges of CO_2, and thus the factors that promote or inhibit plant growth have a major influence on net ecosystem exchange of CO_2 (NEE). It follows that the differences in plant growing conditions in bogs in different parts of the world cause widespread variations in the exchange of CO_2 between bogs in different climatic zones (Lafleur, 2009). The differences in dominant plant species in bogs in the northern and southern hemispheres also have a significant effect on the patterns of CO_2 exchange in these bogs.

2.3.1.1 Sphagnum species

In the northern hemisphere, mosses account for a large proportion of the vegetative biomass in peatlands. In these ecosystems, mosses contribute strongly to net primary production (NPP) (Orwin and Ostle, 2012). *Sphagnum* species are dominant in many northern hemisphere peat bogs, and these ecosystems are recognised as having greater rates of peat accumulation than other bogs. This is thought to be due to the very low rates of *Sphagnum* decomposition; recalcitrant *Sphagnum* material forms the bulk of the peat which is formed. Vascular plant species have been found to have a lower contribution to peat accumulation, and in some cases enhance methane emissions from the peat (Heijmans et al., 2001). In some cases, however, soil oxygen supply (via vascular plant root systems) is greater than demand which results in methane being oxidised before it can be released (Fritz et al., 2011).

Orwin and Ostle (2012) found that *Sphagnum* has a strong effect on NEE, causing the peat to become a carbon sink. *Sphagnum* had more influence on NEE than either of the other two moss genera considered in their study, which were *Plagiothecium* and *Hypnum*. This result is thought to have been caused by the high photosynthetic rate and low gross respiration rate of *Sphagnum*. There are a

range of possible causes of the low respiration rate associated with *Sphagnum*, including the fact that it produces recalcitrant litter, acidifies the surrounding environment, produces anti-microbial compounds and reduces the temperature of the soil. Orwin and Ostle (2012) suggested that *Sphagnum's* high metabolic efficiency of carbon use and the general poor quality of its litter were the main factors controlling the low respiration rates under this vegetation type. Moss species are less effective at carbon sequestration than vascular plant species, however the Orwin and Ostle (2012) study indicated that mosses may be photosynthetically active for a longer portion of the year, which could offset their disadvantage. Research by Zona et al. (2011) suggests that the compact *Sphagnum* canopy structure limits light penetration to the lower moss layers, which reduces damage to the tissues which are photosynthetically active. This stress avoidance mechanism was though to enable longer growing seasons compared to vascular plants and other mosses in the same ecosystem.

A feature which strongly contrasts *Sphagnum* or other moss-dominated vegetation from vascular canopies is that mosses are non-transpiring. Bogs with non-transpiring covers may have the potential for evaporation rates to exceed that of open water, although no firm conclusion has been reached and most research indicates that wetland evaporation rates are lower than the open water potential (Idso and Anderson, 1988; Lafleur and Roulet, 1992). Evaporation in *Sphagnum* dominated communities, which includes most peat bogs in the northern hemisphere, is highly affected by water table fluctuations due to the absence of vascular plant tissues and the low matric potential (Lafleur, 2008).

2.3.1.2 Empodisma robustum

Background on Empodisma

The *Empodisma* plant genus has long been recognised as containing two species which play important ecological roles in wetlands across Australia and New Zealand. *E. gracillimum* is present in wetlands in south-western Australia, while *E. minus* grows in eastern Australia, Tasmania and New Zealand. However, Wagstaff and Clarkson (2012) recently analysed DNA sequenced from 15 individual *Empodisma* samples and discovered a distinct haplotype which is present only in New Zealand north of 38° S latitude. Wagstaff and Clarkson (2012) determined that this haplotype was both physically and ecologically distinct from the recognised *Empodisma* species, and recommended that it be recognised as a

separate species, known as *E. robustum*. The name *robustum* reflects the more robust pattern of growth that this new species demonstrates, compared to *E. minus*, which it was previously thought to be.

The *Empodisma* species primarily occupy peatlands. They tend to grow into very dense and tangled culms, which have given rise to the scientific name *Empodisma*, which is Greek for obstacle, and also to the common name wire rush. *E. robustum* is a rhizomatous perennial which has long scaled stems. The highly branched root structures tend to form clusters which bind litter and bryophytes to the peat surface. The clusters can retain high volumes of water; up to 1500% of the dry weight of the roots. This water holding capacity, along with the acidic conditions created by the roots, led Campbell (1964) to describe *E. robustum* roots as resembling *Sphagnum* in both appearance and behaviour. *E. robustum* is commonly found growing in association with other bog plants, including *Sporadanthus ferrugineus*, *Leptospermum scoparium* (mānuka), *Epacris pauciflora, Baumea teretifolia*, *Schoenus brevifolius* and *Gleichenia dicarpa* (Wagstaff and Clarkson, 2012).

It has been proposed that *Empodisma* species are the "ecosystem engineers" in the transition from fen to bog in New Zealand peatlands. *E. robustum* is tolerant of a wide range of environmental conditions, allowing it to grow in relatively fertile fens before it aids the transition of the ecosystem to an ombrotrophic raised bog by accumulating peat (Hodges and Rapson, 2010). *E. robustum* roots are the primary material making up the peat in these raised bogs, due to the large volume of water which can be held in the root system and the recalcitrance of the dead plant material (Kuder et al., 1998; Wagstaff and Clarkson, 2012). *E. robustum* cluster roots also remove ions from rain and atmospheric particulates, which are the only source of nutrients in a raised bog (Clarkson et al., 2009). The role *E. robustum* plays in these ecosystem functions is thought to be the New Zealand equivalent of the role that *Sphagnum* species play in the formation and functioning of Northern Hemisphere bogs (Agnew et al., 1993). Since *Empodisma* has only recently been subdivided into a third species, research published before 2012 concerning raised bogs in New Zealand north of 38° latitude refer to *E. minus* rather than *E. robustum*. The architecture of these two species is clearly different (Wagstaff and Clarkson, 2012).

Role of E. robustum in CO_2 and H_2O exchange

The development of bogs is highly affected by the balances of carbon and water in these ecosystems. Vascular plants in bogs tend to reduce evaporation in several ways. The raised, rough canopy shelters the bog surface from wind turbulence and radiation, limiting evaporation from the peat surface. Vascular plants are also able to physiologically control transpiration through the conduction of water vapour through leaf stomata (small pores on the leaf surface through which gas exchange occurs). Stomatal conductance varies between different plant functional groups, but is always influenced by the atmospheric vapour pressure deficit (*D*) which is a measure of the ability of the air to take up moisture (Lafleur, 2008).

E. robustum is thought to play a significant role in the water balance of bogs in the northern North Island, where the climate is warm enough, often with dry summers and large water deficits, that the presence of extensive raised bog ecosystems would otherwise be unexpected (McGlone, 2009). The work of Campbell and Williamson (1997) and Thompson et al. (1999) has provided insight into the ways in which *E. robustum* influences water balances, possibly enabling raised bogs such as Kopuatai to form north of 38° S (Kuder et al., 1998; McGlone, 2009; Wagstaff and Clarkson, 2012).

Campbell and Williamson (1997) used the Bowen ratio technique to measure evaporation rates from Kopuatai over the summer of 1993/94. Evaporation rates were found to be much lower than those recorded for other wetlands. Evaporation rates measured during the day ranged from 0.06 – 0.16 mm hr^{-1}, which was notably lower than rates documented for northern hemisphere bogs (Lafleur, 2008). The daily average evaporation rate found at Kopuatai accounted for only 26% of the Penman potential open water rate (Thompson et al., 1999) – despite the fact that the water table remained within 0.2 m of the peat surface throughout the summer.

Campbell and Williamson (1997) measured Bowen ratios for the summer period, which describe the ratio of sensible to latent heat fluxes. Bowen ratios ranged from 3 – 5; values in this range would be expected in a semi-arid climate rather than in a saturated peat bog. Campbell and Williamson (1997) used these Bowen ratios to infer that the dense *E. robustum* canopy strongly restricted evaporation from the surface of the peat. A further anomaly Campbell and Williamson (1997) found in the Kopuatai evaporation regime was the fact that evaporation rates

remained relatively constant throughout the day, rather than following the pattern of net radiation. This implies that stomatal and canopy conductance provide active control of water loss during periods of high radiation.

It was proposed by Campbell and Williamson (1997), and supported by Thompson et al. (1999), that low evaporation rates measured at Kopuatai resulted from strong physiological control of *E. robustum* over water losses, possibly influenced by the low levels of available nutrients in the peat bog. Also, the dense canopy of living and dead *E. robustum* stems were thought to act as mulch, preventing evaporation from the peat surface and simultaneously absorbing a large volume of precipitation. The only time when the Kopuatai evaporation regime appeared to be similar to those reported for other wetlands was after rain, when the canopy was wet and therefore evaporation was not restricted by canopy resistance or mulching. The effectiveness of mulch layers in peatland ecosystems was demonstrated by Petrone et al. (2001), who measured a decreased evaporative flux (354 mm compared to a pre-restoration flux of 433 mm) after applying 3000 kg ha^{-1} of straw mulch to an extracted peatland.

The Campbell and Williamson (1997) study shows that Kopuatai is an ecosystem where the vegetation exerts very strong control over evaporation. The near-permanently saturated soils of Kopuatai combined with a microclimate above the canopy typical of semi-arid conditions have become known as the 'wet desert' paradox. A major question that remains is how the unusual water exchange properties of *E. robustum* affect CO_2 exchange.

2.3.2 Abiotic control: Water table

The two dominant controls on the biomass and species composition of a bog are the water table height and the availability of nutrients (Laine et al., 2011). Water table height is the most influential factor in determining the rate of peat decomposition in bogs, as saturated peat is subjected to anaerobic conditions and decomposition is inhibited (Berglund and Berglund, 2011). Low water tables can occur naturally as a result of drought or seasonal changes in precipitation but are also commonly caused by anthropogenic drainage to enable organic-rich peat soils to be utilised for production, as is the case in the Hauraki Plains (McLay et al., 1992). When bog water tables are lowered, the peat is oxidised and microbial decomposers release stored carbon to the atmosphere as carbon dioxide. If this

oxidation process is on-going, irreversible drying and shrinkage of the peat will occur, which can lead to peatland subsidence (Jaenicke et al., 2010; Schipper and McLeod, 2002). Couwenberg et al. (2010) estimated that in south-east Asian peatlands a 10 cm decrease in the average water table position caused by drainage could lead to the emission of 9 t CO_2 ha^{-1} a^{-1}.

2.4 Influence of canopy architecture on CO_2 and H_2O exchanges

The structure of a canopy can have a strong influence on the exchanges of CO_2 and H_2O in an ecosystem. In most bogs, dead plant litter falls to the peat surface where it decomposes, while decomposition of the plant root material is hindered by anoxic conditions and incorporated into the peat material. However, in ecosystems such as Kopuatai, which have a high proportion of standing-dead plant litter, this dead material can influence the exchange of H_2O between the atmosphere and the ecosystem. A hypothesis of this study is that a similar influence exists over the ecosystem exchanges of CO_2.

Globally, there are a range of ecosystems where the canopy contains a high proportion of standing litter. Examples include freshwater marshes (Kuehn et al., 2004; Rocha et al., 2008) and grasslands (Briggs and Knapp, 1995; Rutledge et al., 2010). The following section reviews the role of canopies in ecosystem CO_2 and H_2O exchanges.

2.4.1 Reduced CO_2 uptake

Rocha et al. (2008) investigated the role that dead standing litter in the San Joaquin Freshwater Marsh, Southern California, had on NEE. This study found that the litter had a significant impact on the carbon flux in the marsh, with NEE reduced by 17 - 47% in treatment plots with the standing litter present. These results are consistent with those of previous research in a range of ecosystems, which indicate that the presence of accumulated litter in a canopy leads to decreased productivity and a decreased response to environmental factors. Standing dead litter in marshes (Bonneville et al., 2008), estuaries (Jordan et al., 1990) and grasslands (Knapp and Seastedt, 1986; Lecain et al., 2000) has been found to contribute to the loss of CO_2 through microbial decomposition, and reduced productivity due to shading.

The decrease in available light energy due to dense standing litter layers is well documented; Rocha et al. (2008) found that light levels in the lower canopy of the

marsh increased by 70% when litter was removed. Briggs and Knapp (1995) conducted research into the factors influencing NEE at the Konza Prairie Research Natural Area (KPRNA), a tallgrass prairie in northeast Kansas. They found that the large volume of dead litter from both the most recent growth period and from previous years had a negative effect on the ecosystem's ability to assimilate CO_2. This was due to a reduction in the penetration of solar radiation, which limited the photosynthetic potential of the canopy. These findings were consistent with other research (Knapp and Seastedt, 1986; van Leeuwen and Huete, 1996). The research by Briggs and Knapp (1995) reflects a more seasonal influence of canopy structure of gas exchange than is found in New Zealand bogs, due to the seasonal nature of grasslands.

The standing dead litter layer is a grassland has also been found to alter the microclimate in the lower canopy (influencing the ability of new shoots to assimilate CO_2) and decrease the soil temperature (leading to decreased root productivity) (Knapp and Seastedt, 1986).

2.4.2 Mulching Effect

The effect standing dead litter layers have in reducing the penetration of radiation to the ecosystem surface often has the follow-on effect of reducing soil evaporation. The presence of standing dead litter influences the partitioning of energy into latent (*LE*) and sensible (*H*) heat. Bremer and Ham (1999) investigated the effects of burning dead biomass in a grassland in Kansas. Burning the dead litter increased the exposure of the moist soil to the atmosphere, increasing the surface conductance and evaporation by 2 – 3 times. Meanwhile, at the unburned site, the mulching effect of the burned litter restricted surface conductance and *LE*. The standing dead litter absorbed radiant energy, which was transported away from the surface as *H*. The layer of standing dead litter at Kopuatai bog is thought to have a significant mulching effect, influencing the rate and pattern of evaporation as described above (Campbell and Williamson, 1997; Thompson et al., 1999).

2.4.3 Decomposition of standing-dead litter

Mineralisation of carbon in wetland sediments is the most well-known source of CO_2 in bogs, but research into the CO_2 evolution from plant litter standing in the canopy suggests that this can represent an appreciable portion of a wetland's C

cycle. A range of studies have been carried out which investigated the rate of CO_2 evolution from decomposing plant litter in wetlands, and the conditions which promote this evolution.

Kuehn et al. (2004) tested CO_2 evolution from standing-dead litter in two Swiss lakes, and found daily fluxes of 51 - 570 mg C m^{-2} (0.01 – 0.15 µmol CO_2 m^{-2} s^{-1}). These rates indicate that microbial decomposition of litter within the canopy can contribute significantly to the overall C flux of the ecosystems. CO_2 evolution was found to be highly dependent on water availability, with up to 30 times increase in CO_2 flux occurring within five minutes of air dried material being wet. This rate of evolution could be maintained for up to 24 hours, and rates were found to increase with temperature. When the material was dried, rates of evolution were found to decrease within two hours.

An increase in CO_2 evolution from standing-dead litter after wetting was also observed by Newell et al. (1985). This study focused on the dead leaves and stems of *Spartina alterniflora* and *Juncus roemerianus*, which represent a large portion of the biomass of the warm temperate coastal marshes dominated by these species. The litter was found to respond strongly to wetting with saltwater, freshwater and water vapour by immediately releasing CO_2. The rate of CO_2 evolution was affected by temperature and water content. When saturated with water, the standing-dead litter was found to release CO_2 at rates as high as 200 µg CO_2 g^{-1} dry hr^{-1} (1.26 x 10^{-6} µmol CO_2 kg^{-1} s^{-1}). An initial burst of CO_2 evolution at a higher rate was detected directly after wetting the material. This peak in respiration rate indicates that the microbial assemblage within the standing dead litter is adapted to rapidly alternating wet/dry conditions, and the metabolism of these microbes becomes highly active almost immediately after wetting (Newell et al., 1985).

The CO_2 emitted from the decomposition of standing litter in the canopy constitutes the aboveground heterotrophic respiration portion of the peatland carbon flux (HR_a in Figure 2.2).

2.4.4 Photodegradation

CO_2 production can also occur from the abiotic breakdown of dead material. Photodegradation is the direct degradation of organic matter (OM) by solar irradiance, and leads to the emission of CO_2 through either photochemical

mineralization or microbial facilitation (where large compounds are broken into molecules small enough for microbes to process following rewetting) (Ma et al., 2012; Rutledge et al., 2010). Photodegradation can contribute significantly to the CO_2 flux in a range of ecosystems win which OM is exposed to radiation, which could include Kopuatai bog. Rutledge et al. (2010) determined the proportion of CO_2 loss from a Californian grassland during the dry season. Photodegradation was found to account for 60% of the dry season CO_2 emissions, and 92% of the summer midday CO_2 flux.

Chapter Three

Site Description

3.1 Background on Kopuatai bog

Kopuatai bog is located in the Hauraki Plains on the North Island of New Zealand (Figure 3.1), and is bordered by the Piako and Waitoa Rivers to the west and the Elstow Canal to the east. Kopuatai is approximately 96 km^2 in area, making it New Zealand's largest raised peat bog. The peat dome undulates, with a flat crown at 6.5 m above sea level, and peat up to 14 m deep. Kopuatai formed from small swamps and mires which dominated the Hauraki Plains around 11,000 BP, which then formed one large bog when the water table rose towards 9,050 BP (Newnham et al., 1995). After this point, the bog developed a domed structure, which led to an increasingly oligotrophic nutrient status. Changes in sea level, fire periodicity and environmental conditions altered the state of the bog, and currently the bog consists of two domes; one at the northern end and one at the southern. Although the Hauraki Plains have been extensively drained for agriculture, Kopuatai itself remains the least modified bog in New Zealand, with only the bog margins being significantly influenced by artificial drainage (Newnham et al., 1995). The mean annual temperature at Kopuatai is 13.4°C, and mean annual rainfall is 1112 mm (Clarkson et al., 2009).

3.2 Vegetation

Kopuatai bog is dominated by its primary peat-forming restiad species, *Empodisma robustum*, which grows in a dense wiry mass over much of the central bog area (Figure 3.2 (a)). The *E. robustum* canopy grows to around 0.7 m height, and contains a network of living and dead stems. The other main restiad, *Sporadanthus ferrugineus* (Figure 3.2 (b)), grows in distinct clusters through the *E. robustum* canopy and can reach a height of 2.5 m. *Leptospermum scoparium*, *Dracophyllum lessonianum* and *Epacris pauciflora* are woody species which also grow through the *E. robustum* canopy. These three species are more prevalent near the edges of the bog. Two species of spiky sedge, *Baumea teretifolia* and *Schoenus pauciflorus*, also have a significant presence in the bog vegetation, with *B. teretifolia* comprising around 15% of the canopy biomass. These sedges grow amongst the *E. robustum*, frequently to heights greater than 1 m (Figure 3.2 (c)).

Gleichenia dicarpa also commonly grows in clusters amongst the *E. robustum* (Figure 3.2 (d)). Intermittent areas of where the *E. robustum* canopy is more open allowing higher levels of light penetration have developed into small moss lawns, where species such as *Sphagnum cristatum* and *Riccardia crassa* dominate (Clarkson et al., 2004). The modern distribution of vegetation is largely determined by the availability of nutrients in the bog and the location of recent fires (Newnham et al., 1995).

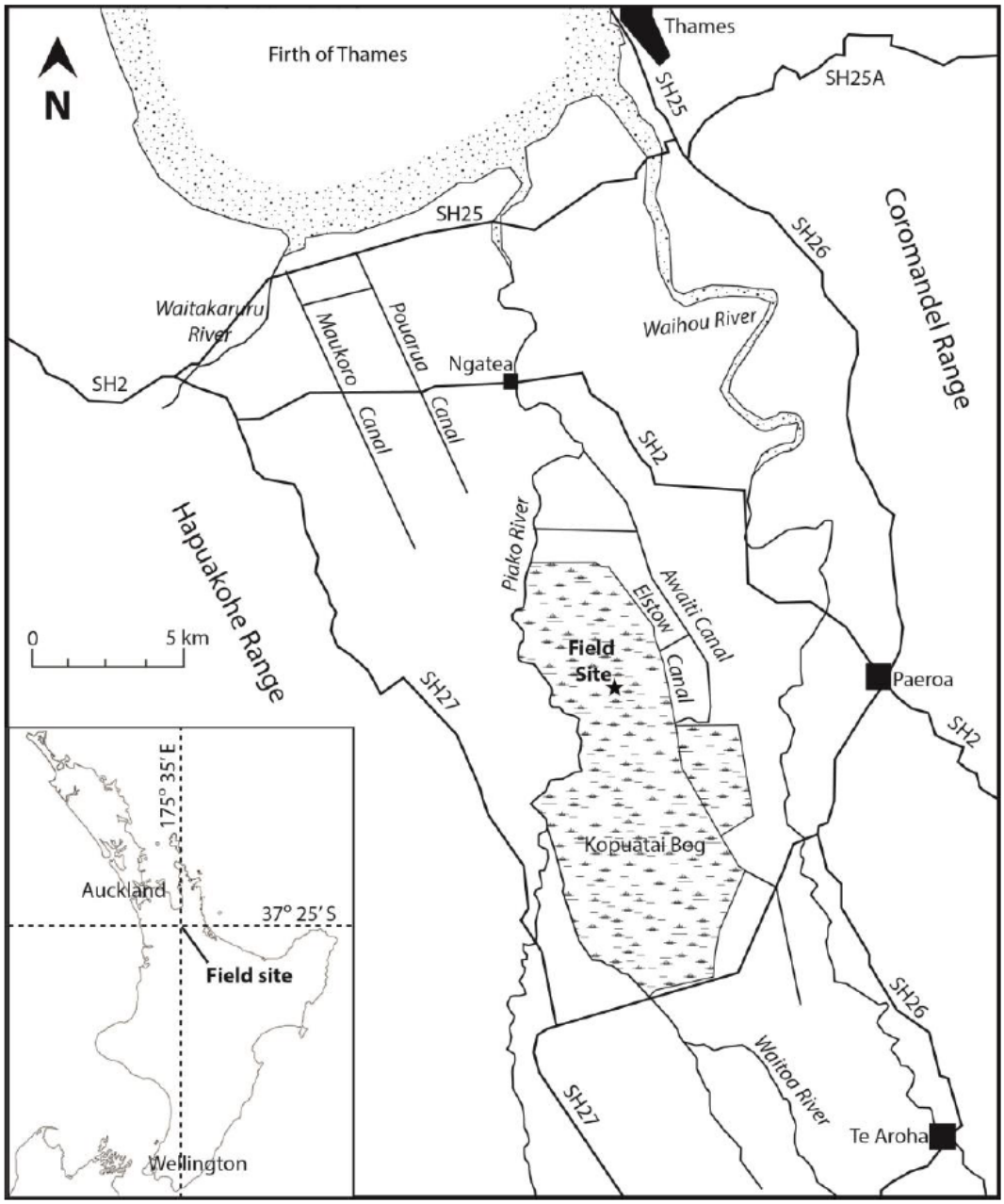

Figure 3.1 The location of Kopuatai bog in the North Island of New Zealand, with the location of the field site indicated. (Source: Sturgeon (2013)).

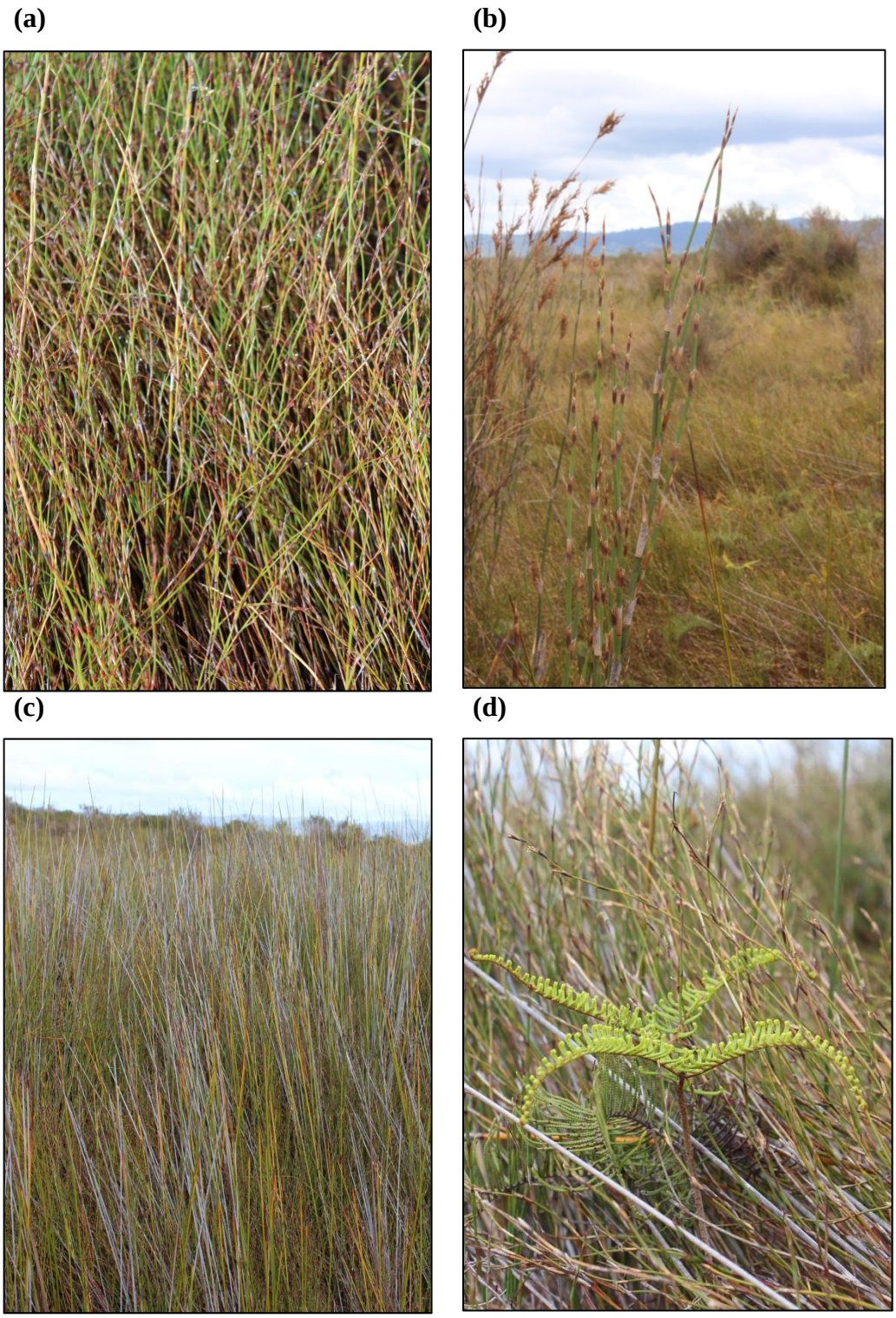

Figure 3.2 Four plant species common at Kopuatai bog (a) the dense *Empodisma robustum* canopy; (b) a cluster of *Sporadanthus ferrugineus* stems; (c) *Baumea teretifolia* and *Schoenus pauciflorus*; and (d) *Gleichenia dicarpa* emerging from the *E. robustum* canopy.

3.3 Research site

A research site was established on the northern dome of Kopuatai bog in 2011 (Figure 3.1). The site is around 2 km from the eastern edge of the bog, and is accessed via private land and a walking track. The research site is a base for high

frequency data collection using an eddy covariance tower. Eddy covariance (EC) is a method of measuring vertical flux densities, and is often used to measure gas exchanges between ecosystems and the atmosphere. EC towers measure vertical wind speed, gas concentrations (CO_2, CH_4, H_2O) and a range of micrometeorological parameters (such as temperature, pressure and humidity) to inform calculations of gas flux. At the research site a 4.5 m high EC tower has instruments mounted on a horizontal arm, approximately 4.25 m high and 1 m from the tower (Figure 3.3). Other measurements made at the site include incoming and outgoing radiation, water table depth, peat and canopy temperature, rainfall and wind direction.

Figure 3.3 The site eddy covariance tower

Chapter Four

Canopy Architecture

4.1 Methodology

4.1.1 Canopy harvest

In order to determine the magnitude of CO_2 emissions from the standing dead litter layer at Kopuatai, the amount of litter in the layer had to be quantified. Canopy vegetation was harvested from 0.25 m^2 plots across the eddy covariance (EC) measurement footprint. The plant species that were present in the canopy, and the proportion of each species that was alive or dead at different heights in the canopy were the main characteristics of interest. The number and locations of these harvests were designed to give a representative spatial sample of the canopy within the EC footprint.

To inform canopy harvest sampling design, a preliminary height survey was carried out, in which 149 measurements of *E. robustum* canopy height were taken within the eddy covariance footprint. A measurement was taken every 10 strides around the loop track (radius approximately 0.2 km, see Figure 4.1), on alternating sides of the track. Measurements were made using a tape measure to visually estimate the highest point of *E. robustum*. The tips of sedge stems (*Baumea teretifolia* and *Schoenus pauciflorus*) often grew much higher than the *E. robustum* canopy, but these were discounted from the height data as they did not appear to represent spatial variation as well as the *E. robustum* canopy height. Summary statistics of these data are presented in Table 4.2, and were assumed to represent the spatial variability of other canopy characteristics within the footprint, which informed the sample design of the canopy harvests. Equation 4.1 (D. Campbell, personal communication, 10 January 2013) was used to estimate the number of samples necessary to achieve different levels of confidence and accuracy in the harvest data. Table 4.1 contains the results of these calculations, with accuracies ranging from 1 - 20% of the true population mean, and confidence levels of 95% and 99%. It was determined that 15 randomly located canopy harvests would achieve ±10% accuracy with 95% confidence (p=0.05).

$$\frac{4 \times \text{Critical t value}^2 \times \text{Standard deviation}^2}{\left(2 \times \left(\frac{\%\ \text{Accuracy}}{100}\right) \times \mu\right)^2} \quad \textbf{(4-1)}$$

The critical t values for 95% and 99% confidence were 1.98 and 2.61 respectively.

Table 4.1 Number of samples required to achieve the stated confidence levels and accuracies, based on canopy height survey and Equation 4.1

	Confidence Level	
% Accuracy	**p=0.05**	**p=0.01**
1	1546	2697
2	387	674
5	62	108
10	15	27
20	4	7

In order to randomly locate the 15 plots to be harvested, five compass bearings (1 – 360°) were randomly generated. These bearings were used as transects which radiated from the eddy covariance tower (Figure 4.1). Three distances less than 200 m were randomly generated for each of the five transects. Each of these points became a sample plot, with the distance value representing the distance along the transect from the EC tower.

Each plot was accessed from the loop track which circles the EC tower, with the exception of those which were within 20 m of the EC tower, in which case they were accessed from the boardwalk to minimise disturbance. Google Earth™ was used to measure the distance from the point at which each transect crossed the loop track to each plot on that transect. In the field, a compass was used to locate the intersection of each transect with the loop track, and the plots were found by measuring the distance towards or away from the EC tower along the transect bearing, using a 50 m tape measure. When a plot was reached, a 0.25 m^2 frame

was placed over the canopy an arm's length to the left of the point (Figure 4.2 (a)) and the co-ordinates of the point were stored on a handheld GPS (Garmin SMap62). Secateurs were used to harvest all of the vegetation growing within the area of the frame. The canopy was first qualitatively divided into three vertical sections: upper canopy (predominantly live green material); mid canopy (green and brown live material, with some dead material); and lower canopy (predominantly dead material) (Figure 4.2 (b)). Each section was harvested and stored separately.

A small error occurred in the division of vegetation into sections, as once material was cut it was difficult to prevent some falling through the canopy into lower sections. This was minimised by cutting only small sections at a time and having one person cut the material while another held the stems being cut. Overall, this error is likely to be negligible.

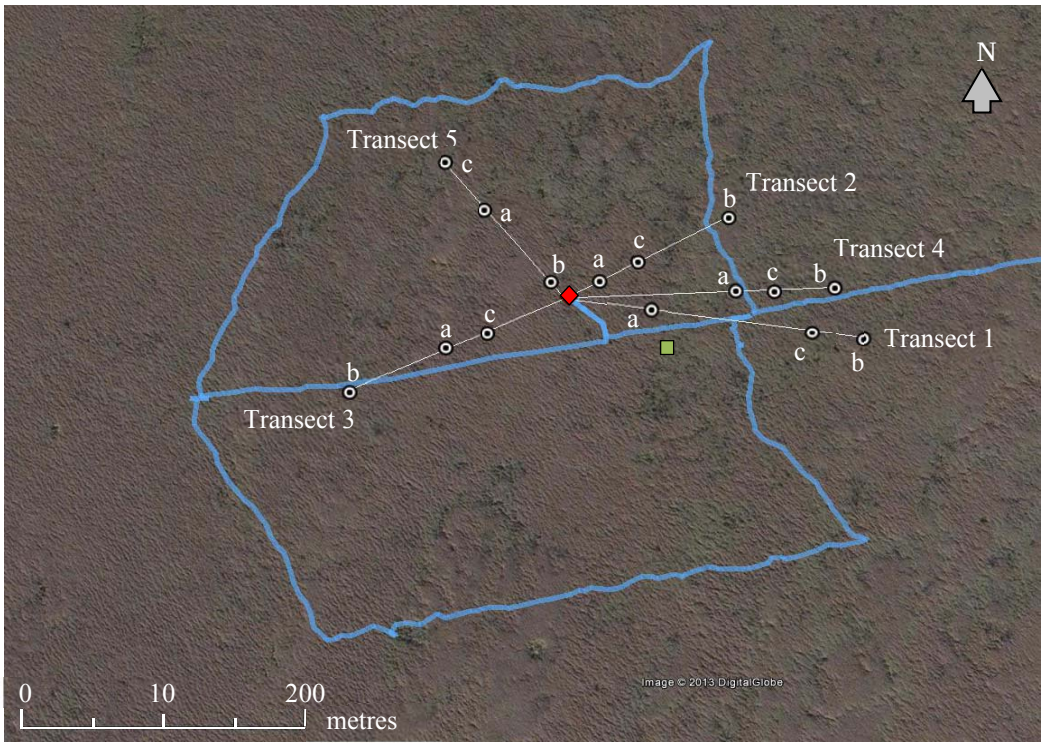

Figure 4.1 Map of the eddy covariance (EC) tower area, with the tower indicated by the red diamond, and the access track and loop track shown in blue. The randomly generated transects used for sample plots are shown as white lines, and the plots themselves are indicated with black and white dots. The loop track was used to take the preliminary height measurements which informed the sample design, and to access transects. The green square indicates the location of the plot harvested by J. Goodrich, referred to in Section 4.3.5. (Source: Adapted from Google Earth™ (2013)).

4.1.2 Canopy sorting

The material from each section of each plot was separately sorted into species and states. *E. robustum* was classified into three states: live green (photosynthesising) material, live brown material and dead material. The sedge species (*B. teretifolia* and *S. pauciflorus*), which were the most dominant plant types after *E. robustum*, were grouped into one category as their physical similarities made it difficult to tell one from the other when examining small sections of the plants. The sedges were sorted into states using the same system as *E. robustum*. Plant material which was neither *E. robustum* nor either of the sedge species was grouped into a class called 'other'. Samples were oven dried at 80°C for around four days before being weighed and discarded.

Figure 4.2 (a) The plot harvest set up, showing the wooden frame used as a boundary for canopy harvests; (b) Cross section of canopy showing the typical structure, including the dense layer of standing dead litter. The vertical sections used for harvesting are labelled.

4.2 Results

4.2.1 Spatial variation of canopy characteristics

4.2.1.1 Height

The canopy height measurements made in the pilot study were used to estimate the spatial variation of canopy characteristics within the EC footprint. The distribution of the 149 canopy height measurements is shown in Figure 4.3 (a), and the statistical properties of these data are presented in Table 4.2. The mean height (±95% confidence interval) of the *E. robustum* canopy was 58.9 cm (±1.9 cm) above the peat surface, so the distribution of heights was roughly normal, with a skewness of 0.3. The kurtosis of these data was calculated to be 2.96, indicating that the distribution had a higher peak and heavier tails than a normal distribution. *E. robustum* was present at all measured sites, and the range in canopy heights was 32 – 91cm.

The distribution of heights of the 15 harvested plots is shown in Figure 4.3 (b), with the statistical properties of these data also presented in Table 4.2. The kurtosis of the heights of the 15 harvested sites was 2.75, and the skewness of this distribution was 0.7. The modal height was 10 cm higher in the preliminary survey than the harvested plots (Figure 4.3).

The difference between the mean canopy heights measured in the preliminary survey and the harvests was compared using a two-sample t-test. An F-test determined that the variances of the two datasets were different (133 cm^2 for the survey and 304 cm^2 for the harvests), so an unequal variances t-test was used. The mean heights were significantly different ($p = 0.02$).

Table 4.2 Statistical properties of the preliminary height survey and 15 harvested plots

	Preliminary survey	**Harvested plots**
Number of samples	149	15
Mean height	58.9 cm	71.1 cm
Standard deviation	11.7 cm	17.5 cm
Minimum	32 cm	46 cm
Maximum	91 cm	110 cm
Confidence level (95%)	1.87	9.66
Kurtosis	2.96	2.75
Skewness	0.3	0.7

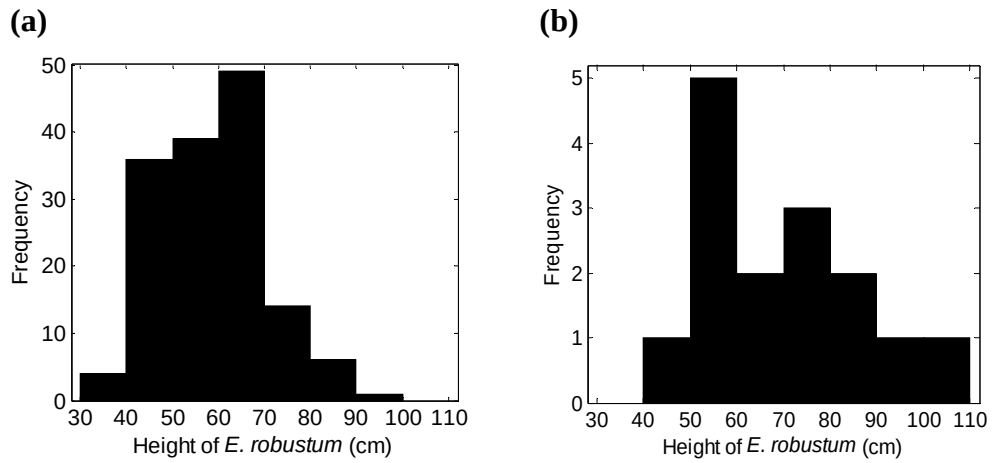

Figure 4.3 Histograms of (a) the distribution of 149 canopy height measurements from the preliminary survey; and (b) the distribution of heights of the 15 harvested plots. Note the different y-axis scales on each figure.

4.2.1.2 Standing mass

The distribution of vegetation mass (kg m^{-2}) across the 15 harvested sites is shown in Figure 4.4. The data have a skewness of 1.09, which gives an indication that the distribution was far from symmetrical, and a kurtosis of 3.38. The range in total

vegetation dry matter density was 1.13 – 3.01 kg m^{-2}, with 73% of sites having densities between 1 – 2 kg m^{-2}.

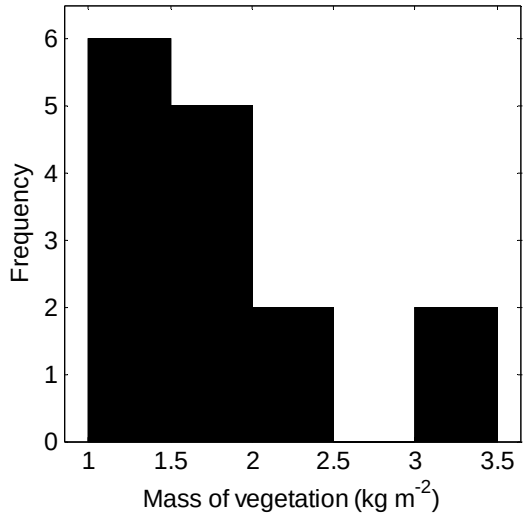

Figure 4.4 Histogram showing the distribution of canopy mass in the 15 harvested plots

4.2.2 Relating canopy height to vegetation mass and density

Since the distributions of height and plot canopy mass were both positively skewed, regression analyses were carried out to determine whether relationships existed between canopy height and the mass of vegetation in the plot, or the volumetric density of vegetation, as it would be easy to assume that the areas with the highest canopy are also the densest. These regression analyses are shown in Figure 4.5, where a poor (R^2 = 0.39) and negative relationship can be seen between the height and density of the harvested plots, and almost no relationship (R^2 = 0.05) exists between the canopy height and vegetation mass. Using the regression equations shown in Figure 4.5, the difference in vegetation densities predicted for the mean heights from the preliminary survey and the harvested plots was 0.5 kg m^{-3}, and the difference in vegetation masses predicted using the two heights was 0.09 kg m^{-2}.

Most of the 15 plots fell into the range of canopy heights 46 – 74 cm, with four particularly tall plots of 88, 89, 94 and 110 cm. The majority of the plots had vegetation masses in the range of 1.1 – 2.0 kg m^{-2}, although two plots had masses of 3.0 kg m^{-2} and heights of 52 and 61 cm. The 110 cm tall plot contained the lowest mass of vegetation, of only 1.1 kg m^{-2}, while the other three tall plots had

masses in the upper half of canopy masses: plots with heights of 88, 89 and 94 cm had masses of 1.8, 1.9 and 2.0 kg m^{-2} respectively.

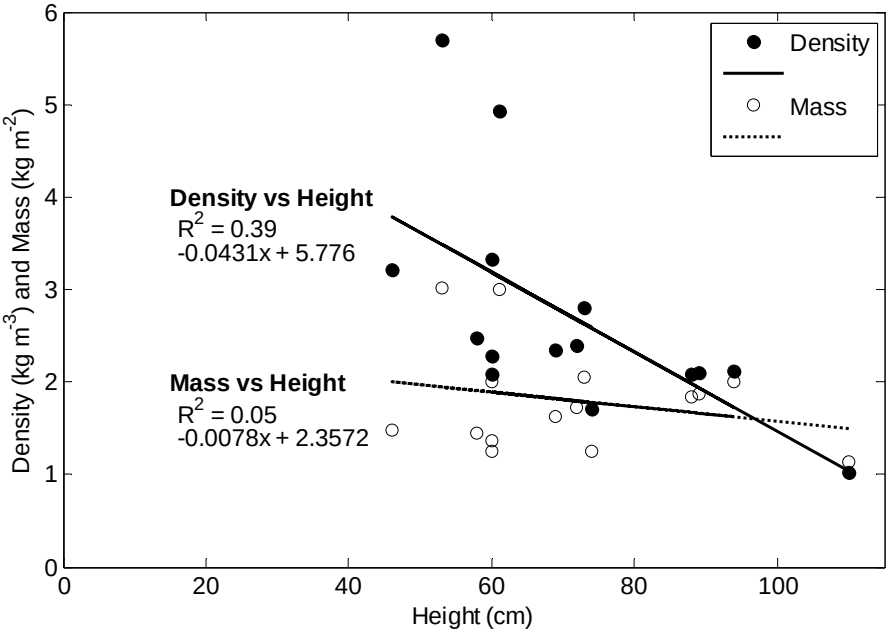

Figure 4.5 Regression analyses of plot height vs vegetation density (kg m^{-3}) and plot height vs vegetation mass (kg m^{-2}), with the R^2 values equations for each regression.

4.2.3 Canopy structure

The thickness of each vertical section used to divide the harvested canopy in the 15 plots is displayed in Table 4.3, and the heights of the sections are shown in Figure 4.6 . In most plots an air space existed between the peat surface and the bottom of the standing dead litter layer, where the only vegetation present was living stems. When harvesting the vegetation this section was incorporated into the lower section. The upper section was the thickest on average, although when the thickness of the airspace was included in the lower canopy (as occurred during harvesting) their average joint thickness (28.7 cm) was approximately equal to the average thickness of the upper section (29.2 cm). The middle section was generally thinner than the upper and lower sections, with an average thickness of 13.2 cm.

Table 4.3 Thickness (cm) of vertical sections within each profile. Refer to Figure 4.1 for location of plots

Plot	Air Space	Lower	Middle	Upper
1a	5	19	7	29
1b	10	22	6	20
1c	10.5	12.5	6	24
2a	4	11	4	42
2b	14	10	17	19
2c	6	14	25	29
3a	23	14	13	38
3b	0	40	30	40
3c	17	17	11	28
4a	18	14	13	44
4b	23	20	17	34
4c	2	25	5	14
5a	9.5	11.5	17	34
5b	12	20	12	25
5c	10	16	15	19

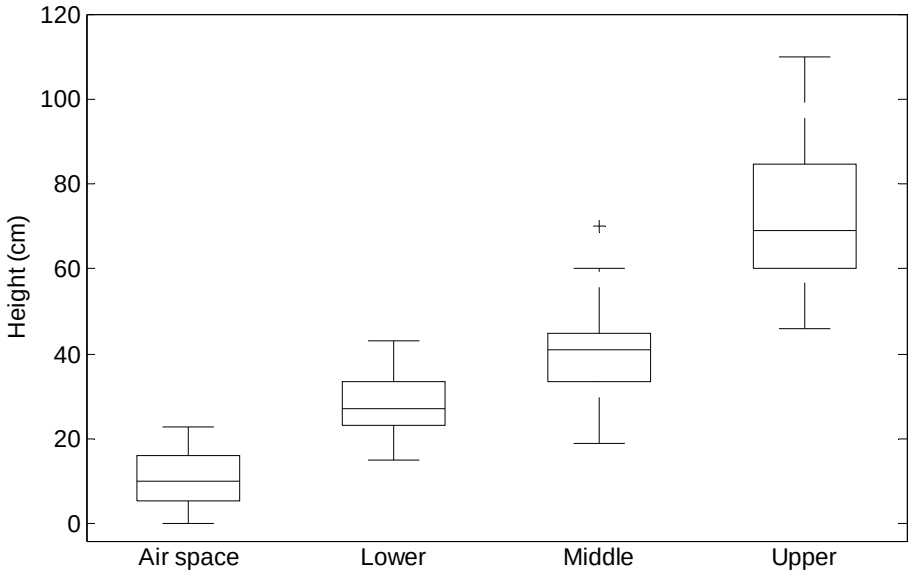

Figure 4.6 Boxplot showing the upper limit of canopy section boundaries in the 15 harvested sites. The horizontal lines in the centre of each box indicate the median height, the upper and lower edges of the boxes represent the 75th and 25th percentiles respectively, the whiskers extend to the most extreme data points and the plus symbol identifies an outlier.

A total of 27 kg of dry vegetation matter (DM) was harvested from the 15 sites. The mass of vegetation of each species and state from all plots combined is shown in Figure 4.7. On average, *E. robustum* constituted 85.6% of total DM: this was comprised of 19% live green, 15% live brown and 51% dead material. Green *E. robustum* dominated the upper section of the canopy, but became less prevalent lower in the canopy. Both live brown and dead *E. robustum* increased in density at lower levels in the canopy. The canopy mass was clearly dominated by the 0.81 ±0.25 kg m^{-2} of dead *E. robustum* in the lower portion of the canopy indicating the layer of standing dead litter. The average volumetric density of *E. robustum* in this layer was 4.5 kg m^{-3}.Two different qualities of litter were apparent in the standing dead layer: material from the upper portion of the layer was more intact, often with long sections of stem evident, while material from the lower part of the layer was much more physically degraded, in the most extreme cases crumbling to a thick dust (Figure 4.8). The air space which exists in the lower portion of most canopy profiles (Figure 4.6) is evidence of the rapid degradation of material at the base of the litter layer, which crumbles to dust and falls on the peat surface.

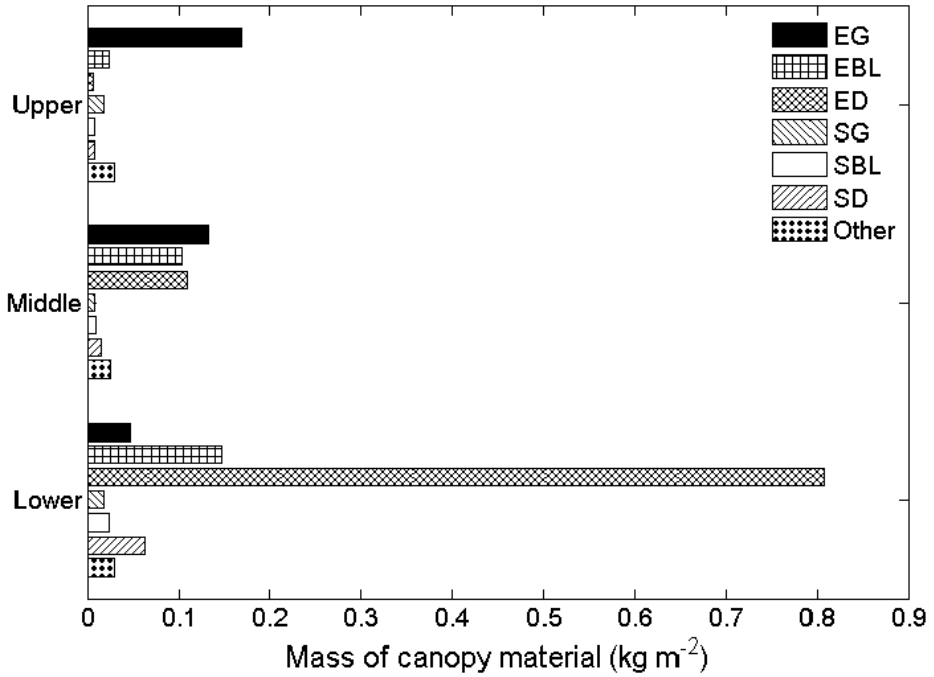

Figure 4.7 Average dry matter mass grouped by vegetation species and state in each vertical section of the harvested plots. S = Sedge (*B. teretifolia* and *S. pauciflorus*), E = *E. robustum*, G = live green material, BL = live brown material, D = dead material.

On average, the two sedge species accounted for 9.7% of the total canopy biomass. Live brown and dead sedge material increased in density with decreasing height.

The 'other' material was predominantly comprised of tangle fern (*Gleichenia dicarpa*) and made up 4.8% of the average canopy biomass. The mass of 'other' material was stable throughout the vertical canopy sections.

(a) **(b)**

Figure 4.8 The two different qualities of E. robustum litter (a) from the upper portion of the standing dead litter layer; and (b) from the lower portion of the layer.

4.3 Discussion

4.3.1 Canopy architecture

The *E. robustum* canopy is around 60 – 70 cm high on average, often with sedge stems growing higher than this. A strong gradient exists though the vertical profile of the canopy, with the upper section (starting at an average of 41 cm above the peat surface) dominated by 0.17 kg m^{-2} living green *E. robustum*, and the lower section dominated by 0.81 kg m^{-2} dead *E. robustum* (total *E. robustum* litter in the canopy was 0.92 kg m^{-2}). This dead material accumulates in a layer of standing dead litter which on average is present between 10 – 28 cm above the peat surface, and has an average volumetric density of 4.5 kg m^{-3}. Dead *E. robustum* litter accounts for 51% of the total canopy biomass. Two sedge species (*B. teretifolia* and *S. pauciflorus*) and 'other' plant material are also present in the canopy, accounting for an average of 9.7% and 4.8% of total canopy biomass, respectively.

The positively skewed distribution of canopy heights in both datasets is likely to reflect the characteristic 'wave crest' formation of the canopy. The canopy forms crests and troughs, where the vegetation appears to have been swept into formation by wind as shown in Figures 4.9 and 4.10. It is likely that the canopy heights which measured between 50 – 70 cm represent the general canopy height, while the heights which are greater than 70 cm represent wave crests. These crests appear to be quite dense, however the poor relationship found between canopy height and vegetation mass indicates that this is not necessarily the case.

4.3.2 Standing dead litter mass in other ecosystems

Table 4.4 lists the density of standing dead litter (SDL) in other ecosystems around the world. Most of these ecosystems are marshes or macrophyte assemblages on lake shores, and one is grassland. All of the ecosystems for which height was reported had much taller canopies than that of *E. robustum* at Kopuatai. Where a range in densities is reported, this is usually a reflection of seasonal variation. The mass of the standing dead litter layer at Kopuatai (0.81 kg m^{-2}) was quite high compared to these examples, with only Gallagher et al. (1980) and Lee (1989) reporting higher masses, at a Georgian salt marsh and a Chinese tidal shrimp pond, respectively.

Figure 4.9 Aerial view of the Kopuatai research site under construction, with examples of wave crests circled, running parallel to the white lines.

Figure 4.10 Close up view of a canopy wave crest

4.3.3 Ecosystem implications of canopy structure

The Waikato region of New Zealand frequently experiences hot summer periods with low rainfall and water deficits: conditions which would not be conducive to bog development in the northern hemisphere. It has been proposed that the restiad peat formers in these bogs (*S. ferrugineus* and *E. robustum*) have properties which support moisture conservation, enabling bogs to develop and survive in the Waikato. The large water holding capacity of restiad roots, and the dense *E. robustum* canopy, which is thought to lower the rate of evaporation, are two

properties which enable these bogs to endure warm dry seasons (Campbell and Williamson, 1997; Hodges and Rapson, 2010; McGlone, 2009). The density of plant material in the standing dead litter layer is likely to contribute to the ecosystem's ability to conserve water.

Table 4.4 Canopy height and litter mass data from studies looking at standing dead litter in different environments

Location	Species	Height (cm)	Density of standing dead litter	Source
Creek bank, Georgia, USA	*Spartina alterniflora*	-	~0.3 - ~1.10 kg m^{-2}	Gallagher et al. (1980)
High marsh, Georgia, USA	*Spartina alterniflora*	-	~0.10 - ~0.44 kg m^{-2}	
Salt marsh, Georgia, USA	*Juncus roemerianus*	-	~0.6 - ~1.4 kg m^{-2}	
Lake Neuchâtel, Switzerland	*Phragmites australis*	311	42 ± 12 shoots m^{-2}	Kuehn et al. (2004)
Lake Hallwil, Switzerland	*Phragmites australis*	305	47 ± 12 shoots m^{-2}	
Lake Tåkern, Sweden	*Phragmites australis*	215 ± 9	61 ± 8 stems m^{-2}	Granéli (1989)
Freshwater marsh, China	*Deyeuxia angustifolia*	-	~0.025 - 0.290 kg m^{-2}	Zhang et al. (2014)
Tidal shrimp pond, Hong Kong	*Kandelia candel*	336	0.96 kg m^{-2}	Lee (1989)
Native mixed-grass rangeland, Wyoming, USA	Grasses, forbes, sedges and half-shrubs	-	0.03 kg m^{-2}	Schuman et al. (1999)
Kopuatai bog, Waikato, New Zealand	***Empodisma robustum***	**71**	**0.81 kg m^{-2}**	**This study**

4.3.4 Canopy height

The fact that the mean canopy heights measured in the preliminary study and at the harvested plots were significantly different indicates that the harvested plots may not accurately represent canopy variation in the EC footprint. The mean height of the harvested plots was 12 cm (20%) higher than that of the preliminary survey. This difference in means was probably caused by four plots which had heights that were either close to or exceeded the maximum height measured in the preliminary survey (91 cm), significantly raising the mean of the 15 samples. These four plots were 3a, 3b, 4a and 4b, which had heights of 88, 110, 89 and 94 cm respectively.

There are several possible explanations for the differences in the heights measured in these samples. The bearings of the five transects were generated randomly and, as Figure 4.1 shows, three of the transects (1, 2 and 4) were located within 54° of each other. The eastern side of the footprint was therefore more heavily sampled than any other part, and the 144° separation between transects 1 and 3 meant that the southern side of the footprint was essentially unsampled. The fact that the four high measurements were made on transects located on opposite sides of the EC footprint (transects 3 and 4) suggests that the bias towards the eastern side was not the cause of the difference in heights measured, but rather that the tall plots happened to fall on discrete areas of high canopy which were not picked up in the preliminary survey.

The loop track which was used for the preliminary survey may have a bias towards low canopy heights. This could have been caused by a tendency to avoid tall canopy when forming the track, as it created an obstacle and it would be hard to maintain a track through very tall vegetation.

Continuing in the assumption that the height of the canopy varies in a similar way to the density and composition, the difference between the mean heights measured in the preliminary survey and the harvested plots may mean that the vegetation mass results from the harvested plots were not an accurate sample of the population. However, the very weak relationship between canopy height and vegetation mass (Figure 4.5) shows that, generally, vegetation mass does not change with canopy height. The height of the plot canopies was much more variable than the mass of vegetation in the plot, and those high volumetric

densities were a reflection of low canopy heights. Taking this into consideration, the observed bias in the harvested plots towards tall canopy heights is unlikely to have caused the vegetation mass to be over- or under-estimated. The assumption that canopy height could be used to gauge the variability of other canopy characteristics was not correct. Future research could use an improved strategy to more accurately gauge the variation in characteristics within the canopy population.

4.3.5 Implications of harvesting methods

It was important to quantify how the mass of different species and states of vegetation varied through the vertical profile of the canopy. The decision to visually estimate the bounds of each vertical section at each plot was made so that the data reflected the structure of each plot individually. An alternative approach would have been to use set height intervals from the peat surface, which would place the emphasis of the data on how high different types of material were. Since the focus of this project is the 'architecture' of the canopy and where different types of vegetation are located within this structure, it was important that the section bounds be relative to the specific architecture and level of development of each plot. Variation in the canopy heights and levels of development within the harvested plots means that the entire profile of some plots was shorter than what was classified as the 'lower' section of others. Thus, separating the canopy sections visually provided more powerful information on the structure of individual plots.

For comparison, an example of a plot which was harvested by separating vegetation by height intervals rather than a subjective analysis of canopy layers is shown in Figure 4.11. The plot was also located within the EC footprint (indicated by the green square in Figure 4.1), and with a height of 75 cm and a density of 4.03 kg m^{-2}, this plot was considerably denser than any harvested in the current study, and taller than the two plots which had relatively high densities. The vegetation at this plot was harvested in vertical increments of 20 cm. The standing litter layer straddled one of the divisions, and was thus divided into two sections: 0 – 20 cm and 20 – 40 cm (Figure 4.11).

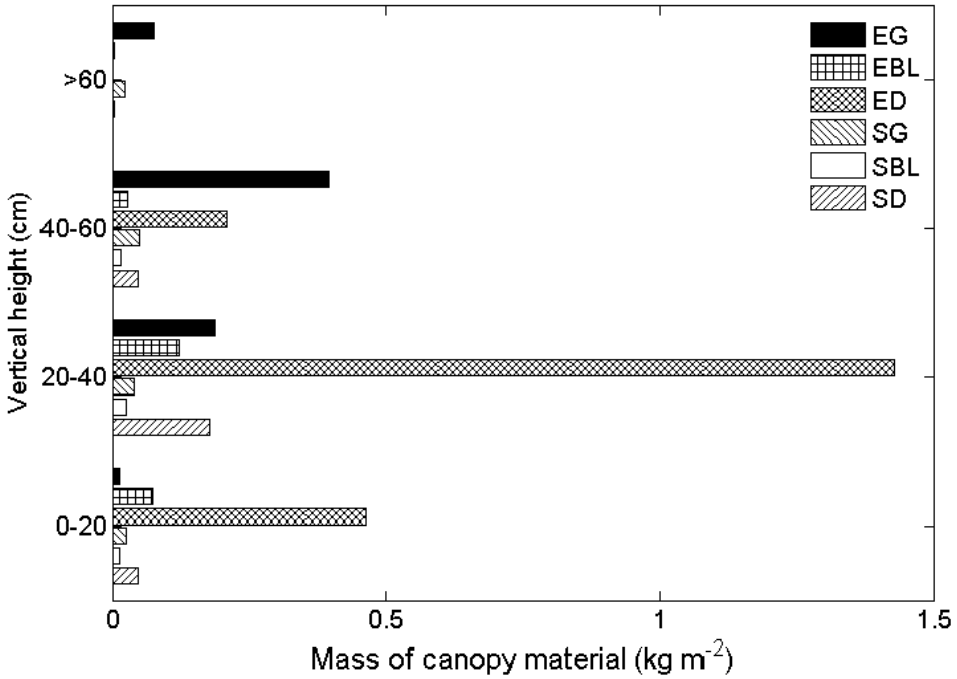

Figure 4.11 Average mass of vegetation canopy at a plot divided by height increments rather than canopy structure (Data from J. Goodrich, personal communication, 12 February 2013)

The height increment approach provided a more detailed analysis of the material present at specific heights in the canopy. However, the two methods ultimately provide the same information on canopy mass. In this study, the emphasis was on understanding the characteristics of the layers which make up the canopy architecture, so using these layers to divide the canopy worked well. The fact that corresponding sections in different plots had different thicknesses was taken into account when processing the data.

Chapter Five

Canopy Litter Respiration

Incubations were carried out in order to determine the rate at which CO_2 was produced by the microbial decomposition of *E. robustum* litter. A multiplexed flask system was built, that was able to measure CO_2 fluxes from eight litter samples in sequence. The moisture contents and temperatures of the samples could be controlled and measured accurately, providing insight into the effect these variables had on the rate of CO_2 emissions.

5.1 Methodology

5.1.1 System design

The incubation system (schematic diagram provided in Figure 5.1) consisted of eight sealable polypropylene containers ('Lock & Lock' Classic containers rectangle 180 ml, Product number HPL805), which were connected to a multiplexer (LI-8150, LI-COR, Lincoln NE), using Bev-a-line tubing. The multiplexer was in turn connected to an infrared gas analyser (LI-8100). Samples were sealed inside the containers, and the multiplexer sampled the headspace gas of each container in turn. The gas analyser measured the change in CO_2 concentration over the measurement period, and calculated the flux of CO_2 in $\mu mol\ kg^{-1}\ s^{-1}$ (i.e. per kg of litter dry mass). A ventilation pump was fitted into the multiplexer system, which vented those chambers not being actively sampled by the multiplexer to prevent CO_2 build up in the chambers.

The containers were housed in a (80 × 50 × 20 cm) lidded polystyrene box (Figure 5.2 (a)) so that the temperature of the containers could be regulated. Temperature was controlled by pumping water of known temperature through plastic tubing which was coiled around the bottom of the polystyrene box. To achieve temperatures above room temperature, water was heated in a water bath, before being pumped though the system (Pump model no. iL200P, 12V, Rule Industries). Colder temperatures were achieved by adding ice to water in a bucket before pumping it through the system. Two computer fans were located at one end of the polystyrene box to circulate air during experiments and prevent stratification. Thermocouples attached to the bottom of each container were

connected to a CR1000 datalogger. Figure 5.2 (b) illustrates the incubation experimental setup.

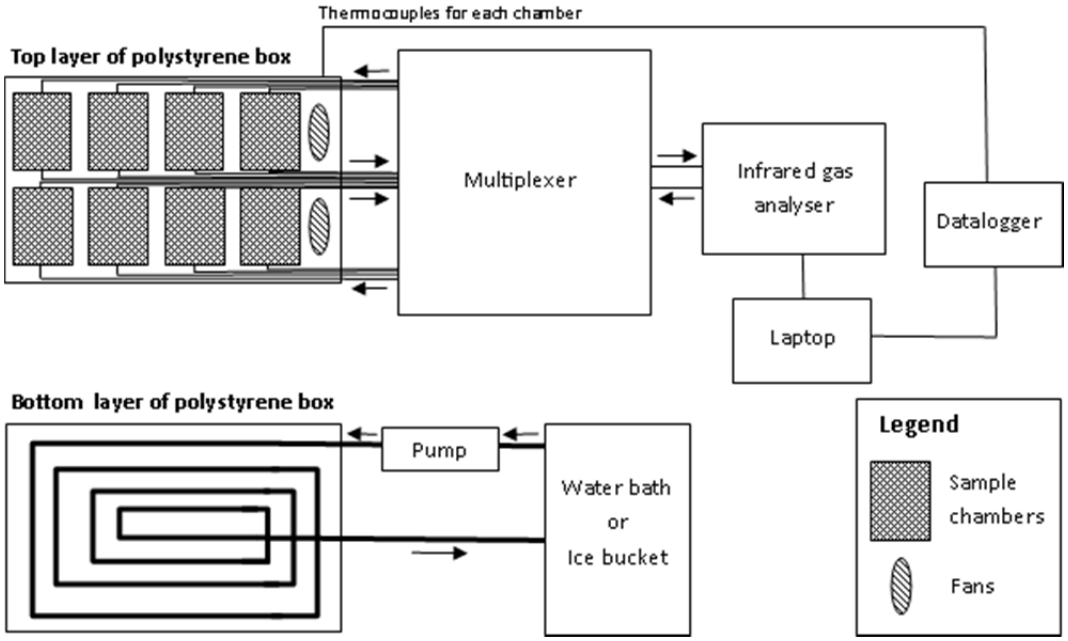

Figure 5.1 A schematic diagram of the incubation system, showing both the top (experimental) and bottom (heating/cooling) layers of the polystyrene box.

5.1.2 Samples

Canopy litter samples were gathered at a variety of locations over several months. Preliminary testing showed notable differences in both moisture uptake and CO_2 flux between different qualities of litter, so material from the upper and lower parts of the standing dead litter layer were treated as different populations. Litter samples were refrigerated (4°C) at field moisture until they were needed, at which point they were air dried for at least 24 hours.

5.1.3 Test for CO_2 pulse

Preliminary tests tracked CO_2 flux from moistened litter over periods of up to 30 hours to test for pulses of CO_2 emitted after wetting. The process used for the experiment that produced the results presented in Figure 5.4 was that moist litter samples from the lower canopy, taken from a bulk sample, were placed in five of the incubation chambers. These were left in sealed containers for four hours, then the CO_2 flux was measured at half hourly intervals for 19 hours.

(a)

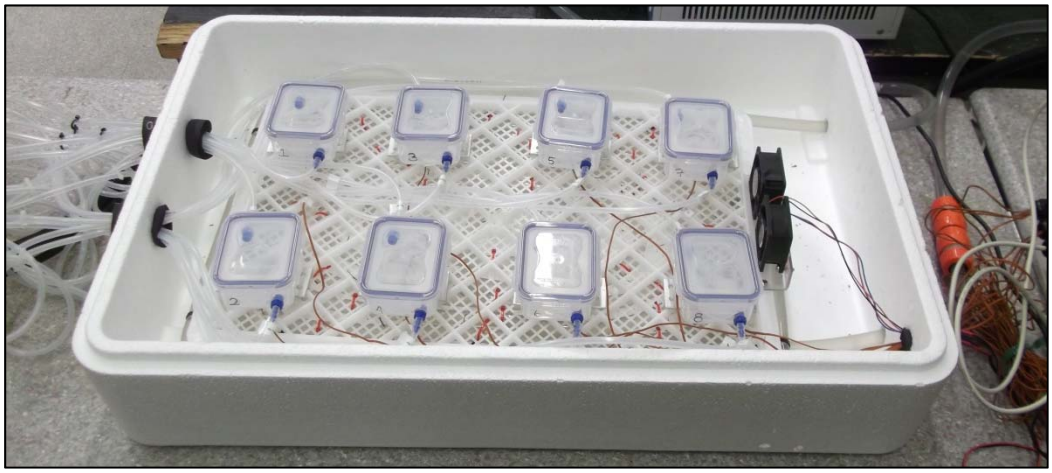

(b)

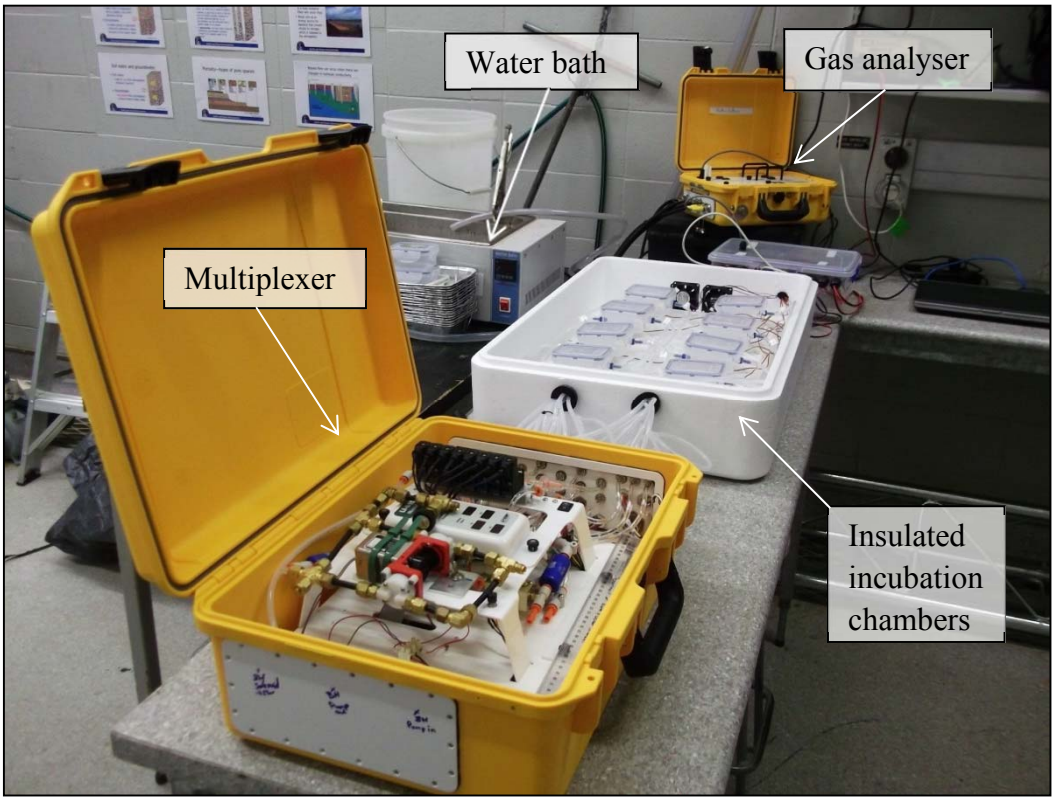

Figure 5.2 (a) The polystyrene box housing eight sealed chambers which held samples of litter. The chambers sat on a plastic shelf separating them from coiled plastic tubing containing temperature controlled water. Brown wires are thermocouples, which were attached to the base of each chamber. Two fans on the right side of the box circulated air to prevent stratification; (b) photo of the incubation setup. Each chamber was connected to the multiplexer which pumped gas samples to the infrared gas analyser. Water of known temperature was pumped from the water bath through the insulated box to control the temperature of the litter samples.

5.1.4 Moisture

Since decomposition rate is moisture limited, it was important to know the moisture content of the samples during incubations. Some experiments used

samples at a variety of different moisture contents, while others focused on samples that were saturated. All samples were initially air dried. All of the sampled material was saturated by being submerged it in deionised water for more than 60 minutes, using fine mesh and weights to prevent any material floating to the surface. The samples were then removed from the water, and surface water droplets shaken off. Saturated samples were taken at this point, by subsampling from the bulk sample, weighing the subsample and placing it in an air tight container to prevent moisture loss. Samples were left in sealed containers for at least 12 hours before experiments were carried out, to allow CO_2 emissions to stabilise. For experiments that required several different moisture contents, the bulk sample was placed in front of a fan and further subsamples taken as drying progressed. Samples were weighed both before and after incubation to determine water loss during the experiments, and again after being oven dried at 80°C for 12 hours, to determine the moisture content of the samples.

5.1.5 Experimental procedures

The experiments included below demonstrate the key findings of the incubation experiments as a whole. Initially, measurements were only taken when all of the containers were within 0.5°C of the target temperature. However, as this was quite time consuming, measurements were later made at approximately the target temperature, and the exact temperature of each chamber was recorded.

The sealed sample containers were not opened at any point between the beginning and end of an incubation experiment, however a ventilation pump was used to return the CO_2 concentration in the containers to ambient when they were not being actively sampled. This helped to ensure accurate CO_2 flux measurements, as it prevented the CO_2 concentration from becoming high enough to limit decomposition and helped to replicate field conditions.

5.1.5.1 Respiration from dry litter

It was important to establish whether respiration could be measured from dry litter in order to confirm that respiration is moisture limited, an assumption that would affect the experimental design of all following incubation experiments. Preliminary incubations had provided strong evidence that CO_2 emissions from dry litter were negligible, but control chambers were used throughout the experiments to reiterate this and provide a check on the other measurements. Two

control chambers were used in the experiment presented in Figure 5.5: one contained dry litter and the other was empty. Of the six remaining chambers, three contained saturated upper litter and three contained saturated lower litter.

5.1.5.2 Temperature response

The experiment presented in Figure 5.5 aimed to establish was the response of litter respiration rates to temperature change, and whether there was a hysteretic response to temperature variations. Initially, the system was heated to 25°C, then 30°C, before being lowered in approximately 5°C steps to 9°C. The temperature was then raised to 17°C. At each temperature step, the temperature was maintained for around one hour, with flux measurements taken repeatedly until they became stable. These stable measurements were then averaged over the chambers with replicated treatments.

5.1.5.3 Respiration from different litter types

This experiment also aimed to determine whether a significant difference in the respiration rate from the upper and lower canopy litters could be measured. This comparison was achieved by including three replications of each litter type in the experiment. An analysis of covariance (ANCOVA) was carried out using the programme SAS 9.3. A general linear modelling procedure was used to determine whether differences between the mean fluxes measured at each temperature from the different treatments were significant. A variance components procedure (REML method) was used to determine the variance between different treatments and between replicate measurements from the same chamber.

5.1.5.4 Effect of moisture content

Two incubation experiments were carried out to produce the data presented in Figure 5.6, each of which focused solely on the influence of moisture content on respiration rate for one litter type. Each experiment included four different moisture treatments: one saturated, two at different stages of drying and one air dry. These four treatments were then repeated in the same experiment, using the eight chamber system. The system was cooled to 5°C, then the temperature was raised in approximately 5°C intervals until it reached 35°C. A flux measurement was taken from each chamber at each temperature increment, and averaged across samples with the same moisture contents.

5.1.5.5 Compiled data and model fitting

A compilation dataset was created with all of the saturated litter data from the experiments carried out with the incubation setup. The Lloyd and Taylor (1994) model (Equation 5.1, a modified version of the Arrhenius model now commonly used to model soil respiration) was fitted to the two datasets, as it was found to describe the data well.

$$R = R_{\mathrm{Ref}}\, e^{E_0\left(\frac{1}{T_{\mathrm{Ref}} - T_0} - \frac{1}{T - T_0}\right)} \qquad \textbf{(5-1)}$$

Where R is the rate of respiration; R_{Ref} is the rate of respiration at a reference temperature (commonly R_{10}, at 10°C); E_0 is an empirical coefficient which is similar to the activation energy of the Arrhenius equation; T_{Ref} is the reference temperature associated with R_{10} (K); T_0 is the lowest temperature respiration occurs at (K); and T is temperature being investigated (K) (Luo and Zhou, 2006).

In the Lloyd and Taylor model, the effective activation energy (E_0) is allowed to vary depending on the temperature, with lower activation energies occurring at higher temperatures. The parameter R_{10} describes the rate of respiration at 10°C, and is commonly used to draw comparisons between datasets. The E_0 parameter is thought to be 308.56 K in a wide variety of ecosystems, so this value is commonly used in the Lloyd and Taylor equation (Lloyd and Taylor, 1994). However it is also possible to calculate an E_0 value which is specific to a dataset. Here, the analysis was performed twice, once using E_0 = 308.56 K and once using an E_0 value that was calculated from the data. Fitting was performed using the "fit" function in MATLAB R2012a (The MathWorks Inc., Natick, MA, 2012).

5.2 Results

5.2.1 Moisture contents of saturated litter

The moisture contents of 16 saturated litter samples (eight of each litter type) were compiled, and are presented as boxplots in Figure 5.3. A distinct difference can be seen between the two different qualities of litter: the lower litter, which was more physically degraded than the upper litter, held an average of three times more water than the upper litter. The maximum moisture content of the upper litter (183.2%) was half the minimum moisture content of the lower litter (366.2%). A two-sample t-test was used to confirm that mean moisture contents of the saturated litter samples were significantly different ($p < 0.001$).

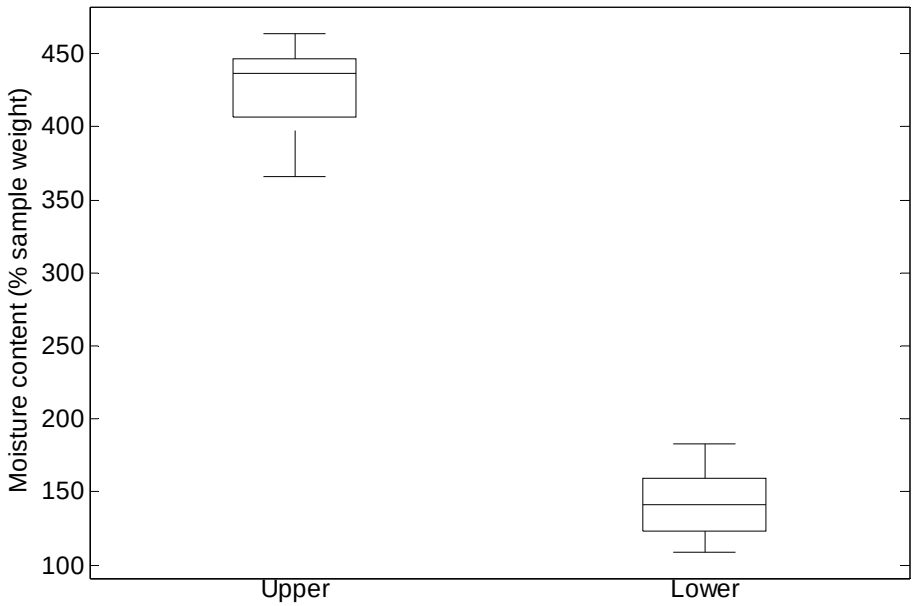

Figure 5.3 Moisture contents of saturated upper (n = 8) and lower (n = 8) canopy litter samples. The horizontal line in the centre of each box indicates the median of the dataset, the upper and lower edges of the boxes represent the 75th and 25th percentiles respectively, and the whiskers extend to the most extreme data points.

5.2.2 CO_2 pulse from moistened litter

The change in CO_2 flux from moistened lower canopy litter over a period of 19 hours (beginning four hours after the litter was wetted) is shown in Figure 5.4. Data shown are the average of the five litter samples. CO_2 flux can be seen to decrease from 1 μmol kg^{-1} s^{-1} to 0.6 μmol kg^{-1} s^{-1} over the first 15 hours. At this point, the flux stabilised and remained constant for the last four hours of the experiment. The initial pulse of CO_2 from microbial respiration immediately after wetting informed the methodology of the rest of the experiments, as moistened

litter samples were left overnight (a minimum of 12 hours) before experiments were conducted.

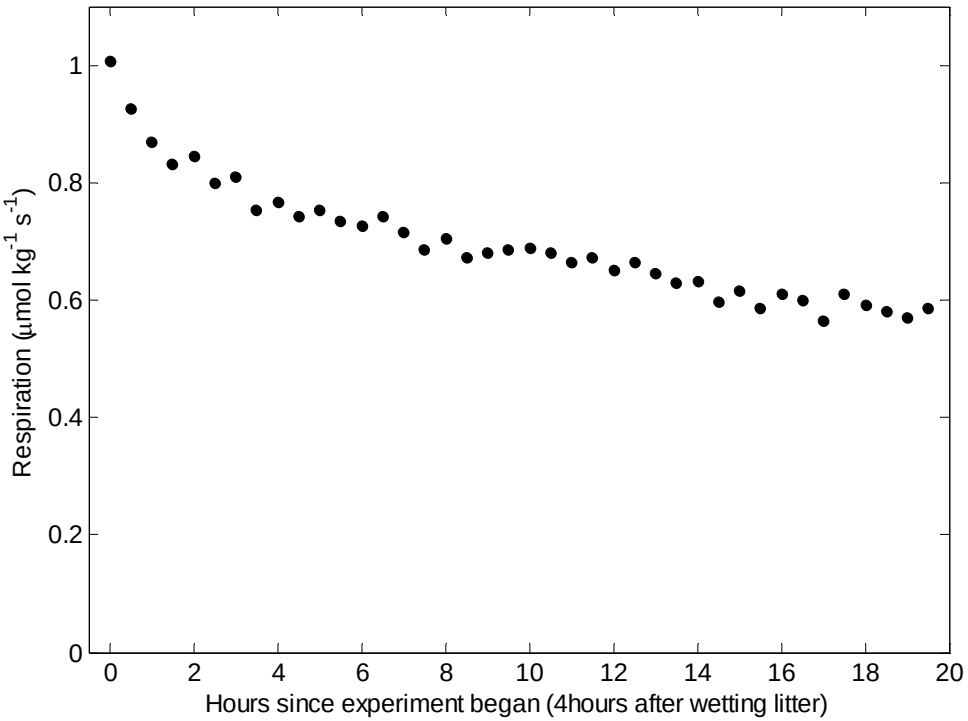

Figure 5.4 CO_2 flux from moistened lower canopy litter (averaged over five chambers) over a 19 hour period at ambient temperature (18-19°C). The litter was wet four hours before this experiment began.

5.2.3 Measuring respiration from litter

Figure 5.5 shows the respiration rates measured over a range of temperatures in experiment 1 (described in Section 1.3.1). A clear temperature response can be seen in the moist samples of upper and lower litter, with respiration rates increasing at higher temperatures. Hysteresis was not found to be an important factor in the temperature response of litter respiration, due to the closeness of the measurements made while heating and cooling the system.

The analysis of covariance allowed the differences in the mean respiration rate of each treatment to be assessed at each temperature. The p-values produced by this analysis are presented in Table 5.1. No significant difference was found between the mean fluxes measured from the empty and dry chambers at any temperature, which confirms the hypothesis that dry litter produces a negligible CO_2 flux. A significant difference ($p < 0.05$, and often $p < 0.01$) between fluxes from the moist litter samples and the empty and dry chambers was measured at every temperature. A significant difference ($p < 0.05$) was found between fluxes from the upper and

lower litters at all but two temperatures: 15°C and 17°C. Lower litter respired at higher rates than the upper litter at all measured temperatures. The difference in respiration rates became larger at higher temperatures, indicating that lower litter has a greater potential to respond to increased temperature. The finer points of the relationship between temperature and respiration rate are the focus of section 5.25.

Table 5.1 Results of the analysis of covariance, indicating the significance of the difference between the least squares means between each of the treatments. The sequence of columns in the table follows the experimental progression of Figure 5.5. p-values which indicate a difference that is significant at the 0.05 level are denoted with *, those significant at the 0.01 level are denoted with **, and those significant at the 0.001 level are denoted with ***.

Treatments	**25°C**	**30°C**	**24°C**	**20°C**	**15°C**	**9°C**	**17°C**
Empty & Dry	0.374	0.481	0.242	0.531	0.770	0.273	0.663
Empty & Lower	0.002 **	0.001 **	0.001 **	0.002 **	0.006 **	0.006 **	0.004 **
Empty & Upper	0.014 *	0.009 **	0.004 **	0.008 **	0.023 *	0.034 *	0.012 *
Dry & Lower	0.001 **	0.001 **	0.000 ***	0.001 **	0.004 **	0.002 **	0.003 **
Dry & Upper	0.006 **	0.005 **	0.002 **	0.004 **	0.017 *	0.009 **	0.008 **
Lower & Upper	0.018 *	0.009 **	0.009 **	0.021 *	0.059	0.038 *	0.110

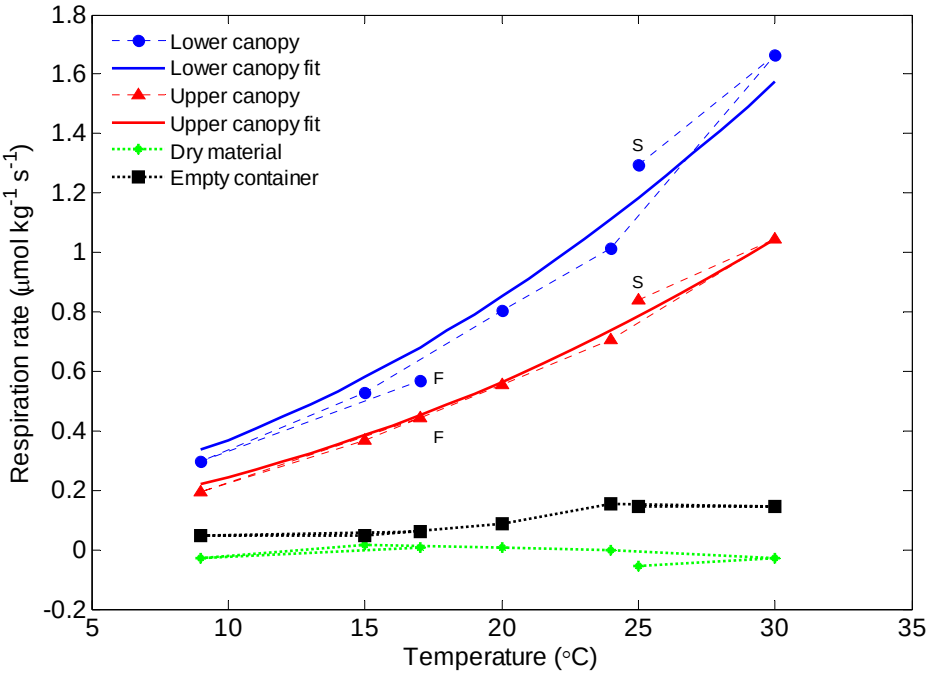

Figure 5.5 Litter respiration rates over a range of ascending and descending temperatures. The dry litter and empty chamber serve as controls. 'S' indicates the start of the experiment, at 25°C, after which the system was heated to 30°C, then lowered to 9°C in approximately 5°C intervals. The temperature was then raised again to 17°C, where 'F' marks the finish point. Symbols for the moist litter samples represent the average of three repeated measurements of each of three different samples (except 17°C, which is the average of two measurements). Markers for the dry litter and empty container represent the same number of measurement at each temperature, but from only one sample. Dashed lines indicate the progression of temperature change. Solid lines represent the Lloyd and Taylor model fitted to moist litter samples.

5.2.4 The effect of moisture content on respiration rates

The effect that moisture content had on respiration rates from upper and lower litter is shown in Figure 5.6. The average moisture contents of the upper and lower litter samples used in the experiments that contributed data to Figure 5.6 are presented in Table 5.2. Samples were dried to different extents in order to achieve a range of moisture contents. Again, the difference in ability of the two litter qualities to hold water is evident in these data.

Figure 5.6 shows that there was a strong similarity between the respiration rates of the drying samples for both the upper and lower litters, while the saturated samples produced notably higher respiration rates than those which were drying.

Again, the air dried samples gave a good indication of the error around measuring a zero flux.

As shown in Figure 5.6, a large decrease in respiration rate occurred at 30°C for the upper litter: respiration rates of the partially dry litter samples at 30 and 35°C were well within the bounds of the 'negligible' fluxes measured from the dry canopy material. This may have been caused by the upper litter material drying out as the experiment progressed, which will be considered further in the discussion.

Table 5.2 Average moisture contents (± standard deviation) of upper and lower litter used in experiments for data presented in Figure 5.6.

	Average Moisture Content (%)			
Litter type	**Saturated**	**Drying Stage 1**	**Drying Stage 2**	**Air Dry**
Upper	136.6 (± 12.3)	109.2 (± 3.4)	84.5 (± 13.0)	9.7 (± 0.02)
Lower	438.4 (± 10.7)	228.8 (± 0.9)	114.4 (± 7.9)	8.7 (± 2.4)

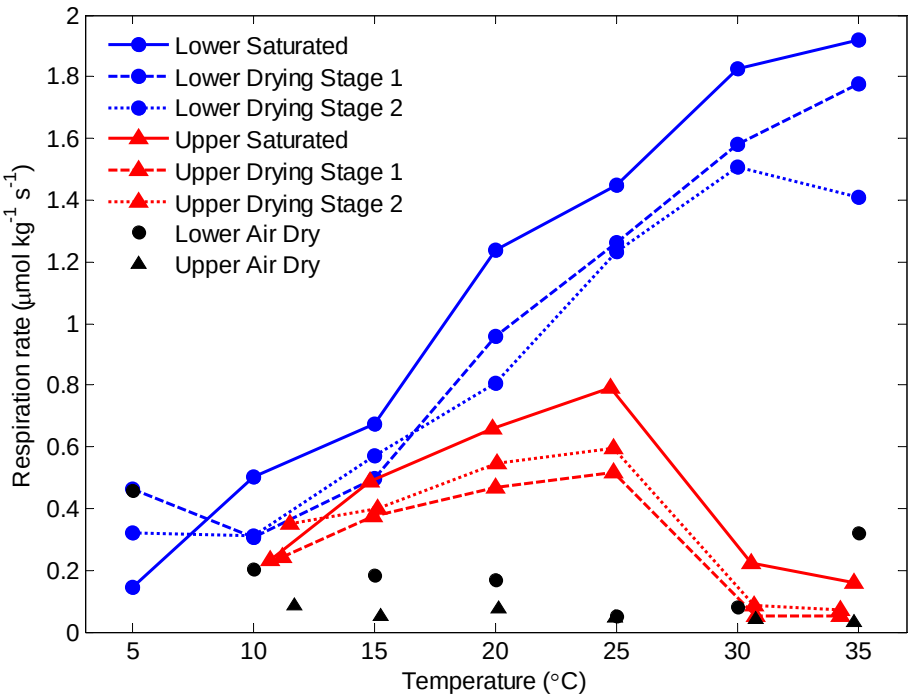

Figure 5.6 Respiration rates from upper and lower litter samples with different moisture contents over a range of temperatures.

The relationship between moisture content and respiration rate for the data in Figure 5.6 at 20°C is shown in Figure 5.7. A hypothesised relationship is shown by the dashed line. This relationship shows insignificant respiration until around 50% moisture content. At this point the rate of respiration rose steadily until a moisture content of around 150%, after which the rate of respiration plateaued, rising only slightly as the moisture content increased to over 400%. At some point, respiration presumably becomes inhibited by saturation, but this point was not reached in any of the experiments. The lower litter fits well to this hypothesised relationship. The upper litter would be expected to plateau at a lower respiration rate, but this is not evident from the range of moisture contents imposed.

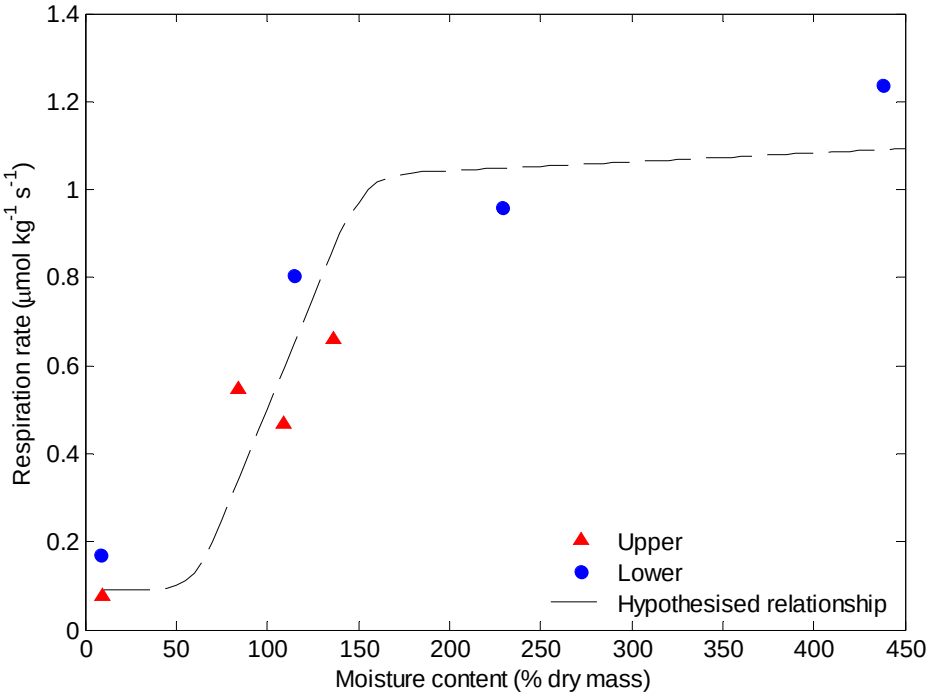

Figure 5.7 Relationship between moisture content and respiration rate at 20°C for the upper and lower litter, with the hypothesised relationship shown.

5.2.5 Temperature response of litter respiration

The compiled data for all incubations of saturated litter provided a clear impression of the pattern of respiration change with temperature, and good fit with the Lloyd and Taylor function (Figure 5.8). In Figure 5.8 (a) the E_0 parameter has been calculated from the data, while in (b) the standard E_0 value of 308.56 K was used to generate the Lloyd and Taylor fit. In both figures, a clear difference in respiration rates can be seen between the upper and lower litter samples. Two data points for the upper litter at 30 and 35°C were removed from

the Lloyd and Taylor fit shown in both (a) and (b), as they appear to be outliers. These are the same data that can be seen in Figure 5.6, with abruptly reduced respiration rates at temperatures greater than 25°C. The remaining data point at 30°C was from a separate experiment with the upper litter, and does not appear to be an outlier. This point was included in the Lloyd and Taylor fit.

The E_0 values calculated for the data (Figure 5.8 (a)) were 275.86 K for the lower litter and 319.15 K for the upper litter. The Lloyd and Taylor model fits very well to the respiration data both when the standard E_0 value is used and when it is calculated. This is evidenced by the very high R^2 values of 0.94 (E_0 calculated) and 0.93 (standard E_0) for the lower litter, and 0.95 in both cases for the upper litter.

The different E_0 values used in Figure 5.8 (a) and (b) influenced the R_{10} value of the lower litter more than the upper litter, as the E_0 value of the upper litter was closer to the standard value. The R_{10} value for the lower litter with E_0 calculated was 0.44 (± 0.1) μmol kg^{-1} s^{-1}, and with standard E_0 the R_{10} was 0.38 (± 0.26) μmol kg^{-1} s^{-1}. The upper litter had an R_{10} value of 0.24 (± 0.05) μmol kg^{-1} s^{-1} when E_0 was calculated and 0.25 (± 0.02) μmol kg^{-1} s^{-1} when the standard value was used. The 95% confidence intervals of the R_{10} values of the upper and lower litter do not overlap in either case.

(a)

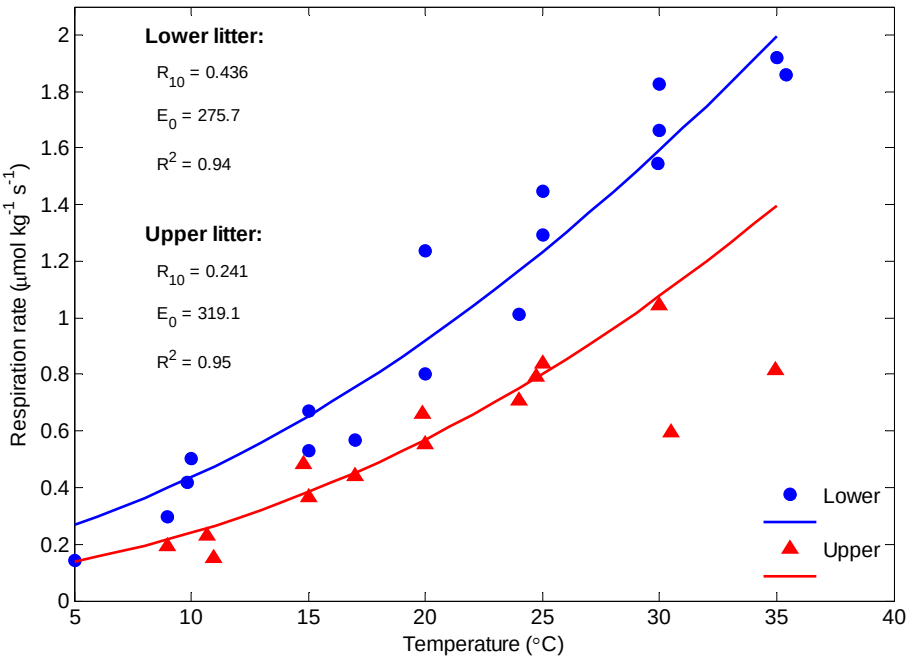

(b)

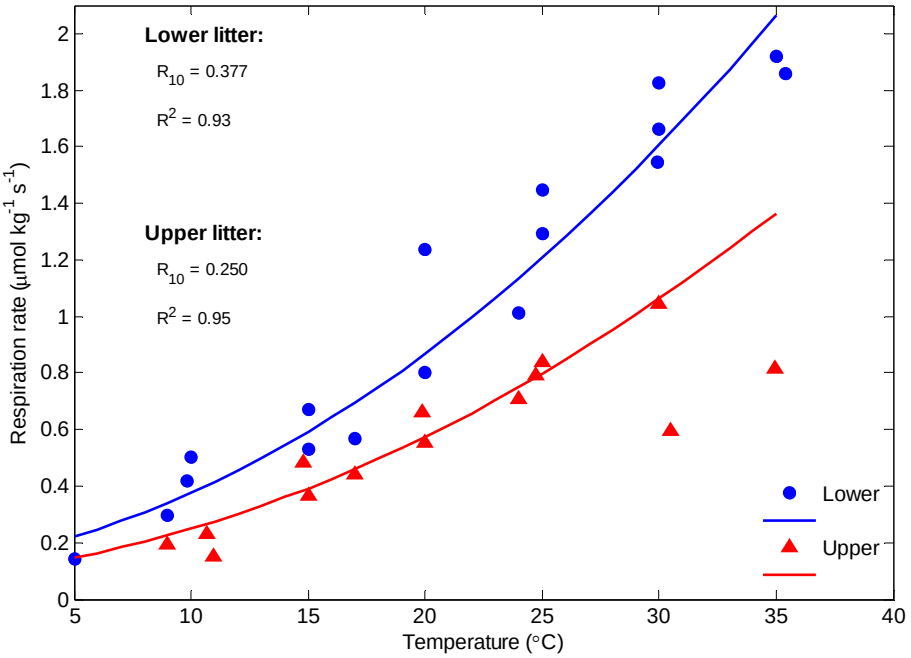

Figure 5.8 Compiled respiration data from multiple experiments. The solid lines show a Lloyd and Taylor fit to each dataset, excluding the outliers at 30 and 35°C. In (a) the Lloyd and Taylor function was fitted using an E_0 value calculated using the data, while in (b) the standard E_0 value of 308.56 K was used. The R_{10} and R^2 values for each dataset are shown on the graph.

5.3 Discussion points

5.3.1 Differences between litter qualities

Two different qualities of *E. robustum* litter have been observed in the canopy (Chapter Four): litter from the upper portion of the standing dead layer, and the more physically degraded litter from the lower portion of the canopy. When wetted, these two litter types had significantly different rates of respiration. The lower litter had consistently higher respiration rates than the upper litter. The lower litter had greater temperature sensitivity than the upper litter, which was modelled in the Lloyd and Taylor function.

The lower rate of microbial respiration of the upper litter implies that the rate of decomposition of *E. robustum* litter increases as the litter breaks down. This is likely to be a result of physical and chemical changes that take place as degradation occurs. For example, it is common for reed species with litter from different parts of the plant structure (for example leaves, stems and culms in species such as *Phragmites australis*) to have different rates of decomposition (Kuehn et al., 2004), however, this is at least partially due to the chemical and structural differences which suit the different plant parts to their individual purpose. In the case of *E. robustum*, the standing dead litter is comprised of only the plant stem, and differs only in age.

Kuder et al. (1998) carried out an analysis of the chemical composition of *E. robustum* and *S. ferrugineus* from Kopuatai and Moanatuatua bogs, and determined that these species contain high proportions of phenolic acids and tannins which, among other influences, increases their resistance to decay. This decay resistance is caused by both the natural inertness of tannin and lignin, and their tendency to inhibit microbial activity. Lignin has hydrophobic properties, and is one of the most slowly decomposing components of dead vegetation: high lignin concentrations are known to inhibit litter decomposition (Girisha et al., 2003; Kuder et al., 1998). Kuder et al. (1998) also found that the xylosan (a molecule produced through the thermochemical decomposition of wood) to glucosan (polysaccharides that produce glucose through hydrolysis, such as cellulose and glycogen) ratio of the plants at Kopuatai suggested that the process

of polysaccharide breakdown was related to the process of disintegration of the plant litter.

The chemical changes that occur during the decomposition of plant litter and the physical degradation of the litter create conditions which may promote further decomposition. Kuehn et al. (2004) related the proportions of arenchymous (spongy, large pored) and sclernchymous (mechanically supporting) tissue in different parts of *P. australis* litter to the water absorption properties of this litter. It is the ability of the litter to absorb water that ultimately determines the colonisation of the litter by decomposing microbes and the subsequent rate of litter decomposition. It is likely that the initial rate of *E. robustum* litter decomposition is limited by the chemical composition of the litter which promotes recalcitrance, one of the features that allows this species to act as a primary peat former. As decomposition occurs, the changing litter chemistry and physical degradation of the litter increase the potential of microbes to act as decomposers and also increase the water absorption potential of the litter material, promoting decomposition. Future research into the microbial assemblages present in the two different qualities of litter would help to confirm this hypothesis.

5.3.2 Temperature response of litter respiration

A positive relationship between respiration rate and temperature was found to exist for *E. robustum* litter from Kopuatai bog. The correlation between temperature and the rate of respiration is widely accepted for litter (Fierer et al., 2005; Howard and Howard, 1979; Kuehn et al., 2004; Salah and Scholes, 2011), as well as in soils (Lloyd and Taylor, 1994) and a wide variety of other contexts. The temperature response seen in the incubation experiments carried out in this study were therefore consistent with expectations.

The temperature responses of both types of *E. robustum* litter were explained well by the Lloyd and Taylor function (Lloyd and Taylor, 1994). The Lloyd and Taylor function produced R_{10} values of 0.24 (± 0.05) μmol kg^{-1} s^{-1} (upper litter) and 0.42 (± 0.1) μmol kg^{-1} s^{-1} (lower litter) when E_0 values were fitted. The calculated E_0 values are used here as they produce a slightly better fit for the lower litter data, which is advantageous for using the fit as the basis of a litter respiration model (Chapter Six). However, the different methods of determining the E_0 parameter have little influence on the results presented in Figure 5.8. The most significant

impact of calculating the E_0 parameter from the data is a 0.06 μmol kg^{-1} s^{-1} increase in the R_{10} of the lower litter.

5.3.3 Rates of respiration from different litter types

The emission of CO_2 from respiring *E. robustum* litter can be compared to that from different species and ecosystems. A wide range of litter respiration rates have been reported in the studies listed in Table 5.3. At 15°C, the standing dead litter from Kopuatai emits between approximately 0.3 μmol kg^{-1} s^{-1} (upper litter) and 0.6 μmol kg^{-1} s^{-1} (lower litter). Most of the respiration rates reported in Table 5.3 for standing dead litter are considerably higher than those found for *E. robustum* litter in the current study, ranging from 5.6 – 22.2 μmol kg^{-1} s^{-1} with the exception of the *Lythrum salicaria* stem litter and *P. australis* culms, which have respiration rates of 2.25 and 0.86 μmol kg^{-1} s^{-1}. Otherwise, the respiration rates of *E. robustum* litter types are most similar to that of the forest floor in Australian Eucalypt forests and Polish beech-pine forests.

5.3.4 Moisture dependence

The availability of moisture has a strong influence on the respiration rate of *E. robustum* litter. The results of experiments using litter samples with different moisture contents suggests that the relationship between moisture availability and litter respiration rate forms a steep-sided plateau, such as that presented in Figure 5.7. In this hypothesised relationship, respiration rates are negligible in dry litter until a threshold moisture content is reached. At this point, the rate of respiration rises steeply before plateauing and rising only slightly as the maximum water holding capacity is approached. This is based on observations that the lower litter has similar respiration rates for a wide range of moisture contents above an apparent threshold separating these rates from negligible fluxes.

This hypothesised relationship can be seen more clearly in litter from the lower portion of the canopy than the upper. The upper litter also seems to have a threshold moisture content between negligible respiration rates when moisture is limited and respiration rates which are relatively constant when adequate moisture is available. The plateau effect that is seen in the lower litter is not as clear in the upper litter. This may be because the upper litter was unable to absorb more than 130% moisture content. Once again, the difference in the ability of the two litter types to take up moisture is probably a result of the changes in the structural and

chemical properties of the litter as it decomposes. If the upper litter was able to take up more water, the resulting respiration rates may well be similar to that of the lower litter.

The very low respiration rates observed for the upper litter samples at high temperatures (Figures 5.6 and 5.8) may be an example of this plateau-threshold being reached. In the experiment which produced these data, the litter samples were heated from 5 – 35°C. It is likely that the sudden decrease in respiration rate above 25°C occurred because the upper litter samples, which all contained less than 136% moisture content, dried out enough through ventilation of the chambers to push them across the moisture threshold to negligible respiration rates.

5.3.5 Implications for using these data for modelling respiration

The good fit between the litter respiration data and the Lloyd and Taylor function creates an opportunity to model litter respiration for temperatures within the range of those included in the experiments. However, it is important to identify limitations in the ability of these data to accurately represent litter respiration in the field. The observed moisture content threshold of the upper litter is an example of this: the above observations imply that the upper litter dries more rapidly than the lower litter. If this is correct, then the immediacy of respiration rate change across this threshold, and the difference in the rate of this change between the litter types would have significant implications for modelling litter respiration in the field. These factors should be incorporated into a model of litter respiration to ensure that the duration of litter respiration is not overestimated.

During the incubation experiments moistened litter was left for at least 12 hours after wetting before the respiration rate was measured. The observed peak fluxes which occur immediately after wetting are likely to occur in the field. These pulses demonstrate the adaptation of the microbial populations of the standing litter to immediately begin metabolising litter on wetting, ensuring that they are able to benefit from even small wetting events (Kuehn et al., 2004). In the present study, stabilised respiration rates, measured after the initial flush of CO_2 from the litter, were used to determine the temperature and moisture sensitivity of the litter. However, these 'steady state' fluxes likely underestimate the full response of litter to wetting.

Table 5.3 A review of litter respiration rates reported in the literature for a variety of ecosystems

Environment	Species	Litter type		Respiration rate (µmol kg^{-1} s^{-1})	Temperature (°C)	Study
Marsh, Sanjiang Plain, China	*Deyeuxia angustifolia*	Standing litter	Culms	6.94 - 11.1	15	Zhang et al. (2014)
			Leaves	13.9 - 22.2	15	
Beech-Pine forest, Poland	-	Forest floor litter		0.71 - 0.75	20	Laskowski et al. (1994)
Eucalypt forest, southwest Australia	*Euculyptus marginora*	Partially decomposed forest floor leaf litter		0.24	Average (temperature adjusted)	O'Connell (1990)
Eucalypt forest, southwest Australia	*Euculyptus diversicolor*	Partially decomposed forest floor leaf litter		0.39	Average (temperature adjusted)	Welsch and Yavitt (2003)
Freshwater marsh, New York, USA	*Lythrum salicaria*	Standing stem litter		2.25		
Littoral zones of lakes Neuchâtel and Hallwil, Switzerland	*Phragmites australis*	Standing litter	Leaves	5.63	10	Kuehn et al. (2004)
			Sheaths	6.39	21	
			Culms	0.86	14	
Kopuatai bog, New Zealand	***E. robustum***	**Standing litter**	**Upper**	**0.24**	**10**	**This study**
			Lower	**0.44**	**10**	

*Malcolm et al. (2009) also reported respiration rates for Pine forest floor litter in the Pennsylvania, USA. However, their reported respiration rate was 40 µmol $hr^{-1}mg^{-1}$ at 17°C, which is equal to 11,100 µmol kg^{-1} s^{-1}, which is clearly incorrect.

Chapter Six

Modelling Canopy Respiration

Understanding the ecosystem carbon flux at Kopuatai requires the partitioning of carbon into specific sources and sinks. This chapter describes the development of a simple model which was used to estimate the amount of CO_2 emitted from the decomposition of standing dead litter at Kopuatai. This litter respiration is the aboveground heterotrophic respiration (HR_a) (Figure 2.2). Finally, the proportion of total ecosystem respiration (ER) sourced from HR_a is estimated.

6.1 Methodology

6.1.1 Wetness Sensors

As litter decomposition has been shown to be moisture limited (Chapter Five), the spatial and temporal variation of water in the canopy needed to be quantified before CO_2 fluxes could be extrapolated to the canopy scale. This was achieved by establishing electronic wetness sensors in the canopy to log the presence of moisture at various heights, and using the sensor data to understand the moisture regime of the canopy. This information was used both as an input to the CO_2 flux model and to test a simple method to predict canopy wetness state based on time and rainfall.

6.1.1.1 Leaf wetness sensor construction

Leaf wetness (LW) sensors are simple electronic circuits which can be used to determine whether water is present in the canopy. LW sensors were constructed following the design of the Campbell Scientific model 237 leaf wetness sensor, using a commercially available grid (Hobby Boards, SKU: LWS1-R2-B). This printed-circuit sensor with interlacing gold-plated copper spokes (Figure 6.2 (a)) acted as a variable resistor in the circuit. The presence of moisture on the flat surface of the sensor bridged the spokes, lowering the resistance. The resistance was used as an indicator of the degree of wetness in the canopy. The surface of the sensor represented the surface of *E. robustum* stems. The sensors originally had gold print on both sides, but the print was sanded off one side of each board in order to prevent water drops accumulating on the underside of the sensor affecting the measurement.

The electronic circuit illustrated in Figure 6.1 was constructed, with the variable resistor (R_s) representing the LW sensor. As the wetness sensors needed to be waterproof and durable, rubber moulds were constructed to encase the body of the sensor in epoxy. This ensured that the electronic circuit was waterproof, with only the sensing grid left exposed. Holes were drilled in the epoxy to enable it to be mounted with cable ties in the canopy.

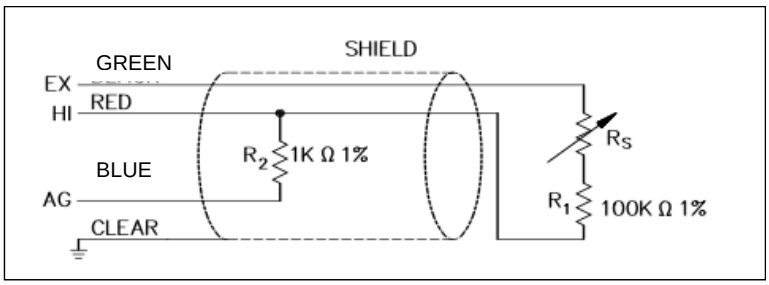

Figure 6.1 Schematic diagram of the electronic circuit used in the leaf wetness sensors (Source: Campbell Scientific Inc., Leaf Wetness Sensor Model 237 Instruction Manual, revision 7/10, 2010)

The surface of the circuit board was coated in one thin coat of 'sateen snow' latex paint (tint formula 42347, Wattyl NZ Ltd) (Figure 6.2 (b)), which has a porous surface that draws water droplets out over the sensor surface, maximising the spread of each drop. Experiments with painted and unpainted sensors showed that this prevented water from beading and running off the sensor surface too quickly to impact on resistance, and reduced the potential for slight differences in the angle at which sensors were placed in the canopy to influence results.

(a) **(b)**

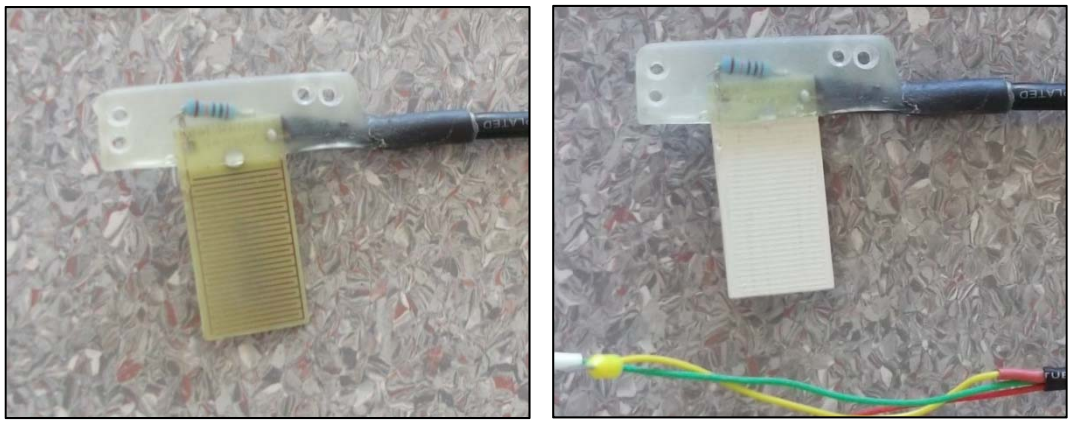

Figure 6.2 LW sensors (a) showing the gold print of the sensor face; and (b) after coating the sensor with latex paint. The epoxy casting covers the R1 100K Ω resistor (Figure 6.1) and soldered joints.

6.1.1.2 Wetness sensor deployment

Eighteen LW sensors were mounted in the canopy using cable ties to attach the sensors to small bundles of *E. robustum* stems (Figure 6.3 (a)). They were positioned at an angle that mimicked the slant of the vegetation, so that water droplets were likely to behave in a similar manner on the sensor surface as the stem surface (Figure 6.3 (b)). Where the canopy was high enough, vertical profiles of 3 – 4 sensors were established, to provide insight into wetting and drying behaviour at different heights. Sensors were placed in all *E. robustum* canopy types common within the eddy covariance footprint: tall, medium and low vegetation heights (each with a vertical profile of 2 – 4 sensors), and small moss lawns.

(a) **(b)**

Figure 6.3 (a) A LW sensor deployed in the upper canopy; (b) the wet canopy on a winter morning after a heavy dewfall.

6.1.1.3 Data logging

The LW sensors were connected to a CR1000 datalogger (CSI) via a multiplexer (AM16/32, CSI). LW sensors were measured every 60 seconds using a half-bridge measurement instruction that enabled sensor resistance (Ω) to be calculated. When sensors dried out, very large resistances resulted, and to counter this, resistances >1000 Ω were set to 1000 Ω, assumed to represent fully dry conditions. Sensor outputs were averaged over half-hour periods and stored in datalogger memory until downloaded. In order to gauge the accuracy of wetness sensor

readings, five samples of litter were taken from the canopy beside LW sensor profiles. The field moisture content of these samples was determined in the lab, and compared to the LW readings at the time of collection.

6.1.2 Antecedent Precipitation Index (API)

Leaf wetness data provides detailed insight into canopy wetness on a small time scale. While the wetness sensor data were useful for investigating canopy wetness behaviour here, an alternative method of gauging canopy wetness was required for long-term modelling of the canopy. The antecedent precipitation index (API) was developed by Woods and Rowe (1996) to estimate catchment moisture before storm events, and was modified by Smith (2003) and Thornburrow (2005) to simulate the wetting and drying of the canopies of Waikato bogs. The API (Equation 6.1) is an exponential function which uses total rainfall depth and the time since rainfall to estimate the duration of canopy wetness. In previous studies, the API has been set to consider precipitation that has occurred within 48 hours of the index time, but here the length of time was able to be adjusted so that suitable API functions could be found for different parts of the canopy, which dry at different rates after rain events.

$$\mathrm{API} = \sum_{i=1}^{j} \frac{P_i}{1.104 \times 1.024^i} \qquad \textbf{(6-1)}$$

Where P_i is the precipitation (mm) measured during the i^{th} half-hour period before the index time, and j is the number of half-hour periods preceding the index time which are considered in the API. When API < 1 the canopy was classified as dry, and wet when API ≥ 1. API functions with different time inputs (amount of preceding time considered in the model) were compared to LW sensor data gathered over the 2013 year to identify time inputs which fitted well to the LW data.

6.1.3 Model of litter respiration

A model was developed which estimated the litter respiration component of the total ecosystem respiration measured at Kopuatai. The model methodology is outlined below, with a simplified methodology shown as a flow chart in Figure 6.4. The model was coded in Matlab, with data inputs of time, LW or API,

ecosystem respiration (ER) and canopy temperature. Parameters set at the beginning of the model were the date range of the analysis, the density of *E. robustum* litter in the canopy (kg m^{-2}), the fraction of this litter classified as 'upper' or 'lower' (this was a subjective estimate, as the canopy harvest data did not distinguish between these two types, but sensitivity testing on the model allowed the impact of this division to be gauged), and the R_{10} and E_0 values for the upper and lower litter reported in Chapter Five.

Two spatially-averaging thermocouples (four measurement junctions each) permanently located in the canopy were identified as being representative of the locations of the upper and lower litter types in the canopy. The model loaded half-hourly averages of the temperature data from each of these thermocouples for the date range specified. The rate of respiration of each litter type was then calculated for each half hour, using the Lloyd and Taylor (1994) function (Equation 5.1) with inputs of temperature, R_{10} and E_0 for each litter type.

Conditions where the canopy was wet enough for litter respiration to occur were identified using either the API (values $\geq$ 1 were defined as wet) or two representative LW sensors (resistances $\leq 350\ \Omega$ were defined as wet). At all other times, respiration was assumed to be negligible and was set to zero.

The respiration rates were then extrapolated to the canopy scale by multiplying the respiration rates (μmol kg^{-1} s^{-1}) by the mass of each litter type in the canopy (total canopy litter mass × fraction of litter estimated for each litter type). The sum of respiration rates from the two litter types was calculated to determine the total litter respiration rate for each half hour period (μmol m^{-2} s^{-1}). Units were converted to g C m^{-2} s^{-1}, and daily and monthly sums of respiration were calculated. Sums of total litter respiration and ER over the whole date range were then used to calculate the percentage of ER represented by respiration from the *E. robustum* litter.

6.1.3.1 Sensitivity testing the model

Several tests were carried out to gauge the sensitivity of the litter respiration model output to changes in the input parameters. These analyses allowed confidence in the choice of parameters used in the model. The effect of changes in the fraction of each litter type input to the model was assessed by comparing the 2013 total litter respiration from the canopy when the litter was defined as 100%

lower litter through to 100% upper litter. A similar technique was used to determine the range of total respiration that depended on the API threshold that predicted whether the canopy was wet or dry. The difference in total carbon emissions from litter respiration over the 2013 year depending on whether the standard value of E_0 was used in the Lloyd and Taylor model or whether it was fitted (see Chapter Five) was also investigated.

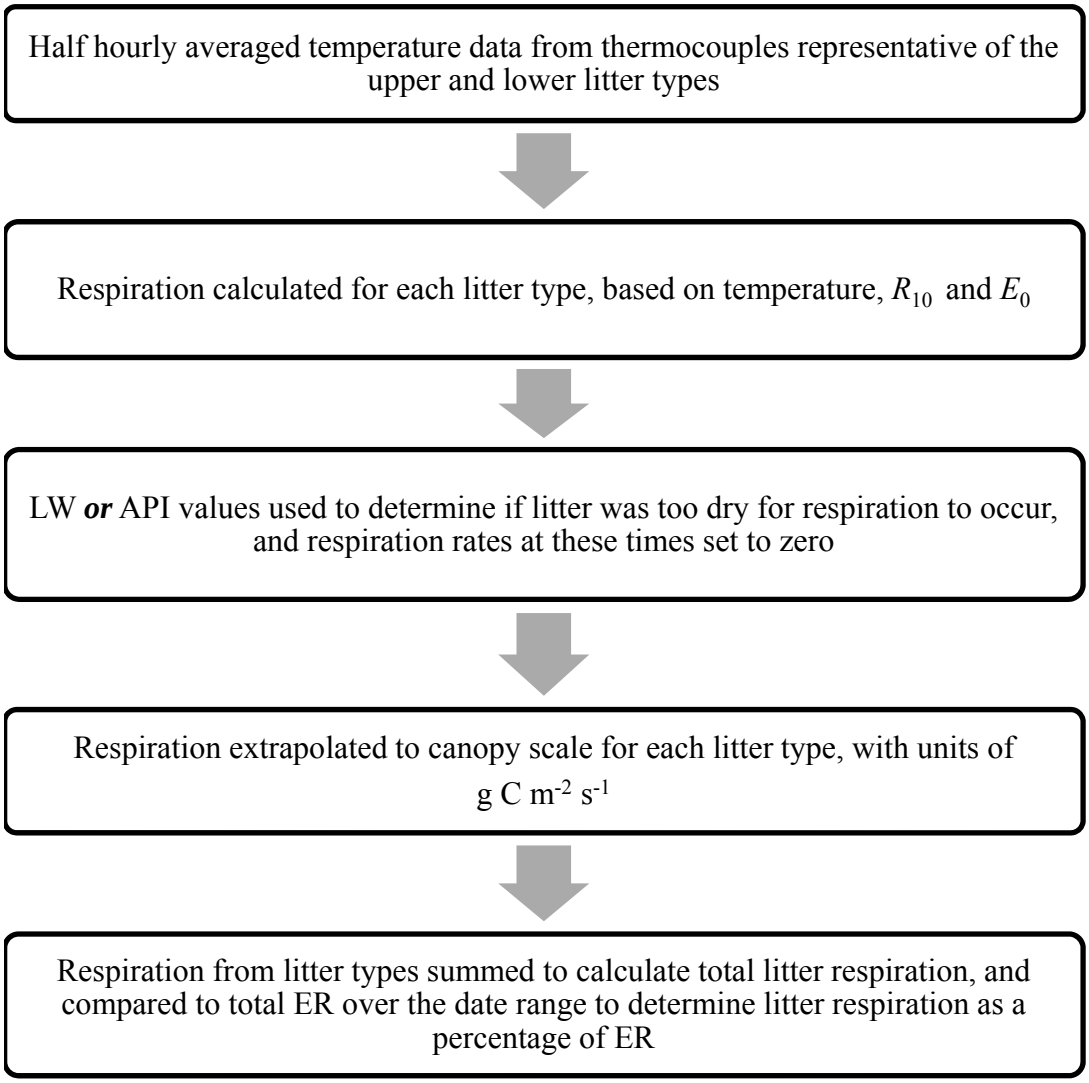

Figure 6.4 Flow chart describing the litter respiration model

6.1.4 Ecosystem respiration

The ER data which was used in the litter respiration model was estimated based on measurements from the EC system. The calculation was based on night-time measurements of ER which were filtered for periods with adequate turbulence (friction velocity > 0.15 m s^{-1}). The Lloyd and Taylor model was fitted to these

data over monthly periods, based on air temperature measurements. ER was then calculated for half-hour periods (day- and night-time) using the Lloyd and Taylor model and the parameters generated from the monthly fitting.

6.1.5 Recalcitrance of canopy litter

The amount of time that the mass of *E. robustum* litter quantified in Chapter Four would be expected to remain in the canopy given the modelled rate of respiration was calculated. *E. robustum* stem litter has a reported carbon content of 49.3% (Clarkson et al., 2014).

6.2 Results

6.2.1 Matching LW data with litter field moisture contents

The moisture contents of litter samples taken from the canopy near LW sensors and the corresponding LW readings at those times are presented in Table 6.1. The LW data signals are given with units of Ω as they are a measurement of resistance, however they are best considered as representing a relative scale of wet (approaching 0 Ω) to dry (1000 Ω). One sensor reading showed 1000 Ω, which is indicative of a dry canopy. The moisture content for the litter at that location and time was 34%, which was higher than the moisture contents of air dry litter observed in the laboratory during the incubation experiments (between 5 – 11%), but far below the respiration threshold determined in Chapter Five. Table 6.1 shows a clear pattern of increasing moisture content and decreasing LW reading, which is expected with wet conditions. The only exception is the highest recorded moisture content, 329%, which is indicative of near saturated litter, but relates to a LW reading of 340 Ω, which is the second 'driest' signal, and similar to the signal for the litter with 127% moisture content. Considering the data in Table 6.1, the LW threshold between wet and dry canopy was set to 350 Ω.

Table 6.1 Comparison of litter field moisture and LW data at the same time and location. Litter samples were taken near the lowest sensor in each profile. LW data is a relative scale, with 1000 Ω representing dry conditions and 0 Ω wet conditions.

Date and time	Sensor	Moisture content	LW reading
23 July 4pm	LW_{10}	34%	1000 Ω
23 July 4pm	LW_5	127%	300 Ω
21 August 3pm	LW_8	129%	200 Ω
21 August 3pm	LW_5	207%	45 Ω
23 July 4pm	LW_8	329%	340 Ω

6.2.2 Leaf wetness sensor data

The data from the leaf wetness sensors provided a high-frequency record of when and where moisture was likely present in the canopy. After a wetting event, LW

sensors detected canopy drying at different rates depending on the position of the sensor in the canopy.

An example of a drying cycle is shown in Figure 6.5, which includes three LW sensors positioned in a vertical profile in a tall stand of *E. robustum*. In this example, all of the sensors shown in Figure 6.5 registered a dry signal (≈1000 Ω) before the rain event which occurred at 18:00 hours on 15 April. After the rain, all of the sensors registered a wet signal, with resistances well below 350 Ω. The sensor in the upper canopy was the first to respond to the wet conditions, followed by the sensor in the standing dead litter (SDL) layer and then that in the lower canopy. This progression shows the movement of water through the dense canopy over time. A 12 hour break in rainfall on 16 April enabled the top sensor to dry out, registering a dry signal at around 09:00 hours while the lower two sensors remained wet throughout the day. Several small rainfall events were recorded over the following 30 hours, which caused the upper canopy sensor to fluctuate as it was wetted and dried. At around 18:00 on 17 April, the sensor in the SDL layer began to dry. A small rain event at 23:00 on 17 April slightly wetted the upper canopy, but did not appear to penetrate to the SDL layer. The lowest sensor remained wet for 24 hours after the others began to dry, slowly trending towards a dry signal in the early hours of the 19 April.

This drying sequence is typical of the data gathered from the LW sensors. The upper sensors were clearly more variable than those lower in the profile, fluctuating frequently between wet and dry signals as they responded quickly to environmental conditions. The sensors in the lower parts of the canopy were protected from environmental conditions which caused both wetting and drying by the dense canopy, and therefore had slower response times. The canopy also appears to have insulated these sensors, trapping moisture near the peat surface at times when the upper sensor indicated that environmental conditions were dry. The sensors did not always change between wet and dry as rapidly as indicated in Figure 6.5. Sensors frequently took a period of days to reach a dry signal, with a large amount of fluctuation in the intermediate ‘drying’ stages.

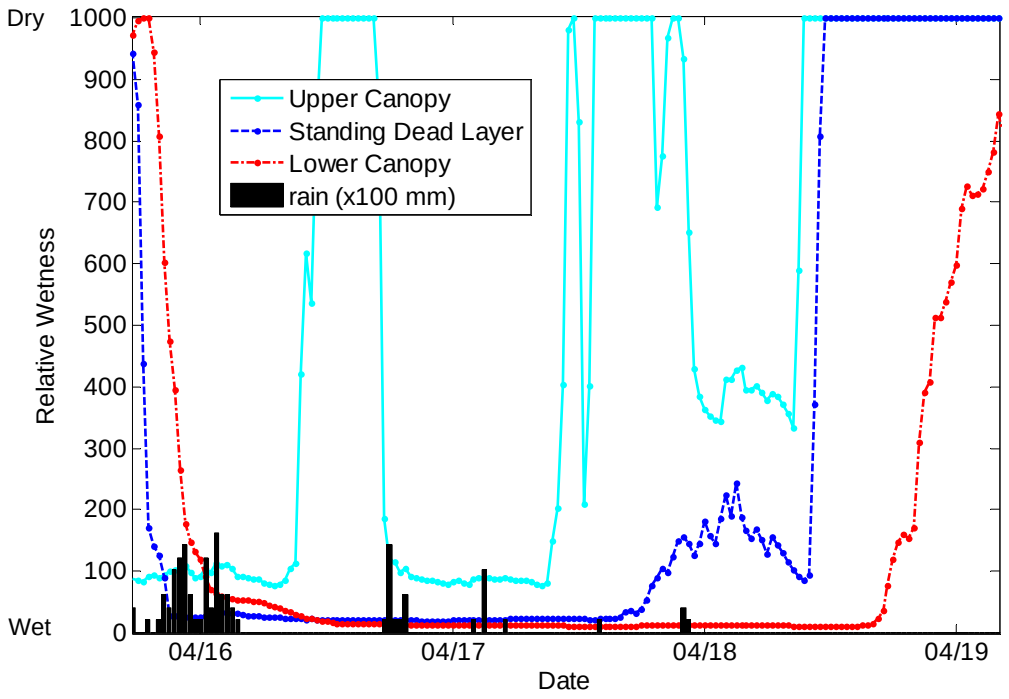

Figure 6.5 Wetting and drying cycles recorded by leaf wetness sensors positioned in a tall stand of *E. robustum*. The sensors were positioned in a vertical profile, positioned at the top of the upper canopy, in the layer of standing dead litter (SDL) and under this layer in the lower canopy. Data shown were collected over a four day period, from 15 – 19 April 2013. The y-axis is a scale of relative wetness, where 1000 represents a dry canopy, and 0 represents a wet canopy. Black bars show rainfall measured in half hour periods.

6.2.3 Canopy wetness and energy flux

Figures 6.6 and 6.7 show the relationships between different elements of the wetness and energy balance data available for the EC footprint following two rainfall events. The data in Figure 6.6 span five days, from 4 – 9 June 2013, during which a rainfall event occurred on the first day, and the four subsequent days were rain-free. Figure 6.7 spans four days in late-spring, from 8 – 12 November, again with a rainfall event on the first day.

6.2.3.1 LW sensor data

Output from three representative LW sensors are presented in Figure 6.6 (a) and Figure 6.7 (a), from the upper canopy, SDL layer and the lower portion of the canopy. In Figure 6.6, all three sensors registered a wet signal shortly after rainfall began on 4 June, and remained wet for around 24 hours. The upper sensor dried quickly, reaching a dry signal around midday on 5 June, while the SDL sensor fluctuated in a drying state before reaching a dry signal on 6 June, and the lower

sensor remained wet for longer than the other two, fluctuating before reaching a dry state on 7 - 8 June.

The rainfall event in Figure 6.7, at midday on 8 November, was short and intense. Preceding this rainfall, the canopy was in the process of drying from a separate wetting event. The maximum half-hourly rainfall volume on 8 November was 12 mm, in comparison to the maximum of less than 2.5 mm recorded for the rain event on 4 June. Before the 8 November rainfall, the three LW sensors shown in Figure 6.7 (a) had registered trending towards dry conditions. When the rainfall occurred, all three sensors registered a wet signal. The upper sensor remained wet for several hours, before rapidly returning to a dry signal that afternoon. The SDL sensor remained wet until midmorning on 9 November, when it dried rapidly. The LW sensor in the lower canopy recorded fluctuating resistances over 8 – 9 November, before reaching a dry signal late on 9 November. The lower canopy LW sensor registered resistances between 400 – 600 Ω twice more on both 10 and 11 November, without any recorded rainfall. The short duration of wetness remaining in the canopy compared to the example in Figure 6.6 is likely to have been caused by warmer temperatures and the lower overall volume of rainfall.

6.2.3.2 Energy Balance

In Figure 6.6 (b), the dynamics of four components of the energy balance can be seen responding to the changing canopy wetness during and after the rain event. The net radiation (R_n) is the balance of incoming and outgoing radiation in the ecosystem. The overcast conditions on 4 June led to a very low R_n, where the incoming and outgoing radiation almost cancel each other out. In the subsequent days, which had clearer skies, R_n was high during the day due to high incoming radiation, and negative during the night when outgoing radiation dominated. The latent heat flux (LE) describes the flux of heat associated with phase changes of water, such as evaporation, transpiration and condensation. The sensible heat flux (H) describes the flux of heat energy from the canopy to the atmosphere. When the canopy was wet, from 4 – 6 June, LE dominated as evaporation from the canopy was the main driver of the heat flux. On 7 June, when the upper and SDL parts of the canopy were dry but the lower canopy was still wet, LE and H were approximately equal. On 8 June, when the lower canopy reached a dry state, H exceeded LE since water supply was restricted by the dry canopy. The ratio of H to LE is known as the Bowen ratio (β). A wetted canopy leads to $\beta < 1$ (such as 5

– 6 June), a drying canopy would have $\beta \approx 1$ (7 June), and a dry canopy leads to $\beta > 1$ (8 June).

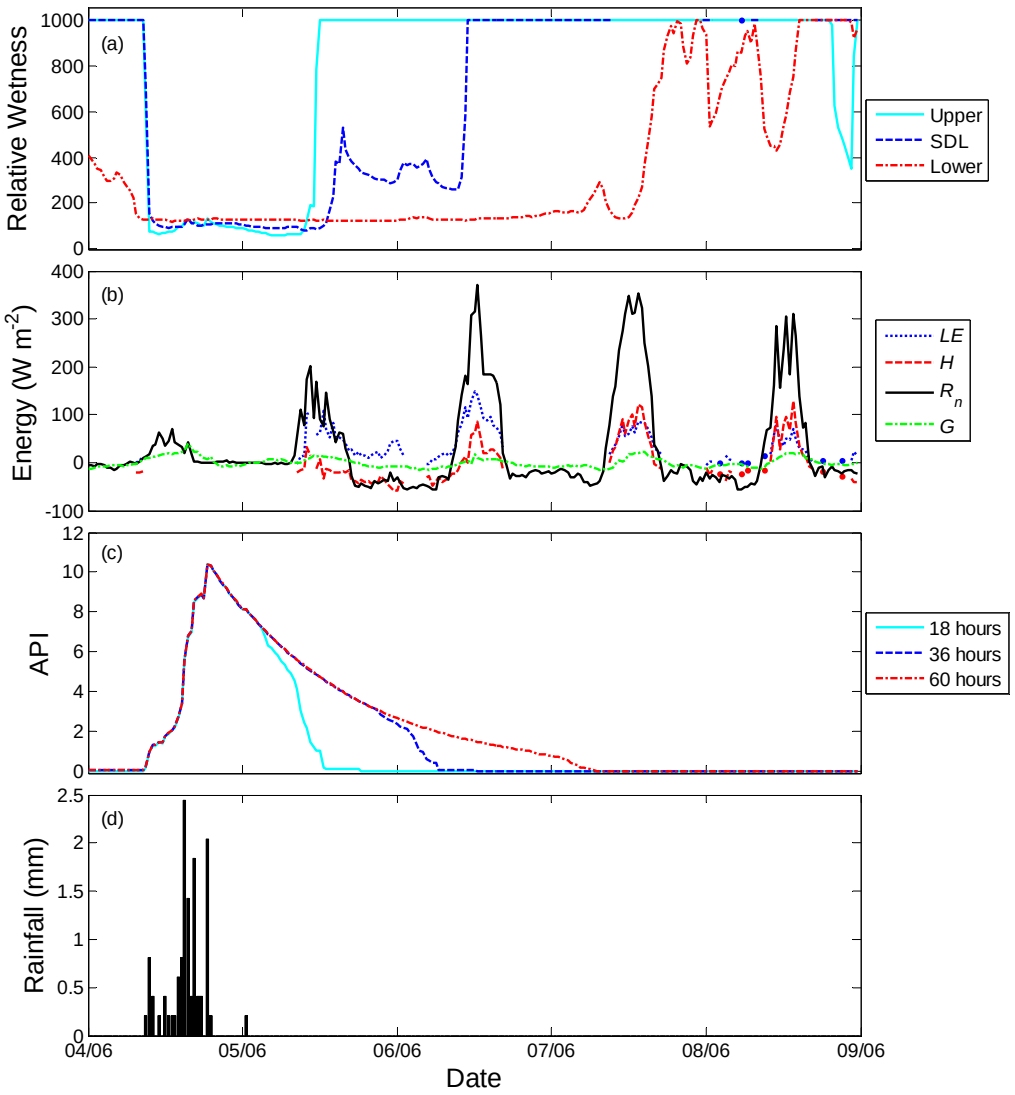

Figure 6.6 Example time series showing the relationships between (a) leaf wetness sensor data from the upper canopy, standing dead layer (SDL) and lower canopy; (b) energy flux densities: latent heat (*LE*), sensible heat (*H*), net radiation (R_n) and soil heat flux (*G*); (c) API calculated for i = 18, 36 and 60 hours; and (d) half hourly rainfall totals over a five day period in June 2013.

The scale of energy flux in Figure 6.7 (b) is twice that of Figure 6.6 (b), due to the seasonal difference between the two examples. The fluctuations in R_n over 8 November suggest cloudy conditions, while the subsequent three days were clear or partly cloudy. The Bowen ratio was less affected by the rainfall event on 8 November than that on 4 June: *LE* exceeded *H* by a small amount on the day of the rainfall ($\beta < 1$), although these data are missing for the time over which the rain occurred due to wet sensors. In the following days, *H* consistently exceeded

LE as *LE* decreased as the lower parts of the canopy became dry ($\beta > 1$), except on the morning of 9 November, when $\beta \approx 1$. These two examples of energy balance data (Figures 6.6 and 6.7) show the important role that canopy wetness plays in the ecosystem energy fluxes. Energy balance data are also a useful diagnostic tool, allowing the accuracy of the LW sensors to be checked.

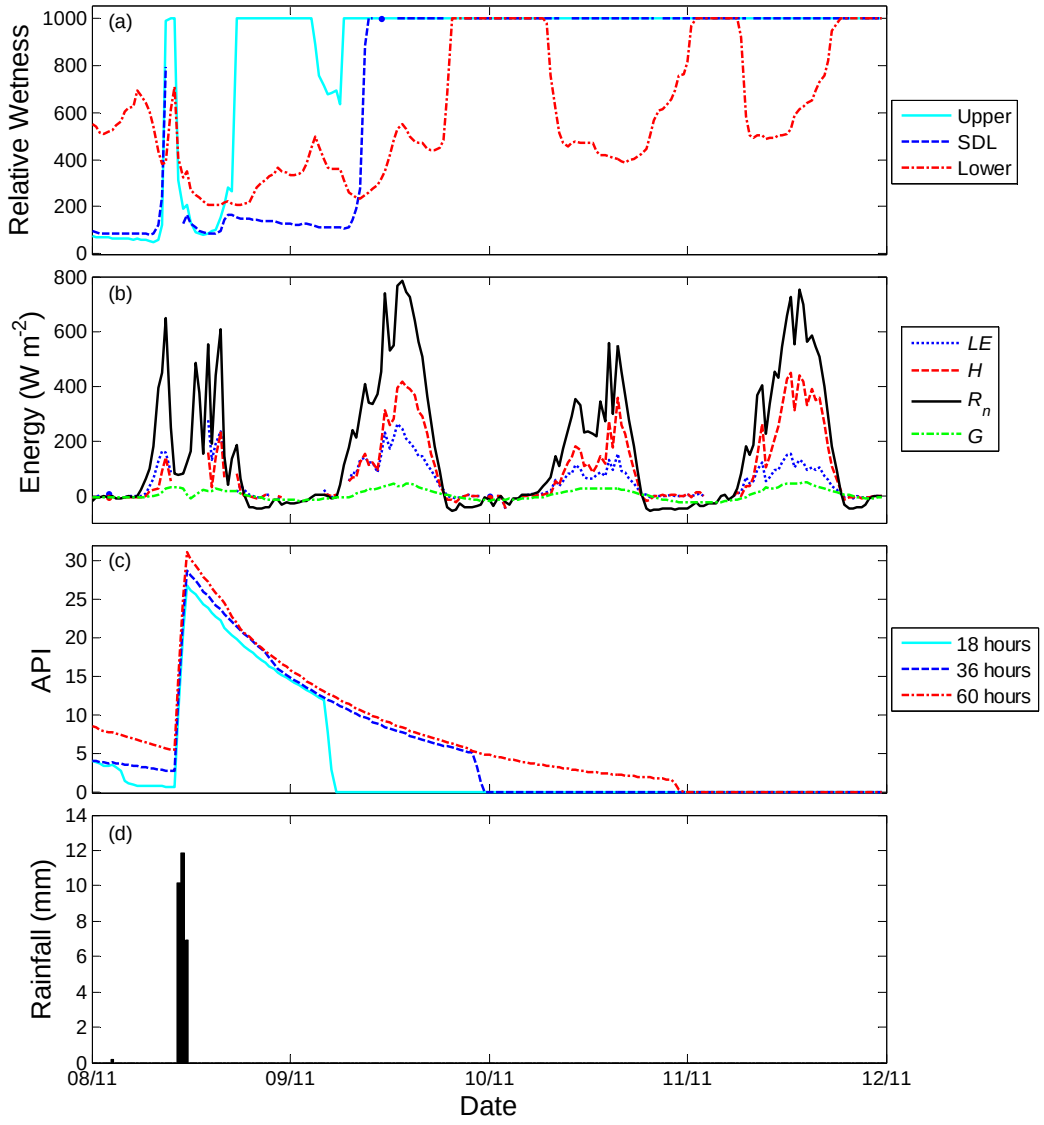

Figure 6.7 Equivalent to the example in Figure 6.6, but for a late-spring period, from 8 – 12 November 2013. Time series showing the relationships between (a) leaf wetness sensor data from the upper canopy, standing dead layer (SDL) and lower canopy; (b) energy flux densities: latent heat (*LE*), sensible heat (*H*), net radiation (R_n) and soil heat flux (*G*); (c) API calculated for i = 18, 36 and 60 hours; and (d) half hourly rainfall totals.

6.2.3.3 API

The behaviour of the API was influenced by the amount of rainfall experienced: in Figures 6.6 (c) and 6.7 (c), increases in API can be seen to correlate to half hour

periods with large rainfall volumes measured. When rainfall stopped, the API decreased in a pattern which is influenced by the length of time considered in the API function. The 18 hour API shown in Figure 6.6 (c) reached 0 around 18 hours after the major rainfall events stopped on 4 June. A small bulge in the 18 hour API can be seen where the small rain event in the early hours of 5 June slowed the decline in API slightly. The 36 and 60 hour API functions also reached 0 around 36 and 60 hours after the rainfall stopped, respectively. In Figure 6.7, (c) the shape of the API is very triangular due to the short duration of rainfall, and almost three times larger, due to the large volume of rain recorded. In this example, each API rapidly shifts to 'dry' after the specified length of time (*i*) after rainfall. In this summer example, the API's appear to slightly overestimate the duration of canopy wetness compared to the LW data.

The relationship between the API functions and the LW data for individual rain events over the 2013 year was closely inspected. The three API functions shown here were found to correspond well to sensors in the upper canopy (18 hour API), standing dead layer (36 hour API) and lower layer (60 hour API).

Comparisons of LW and API data over the 2013 year showed some examples where the API functions matched the data well (such as in Figure 6.6), and others where the signals were quite different (such as in Figure 6.7). A key reason for discrepancies between the datasets is that API estimated drying time is not influenced by the variable evaporation conditions which occur in reality, driven by temperature, radiation and humidity. The API is also unable to differentiate between wetting and drying patterns at different positions in the canopy: although a light shower which saturates the upper canopy may have no influence on the lower canopy, the API only takes the volume of rainfall into account. The LW data also has shortcomings in measuring canopy wetness, as shown in the comparison of field moisture contents and LW readings (Table 6.1). In the example of Figure 6.7, the discrepancy between the LW and API signals of canopy wetness may have been caused by either inaccurate LW readings (the fluctuation in the lower sensor signal after it has reached 'dry' indicates that the lower canopy probably contained a notable amount of moisture throughout the days following the rain event, which reinforces that these data may only be used as indications of wetness), or theoretical flaws in the API (water from the shower

may not have actually contributed much water to the lower canopy, but the API is unable to distinguish between canopy heights).

6.2.4 Litter respiration model outputs

6.2.4.1 Model settings

The variable parameters which were set for the canopy respiration model are listed in Table 6.2. The date range used for most analyses here was the calendar year from 1 January – 31 December 2013. The mass of *E. robustum* litter was the average mass of litter (kg m^{-2}) determined from harvests described in Chapter Four. The fraction of litter classified as each of the two litter types was estimated, and the impact of this is examined. The R_{10} and E_0 values for each litter type were determined in Chapter Five, and the impact of choosing calculated E_0 values rather than using 308.56 K is examined. The time constant (i) of the API function was determined by carefully examining LW and API data over the 2013 year, and choosing API time frames which gave similar signals to LW sensors in the lower canopy and SDL layer.

6.2.4.2 Seasonal change in litter respiration

Figure 6.8 shows the monthly sums of carbon respired through both ER and litter respiration, which was modelled using both API and LW sensors. The LW sensors used to produce the data shown in this figure had been identified as producing a consistently reliable signal of wet and dry conditions. The LW data used in Figure 6.8 only span the 10 month period from 1 March to 30 November 2013, as this was the period of operation for the LW sensors. The model was also run over this time frame using different LW sensors (data not shown), which were identified as producing a less consistent signal over the year, in order to gauge the impact of wetness sensor accuracy on the model's results. Although these alternate LW data frequently registered different signals from the LW data selected for use in the model, the monthly sums of respiration produced by each dataset were almost equal (not shown).

The seasonal variation in the monthly sums of both litter respiration and ER is evident in Figure 6.8. ER was highest during the summer months and lowest during winter. Litter respiration had peaks in autumn (April and May) spring (August and September) and early summer, while January to March, July and October had very little respiration. The API and LW data produced similar

modelled monthly sums of litter respiration between March and July. A difference in the respiration output generated by the API and LW emerged from August to November, with the API producing a consistently higher respiration rate than the LW data in these months, possibly because API overestimated the duration of canopy wetness in spring and summer.

Table 6.2 Parameter values used in the litter respiration model

Date range		Adjusted to suit period of interest
Mass of *E. robustum* litter		0.92 kg m^{-2}
Fraction of litter types	Upper litter	0.4
	Lower litter	0.6
$\boldsymbol{R_{10}}$	Upper litter	0.241 μmol kg^{-1} s^{-1}
	Lower litter	0.436 μmol kg^{-1} s^{-1}
$\boldsymbol{E_0}$	Upper litter	319.15 K
	Lower litter	275.86 K
API time constant (*i*)	Upper litter	36 hours (1.5 days)
	Lower litter	60 hours (2.5 days)
API wetness threshold	Wet	API ≥ 1
	Dry	API < 1
LW sensor threshold	Wet	≤ 350 Ω
	Dry	> 350 Ω

6.2.4.3 Annual litter respiration

Using the settings in Table 6.2, the litter respiration model calculated a total loss of 58.8 g C over the 2013 calendar year (1 January – 31 December) from the respiration of *E. robustum* litter. This represents 8.8% of the total annual ER estimated by the EC system. Monthly litter respiration ranged from 2% – 16.5%

of monthly ER over the 2013 year, with litter contributing the lowest proportion of ER in February and the highest in September.

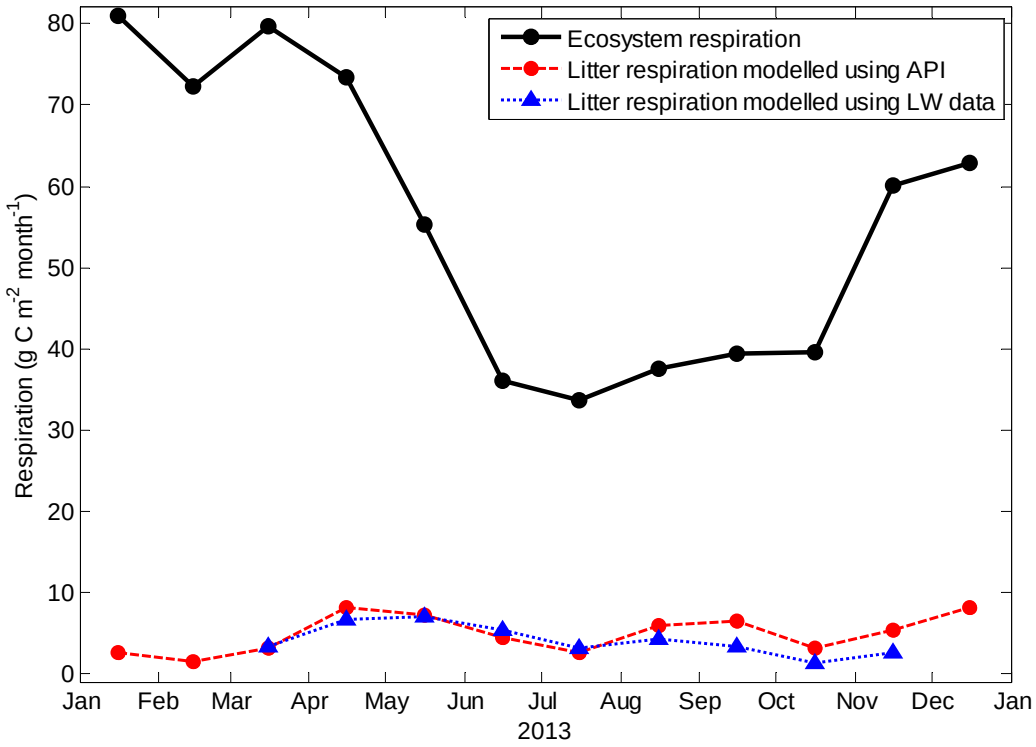

Figure 6.8 Monthly sums of ecosystem and litter respiration for the period 1 January – 31 December 2013, calculated by the respiration model. Litter respiration rates shown were calculated using two indicators of canopy wetness: the API functions listed in Table 6.2, and representative LW sensors which were identified as producing consistent data.

6.2.5 Model sensitivity testing

6.2.5.1 The estimated fraction of upper and lower litter

The annual 2013 carbon emission from litter respiration was 36.3 g C m^{-2} when the litter was defined as 100% upper litter, and 73.8 g C m^{-2} when it was defined as 100% lower litter. The relationship between total litter respiration and the proportion of each litter type in the canopy was linear. Field and laboratory observations indicated that there is slightly more lower litter than upper litter, and that the divide is likely between 50 – 70% lower litter. The range in modelled carbon emission from litter respiration between these limits was 55 – 63 g C m^{-2} yr^{-1}. This 8 g C m^{-2} yr^{-1} difference is equivalent to 1.2% of the total annual ER.

6.2.5.2 API threshold between wet and dry

Smith (2003) and Thornburrow (2005) used an API value of 1 as the threshold between wet and dry canopy conditions. The total litter respiration over 2013 was calculated for API with thresholds of 0.5 – 5. Again, the relationship between total litter respiration and API threshold was linear. When the thresholds were changed between API 0.5 – 5, the difference in the total carbon emissions from litter respiration in the 2013 calendar year was 3 g C m^{-2}, which was equivalent to 0.4% of the total ER.

6.2.5.3 Difference between using fitted E_0 and standard value

The litter respiration model was run using the standard E_0 value (308.56 K), and the result compared to that when the E_0 was calculated for the data. Total litter respiration over the 2013 calendar year was 1.1 g C m^{-2} higher when the standard E_0 value was used, which is equivalent to 0.16% of ER calculated over the same period.

6.2.6 Recalcitrance of canopy litter

Based on a canopy litter mass of 920 g m^{-2}, the carbon content of the litter was calculated to be 454 g C m^{-2}. Using the modelled litter respiration rate for the 2013 calendar year, 58.8 g C m^{-2} yr^{-1}, it was calculated that the estimated mass of litter in the canopy would take 7.71 years to decompose. Since new litter is continually being added to the canopy stock, this time period may be considered as an estimate of the litter turnover time.

6.3 Discussion

6.3.1 Modelled canopy litter respiration

Using a litter respiration model based on the Lloyd and Taylor (1994) function, with inputs of R_{10}, temperature and a wetness threshold, it was calculated that 58.8 g C m^{-2} was respired by *E. robustum* litter from 1 January – 31 December 2013. This represents 8.8% of the total ER as estimated by EC measurements over this time period. The model appeared to be relatively insensitive to a range of input parameters, which provided some confidence in the model output despite some parameters being estimated.

Over the 2013 year, the percentage of monthly ER represented by monthly litter respiration ranged from 2% in February to 16.5% in September. This range was caused by differences in the drivers of the two respiration components. ER is driven primarily by temperature and water table position, and is highest in the summer months and lowest during winter. Litter respiration is driven by a combination of temperature and water availability, and was therefore highest in the spring and autumn months when temperatures were moderate and frequent rainfall kept the canopy moist for a large proportion of time. Litter respiration represented a particularly low proportion of ER in February 2013 due to drought conditions which limited wetness and led to only 1.4 g C m^{-2} being respired in this month.

The analysis of litter respiration with respect to ER is influenced by the fact that the ER measurement used is only an estimate of the actual respiration from the ecosystem. The measurements that the ER model is based on are taken only from night-time data, which are assumed to be representative of day-time data. The collected ER data incorporate a range of canopy wetness conditions, so they are assumed to be representative of an 'average' canopy wetness state.

Zhang et al. (2014) measured respiration from *Deyeuxia angustifolia* culm and leaf litter in a freshwater marsh, and used standing litter mass to extrapolate these measurements to the ecosystem scale. They estimated that culms and leaves respired 3.07 g C m^{-2} yr^{-1} and 6.81 g C m^{-2} yr^{-1} respectively, which combine to represent 1.12% of total ER (880 g C m^{-2} yr^{-1}). Kuehn et al. (2004) estimated that the combined standing litter of *Phragmites australis* leaves, sheaths and culms respired in the range of 18 – 208 g C m^{-2} yr^{-1}. The results of the present study

indicate that *E. robustum* standing litter respires at a considerably higher rate than *D. angustifolia* litter, but in the range of that estimated for *P. australis*.

6.3.2 Litter recalcitrance

The modelled litter respiration gives an indication of the rate of decomposition of *E. robustum* litter in the canopy. This litter is known to be recalcitrant (Hodges and Rapson, 2010; Kuder et al., 1998), and its ability to remain in the canopy for long periods of time enables it to perform a key role in the function of Waikato bogs such as Kopuatai. The calculated litter turnover time of 7.7 years is likely to be an overestimate (as discussed below). However, knowing that the presence of litter in the canopy is on the scale of years is important for reinforcing the notion of litter recalcitrance and the role that litter plays in the canopy over its lifespan (Clarkson et al., 2014).

6.3.3 Implications of CO_2 pulse on wetting

The litter respiration model uses the same R_{10} value for the litter respiration at all times. In reality, the litter incubation experiments presented in Chapter Five detected an initial pulse of CO_2 from wet litter which takes at least 12 hours to stabilise. This stage of the litter wetness response was deliberately excluded from the experiments which informed the R_{10} input to the litter respiration model. On an annual scale, 12 hours of enhanced CO_2 flux for every transition from dry to wet litter would represent a large source of underestimation in the litter respiration model. A mitigating factor is that in times of frequent wetting events, for example during winter, this increased rate of respiration is likely to have occurred less frequently, as much of the canopy would remain moist between events. Also, the cause of the elevated CO_2 respiration is unknown, and whether it occurs in the field (i.e., the pulse may be an artefact of disturbing the litter samples).

6.3.4 Relationship between wetness and the energy balance

Energy balance data provided a useful alternative for gauging the state of canopy wetness and therefore the accuracy of LW data and the API models. Campbell and Williamson (1997) and Thompson et al. (1999) described the energy balance at Kopuatai for days with different weather conditions and canopy wetness states. These studies presented several different energy partitioning patterns, depending on R_n and the availability of water in the canopy, which were consistent with

those observed in Figures 6.6 and 6.7. These studies also observed Bowen ratios <1 when the canopy was wet and >1 when it was dry.

6.3.5 Methods of determining canopy wetness

6.3.5.1 Leaf wetness sensors

The LW sensors produced comprehensive data on the spatial and temporal variation of moisture in the canopy, which informed the API model and developed understanding of the patterns of wetting and drying at different heights in the canopy. The LW data correlated well to patterns in energy fluxes over the same period, which supports its use as a large scale indication of canopy wetness conditions. However, some discrepancies occurred between the data and observed drying rates, and the moisture contents of litter samples did not always relate well to the signal registered by the LW sensor.

One drawback to using LW data is that the measurement of resistance cannot be used to quantify wetness, but is rather used as a relative scale to indicate the degree of wetness. This means that the threshold between wet and dry conditions was based on a subjective analysis of the data. Another drawback is that sensors placed in similar positions in the canopy often produced different signals, and some sensors appeared to become less responsive during the year. Data from the sensors that were chosen for analyses involving LW data were closely examined for consistency, which was a labour intensive process. The resulting data can only be considered an indication of canopy wetness conditions.

6.3.5.2 API

Considering the simplicity of the litter respiration model, API appears to be a suitable substitute for LW sensor data in determining the wetness state of the canopy. Although the API signals did not match those of the LW sensors in Figure 6.7 as closely as in Figure 6.6, this discrepancy cannot be conclusively attributed to either method. The API signal related satisfactorily to changes in the energy flux. A future improvement for the model may be to refine the API values, perhaps with seasonally varying i values.

6.3.5.3 Comparison of API and LW data

Both the API and LW sensor methods have limitations, and neither can provide a conclusive indication of wetness. The difference between monthly litter

respiration modelled using API and LW sensors increased in the last four months shown in Figure 6.8. In the last four to five months of LW data collection, several sensors produced signals that were less consistent with those in similar canopy positions than they had been earlier in the year. This may have been caused by physical degradation of some LW sensors, making the sensors less responsive as the year progressed. One of the advantages that the API has over LW data for long-term modelling is that it is theoretical and based only on rainfall volume, so the lifespan of the sensors does not have to be taken into account.

The differences in patterns of wetting, drying and energy flux between Figures 6.6 and 6.7 can mostly be attributed to the differences in season and type of rainfall event. For example, the sustained period of rain on 4 June combined with low winter temperatures caused the canopy to remain wet for a number of days. In comparison, the short-lived but high volume rain event on 8 November was dried from the canopy relatively quickly, and the energy flux quickly returned to conditions typical of dry early summer conditions.

Chapter Seven

Synthesis and conclusions

7.1 The contribution of *E. robustum* litter respiration to ER

The *E. robustum* canopy contains a large mass of recalcitrant standing dead litter, which may actively contribute to conserving water in the bog and consequently to bog formation in the Waikato region (McGlone, 2009). Previously published studies have commented on the density of the *E. robustum* canopy, the distinctive standing dead litter layer suspended in it, and its evident role in ecohydrological processes (Agnew et al., 1993; Campbell and Williamson, 1997; Hodges and Rapson, 2010; Thompson et al., 1999).

The results of canopy harvests at Kopuatai in this study indicate that there is a remarkably large mass of standing litter in the canopy (an average of 0.92 kg m^{-2} litter in 1.8 kg m^{-2} canopy), greater than that reported in similar studies from other wetland ecosystems.

E. robustum litter is chemically inclined to recalcitrance (Kuder et al., 1998), which leads to very slow decomposition rates (Clarkson et al., 2014). Incubations of canopy litter from Kopuatai bog showed that freshly dead material from near the top of the canopy litter layer had significantly lower respiration rates (R_{10} = 0.24 (± 0.05) μmol kg^{-1} s^{-1}) than the more physically degraded litter lower in the canopy (R_{10} = 0.44 (± 0.1) μmol kg^{-1} s^{-1}). Freshly dead litter also had lower maximum moisture contents than the more degraded litter, leading to more rapid drying. Respiration rates from both litter types showed a clear temperature response. *E. robustum* litter respiration rates were lower than rates reported for litters from other ecosystems, providing supporting evidence of recalcitrance.

Two methods of gauging the state of canopy wetness were developed, which enabled conditions conducive to litter respiration to be identified. A simple model of litter respiration estimated that microbial decomposition of the canopy litter contributed 59 g C m^{-2} yr^{-1} (8.8%) to total ecosystem respiration of 670 g C m^{-2} s^{-1} over the 2013 calendar year. This represents a turnover time of litter in the canopy of 7 – 8 years.

7.2 The role of litter in ecosystem engineering

E. robustum acts as an ecosystem engineer in New Zealand fens and bogs by generating conditions suitable for the formation of peat in areas which frequently experience annual rainfall deficits (Hodges and Rapson, 2010; McGlone, 2009). The large mass of recalcitrant *E. robustum* litter in the canopy is part of the "engineered" biogeochemical structure which controls the movement of water through the ecosystem. The term canopy 'architecture' rather than 'structure' was chosen to emphasise that this formation is not accidental. The recalcitrant standing dead litter layer plays an integral part in this architecture as it effectively doubles the canopy vegetation density, and increases the mulching effect of the canopy, which insulates the moist peat from the drying conditions of the atmosphere. As well as conserving water in the lower canopy and peat, *E. robustum* litter can hold large volumes of water (up to 450% of its dry mass when it is in the later stages of decomposition) which enhances its ability to retain water in the canopy.

The architecture and function of the *E. robustum* canopy is integral to the peat forming ability of this species, and to the formation of peatlands in the Waikato region. The results of the present study support and contribute to this hypothesis, providing new knowledge on the mass, recalcitrance and longevity of the standing dead litter and its water holding characteristics.

7.3 Further Research

Future research into the role that *E. robustum* litter plays in the carbon and water balances at Kopuatai bog would support and build on the present study. The following is a list of areas that would be beneficial for further study:

- Further investigation into the measured pulse of CO_2 from litter after wetting, to explore whether this is an artefact of the disturbed samples or a phenomenon that occurs every time the litter is wetted in the field;
- Increased accuracy of the model of litter respiration by:
    - Improved canopy wetness predictions, possibly by developing seasonal *i* values for the API method;
    - Accounting for the increased litter respiration rate during the pulse of CO_2 after wetting (if this exists in the field); and

  - Calculating litter respiration over multiple years to develop an understanding of annual and seasonal variation and the main forcing factors;

- An investigation of the spatial variation of canopy characteristics, in particular the causes of the peculiar "wave" formations that are such a prominent feature of the *E. robustum*-dominated canopy in the vicinity of the EC site;
- An analysis of the microbial assemblages in *E. robustum* litter at different stages of decomposition, and whether these provide insight into the decomposition process of the litter; and
- The quantification of CO_2 fluxes from the remaining elements of the NECB, including peat respiration, photodegradation of the litter and plant respiration.

References

Agnew, A.D.Q., Rapson, G.L., Sykes, M.T. and Wilson, J.B., 1993. The functional ecology of Empodisma-minus (Hook f) Johnson and Cutler in New-Zealand ombrotrophic mires. New Phytologist, 124(4): 703-710.

Benvenuto, M.L., Honaine, M.F., Osterrieth, M., Coronato, A. and Rabassa, J., 2013. Silicophytoliths in Holocene peatlands and fossil peat layers from Tierra del Fuego, Argentina, southernmost South America. Quaternary International, 287: 20-33.

Berglund, O. and Berglund, K., 2011. Influence of water table level and soil properties on emissions of greenhouse gases from cultivated peat soil. Soil Biology & Biochemistry, 43(5): 923-931.

Bonneville, M.-C., Strachan, I.B., Humphreys, E.R. and Roulet, N.T., 2008. Net ecosystem CO_2 exchange in a temperate cattail marsh in relation to biophysical properties. Agricultural and Forest Meteorology, 148(1): 69-81.

Bremer, D.J. and Ham, J.M., 1999. Effect of spring burning on the surface energy balance in a tallgrass prairie. Agricultural and Forest Meteorology, 97(1): 43-54.

Briggs, J.M. and Knapp, A.K., 1995. Interannual variability in primary production in tallgrass prairie - climate, soil-moisture, topographic position, and fire as determinants of aboveground biomass. American Journal of Botany, 82(8): 1024-1030.

Brown, D.A., 1998. Gas Production from an Ombrotrophic Bog-Effect of Climate Change on Microbial Ecology. Climatic Change, 40(2): 277-284.

Campbell, D.I. and Jackson, R., 2004. Hydrology of Wetlands. In: J.S. Harding, P. Mosley, C.P. Pearson and B.K. Sorrell (Editors), Freshwaters of New Zealand. New Zelaand Hydrological Society Inc. and New Zealand Limnological Society Inc., Christchurch, New Zealand.

Campbell, D.I., Smith, J., Goodrich, J.P., Wall, A.M. and Schipper, L.A., in press. Year-round growing conditions explains large CO2 sink strength in a New Zealand raised peat bog. Agricultural and Forest Meteorology.

Campbell, D.I. and Williamson, J.L., 1997. Evaporation from a raised peat bog. Journal of Hydrology, 193(1–4): 142-160.

Campbell, E.O., 1964. The restiad peat bogs at Motumaoho and Moanatuatua. Transactions of the Royal Society of New Zealand, 2(16): 219 - 227.

Chapin, F.S., Woodwell, G.M., Randerson, J.T., Rastetter, E.B., Lovett, G.M., Baldocchi, D.D., Clark, D.A., Harmon, M.E., Schimel, D.S., Valentini, R., Wirth, C., Aber, J.D., Cole, J.J., Goulden, M.L., Harden, J.W., Heimann, M., Howarth, R.W., Matson, P.A., McGuire, A.D., Melillo, J.M., Mooney, H.A., Neff, J.C., Houghton, R.A., Pace, M.L., Ryan, M.G., Running, S.W., Sala, O.E., Schlesinger, W.H. and Schulze, E.D., 2006. Reconciling

carbon-cycle concepts, terminology, and methods. Ecosystems, 9(7): 1041-1050.

Clarkson, B., Schipper, L. and Lehmann, A., 2004. Vegetation and peat characteristics in the development of lowland restiad peat bogs, North Island, New Zealand. Wetlands, 24(1): 133-151.

Clarkson, B.R., Moore, T.R., Fitzgerald, N., Thornburrow, D., Watts, C. and Miller, S., 2014. Water table regime regulates litter decomposition in restiad peatlands, New Zealand. Ecosystems.

Clarkson, B.R., Schipper, L.A. and Silvester, W.B., 2009. Nutritional niche separation in coexisting bog species demonstrated by N-15-enriched simulated rainfall. Austral Ecology, 34(4): 377-385. DOI: 10.1007/s10021-013-9726-4

Couwenberg, J., Dommain, R. and Joosten, H., 2010. Greenhouse gas fluxes from tropical peatlands in south-east Asia. Global Change Biology, 16(6): 1715-1732.

de Lange, P.J., Heenan, P.B., Clarkson, B.D. and Clarkson, B.R., 1999. Taxonomy, ecology, and conservation of Sporadanthus (Restionaceae) in New Zealand. New Zealand Journal of Botany, 37(3): 413-431.

Devito, K.J., Waddington, J.M. and Branfireun, B.A., 1997. Flow reversals in peatlands influenced by local groundwater systems. Hydrological Processes, 11(1): 103-110.

Fierer, N., Craine, J.M., McLauchlan, K. and Schimel, J.P., 2005. Litter quality and the temperature sensitivity of decomposition. Ecology, 86(2): 320-326.

Fraser, C.J.D., Roulet, N.T. and Lafleur, M., 2001. Groundwater flow patterns in a large peatland. Journal of Hydrology, 246(1–4): 142-154.

Fritz, C., Pancotto, V.A., Elzenga, J.T.M., Visser, E.J.W., Grootjans, A.P., Pol, A., Iturraspe, R., Roelofs, J.G.M. and Smolders, A.J.P., 2011. Zero methane emission bogs: extreme rhizosphere oxygenation by cushion plants in Patagonia. New Phytologist, 190(2): 398-408.

Frolking, S. and Roulet, N.T., 2007. Holocene radiative forcing impact of northern peatland carbon accumulation and methane emissions. Global Change Biology, 13(5): 1079-1088.

Gallagher, J.L., Reimold, R.J., Linthurst, R.A. and Pfeiffer, W.J., 1980. Aerial production, mortality, and mineral accumulation-export dynamics in spartina-alterniflora and juncus-roemerianus plant stands in a georgia salt-marsh. Ecology, 61(2): 303-312.

Girisha, G.K., Condron, L.M., Clinton, P.W. and Davis, M.R., 2003. Decomposition and nutrient dynamics of green and freshly fallen radiata pine (Pinus radiata) needles. Forest Ecology and Management, 179(1-3): 169-181.

Granéli, W., 1989. Influence of standing litter on shoot production in reed, Phragmites australis (Cav.) Trin. ex Steudel. Aquatic Botany, 35(1): 99-109.

Heijmans, M., Berendse, F., Arp, W.J., Masselink, A.K., Klees, H., de Visser, W. and van Breemen, N., 2001. Effects of elevated carbon dioxide and increased nitrogen deposition on bog vegetation in the Netherlands. Journal of Ecology, 89(2): 268-279.

Hodge, P.W., 2002. Respiration processes in Waikato peat bogs, The University of Waikato, Hamilton, New Zealand, 137 pp.

Hodges, T.A. and Rapson, G.L., 2010. Is Empodisma minus the ecosystem engineer of the FBT (fen-bog transition zone) in New Zealand? Journal of the Royal Society of New Zealand, 40(3-4): 181-207.

Holden, J., 2005. Peatland Hydrology and Carbon Release: Why Small-Scale Process Matters. Philosophical Transactions: Mathematical, Physical and Engineering Sciences, 363(1837): 2891-2913.

Howard, P.J.A. and Howard, D.M., 1979. Respiration of decomposing litter in relation to temperature and moisture - Microbial decomposition of tree and shrub leaf litter-2. Oikos, 33(3): 457-465.

Idso, S.B. and Anderson, M.G., 1988. A comparison of two recent studies of transpirational water loss from emergent aquatic macrophytes. Aquatic Botany, 31(1–2): 191-195.

Jaenicke, J., Wosten, H., Budiman, A. and Siegert, F., 2010. Planning hydrological restoration of peatlands in Indonesia to mitigate carbon dioxide emissions. Mitigation and Adaptation Strategies for Global Change, 15(3): 223-239.

Johnson, P.N. and Gerbeaux, P.J., 2004. Wetland types in New Zealand. Dept. of Conservation, Wellington [N.Z.], 184 pp.

Jordan, T.E., Whigham, D.F. and Correll, D.L., 1990. Effects of nutrient and litter manipulations on the narrow-leaved cattail, Typha angustifolia L. Aquatic Botany, 36(2): 179-191.

Kimmel, K. and Mander, U., 2010. Ecosystem services of peatlands: Implications for restoration. Progress in Physical Geography, 34(4): 491-514.

Knapp, A.K. and Seastedt, T.R., 1986. Detritus Accumulation Limits Productivity of Tallgrass Prairie. BioScience, 36(10): 662-668.

Kuder, T., Kruge, M.A., Shearer, J.C. and Miller, S.L., 1998. Environmental and botanical controls on peatification—a comparative study of two New Zealand restiad bogs using Py-GC/MS, petrography and fungal analysis. International Journal of Coal Geology, 37(1–2): 3-27.

Kuehn, K.A., Steiner, D. and Gessner, M.O., 2004. Diel mineralization patterns of standing-dead plant litter: Implications for CO2 flux from wetlands. Ecology, 85(9): 2504-2518.

Lafleur, P.M., 2008. Connecting Atmosphere and Wetland: Energy and Water Vapour Exchange. Geography Compass, 2(4): 1027-1057.

Lafleur, P.M., 2009. Connecting Atmosphere and Wetland: Trace Gas Exchange. Geography Compass, 3(2): 560-585.

Lafleur, P.M. and Roulet, N.T., 1992. A comparison of evaporation rates from two fens of the Hudson Bay Lowland. Aquatic Botany, 44(1): 59-69.

Laine, A.M., Bubier, J., Riutta, T., Nilsson, M.B., Moore, T.R., Vasander, H. and Tuittila, E.-S., 2011. Abundance and composition of plant biomass as potential controls for mire net ecosytem CO2 exchange. Botany, 90(1): 63-74.

Laskowski, R., Maryański, M. and Niklińska, M., 1994. Effect of heavy metals and mineral nutrients on forest litter respiration rate. Environmental Pollution, 84(1): 97-102.

Lecain, D.R., Morgan, J.A., Schuman, G.E., Reeder, J.D. and Hart, R.H., 2000. Carbon exchange rates in grazed and ungrazed pastures of Wyoming. Journal of Range Management, 53(2): 199-206.

Lee, S.Y., 1989. Litter production and turnover of the mangrove kandelia-candel (l) druce in a hong-kong tidal shrimp pond. Estuarine Coastal and Shelf Science, 29(1): 75-87.

Limpens, J., Berendse, F., Blodau, C., Canadell, J.G., Freeman, C., Holden, J., Roulet, N., Rydin, H. and Schaepman-Strub, G., 2008. Peatlands and the carbon cycle: from local processes to global implications – a synthesis. Biogeosciences, 5(5): 1475-1491.

Lloyd, J. and Taylor, J.A., 1994. On the Temperature Dependence of Soil Respiration. Functional Ecology, 8(3): 315-323.

Luo, Y. and Zhou, X., 2006. Soil respiration and the environment. Academic Press, Boston, MA, USA, 316 pp.

Luyssaert, S., Inglima, I., Jung, M., Richardson, A.D., Reichstein, M., Papale, D., Piao, S.L., Schulze, E.D., Wingate, L., Matteucci, G., Aragao, L., Aubinet, M., Beer, C., Bernhofer, C., Black, K.G., Bonal, D., Bonnefond, J.M., Chambers, J., Ciais, P., Cook, B., Davis, K.J., Dolman, A.J., Gielen, B., Goulden, M., Grace, J., Granier, A., Grelle, A., Griffis, T., GrÜNwald, T., Guidolotti, G., Hanson, P.J., Harding, R., Hollinger, D.Y., Hutyra, L.R., Kolari, P., Kruijt, B., Kutsch, W., Lagergren, F., Laurila, T., Law, B.E., Le Maire, G., Lindroth, A., Loustau, D., Malhi, Y., Mateus, J., Migliavacca, M., Misson, L., Montagnani, L., Moncrieff, J., Moors, E., Munger, J.W., Nikinmaa, E., Ollinger, S.V., Pita, G., Rebmann, C., Roupsard, O., Saigusa, N., Sanz, M.J., Seufert, G., Sierra, C., Smith, M.L., Tang, J., Valentini, R., Vesala, T. and Janssens, I.A., 2007. CO2 balance of boreal, temperate, and tropical forests derived from a global database. Global Change Biology, 13(12): 2509-2537.

Ma, S.Y., Baldocchi, D.D., Hatala, J.A., Detto, M. and Yuste, J.C., 2012. Are rain-induced ecosystem respiration pulses enhanced by legacies of

antecedent photodegradation in semi-arid environments? Agricultural and Forest Meteorology, 154: 203-213.

Malcolm, G.M., Lopez-Gutierrez, J.C. and Koide, R.T., 2009. Temperature sensitivity of respiration differs among forest floor layers in a Pinus resinosa plantation. Soil Biology & Biochemistry, 41(6): 1075-1079.

McGlone, M.S., 2009. Postglacial history of New Zealand wetlands and implications for their conservation. New Zealand Journal of Ecology, 33(1): 1-23.

McLay, C.D.A., Allbrook, R.F. and Thompson, K., 1992. Effect of development and cultivation on physical-properties of peat soils in New-Zealand. Geoderma, 54(1-4): 23-37.

Myers, S.C., Clarkson, B.R., Reeves, P.N. and Clarkson, B.D., 2013. Wetland management in New Zealand: Are current approaches and policies sustaining wetland ecosystems in agricultural landscapes? Ecological Engineering, 56(0): 107-120.

Newell, S.Y., Fallon, R.D., Rodriguez, R.M.C. and Groene, L.C., 1985. Influence of Rain, Tidal Wetting and Relative Humidity on Release of Carbon Dioxide by Standing-Dead Salt-Marsh Plants. Oecologia, 68(1): 73-79.

Newnham, R.M., de Lange, P.J. and Lowe, D.J., 1995. Holocene vegetation, climate and history of a raised bog complex, northern New Zealand based on palynology, plant macrofossils and tephrochronology. The Holocene, 5(3): 267-282.

O'Connell, A.M., 1990. Microbial decomposition (respiration) of litter in eucalypt forests of South-Western Australia: An empirical model based on laboratory incubations. Soil Biology and Biochemistry, 22(2): 153-160.

Orwin, K.H. and Ostle, N.J., 2012. Moss species effects on peatland carbon cycling after fire. Functional Ecology, 26(4): 829-836.

Petrone, R.M., Waddington, J.M. and Price, J.S., 2001. Ecosystem scale evapotranspiration and net CO2 exchange from a restored peatland. Hydrological Processes, 15(14): 2839-2845.

Ponton, S., Flanagan, L.B., Alstad, K.P., Johnson, B.G., Morgenstern, K., Kljun, N., Black, T.A. and Barr, A.G., 2006. Comparison of ecosystem water-use efficiency among Douglas-fir forest, aspen forest and grassland using eddy covariance and carbon isotope techniques. Global Change Biology, 12(2): 294-310.

Rocha, A.V., Potts, D.L. and Goulden, M.L., 2008. Standing litter as a driver of interannual CO(2) exchange variability in a freshwater marsh. Journal of Geophysical Research-Biogeosciences, 113(G4).

Roulet, N.T., Lafleur, P.M., Richard, P.J.H., Moore, T.R., Humphreys, E.R. and Bubier, J., 2007. Contemporary carbon balance and late Holocene carbon accumulation in a northern peatland. Global Change Biology, 13(2): 397-411.

Rutledge-Jonker, S., 2010. Carbon dioxide losses from terrestrial organic matter resulting from photodegradation and microbial respiration, University of Waikato, Hamilton, New Zealand, 303 pp.

Rutledge, S., Campbell, D.I., Baldocchi, D. and Schipper, L.A., 2010. Photodegradation leads to increased carbon dioxide losses from terrestrial organic matter. Global Change Biology, 16(11): 3065-3074.

Salah, Y.M.S. and Scholes, M.C., 2011. Effect of temperature and litter quality on decomposition rate of Pinus patula needle litter. In: S. Cornell, C. Downy and M. Rounsevell (Editors), Earth System Science 2010: Global Change, Climate and People. Procedia Environmental Sciences, pp. 180-193.

Schipper, L.A. and McLeod, M., 2002. Subsidence rates and carbon loss in peat soils following conversion to pasture in the Waikato Region, New Zealand. Soil Use and Management, 18(2): 91-93.

Schuman, G.E., Reeder, J.D., Manley, J.T., Hart, R.H. and Manley, W.A., 1999. Impact of Grazing Management on the Carbon and Nitrogen Balance of a Mixed-Grass Rangeland. Ecological Applications, 9(1): 65-71.

Smith, J., 2003. Fluxes of carbon dioxide and water vapour at a Waikato peat bog, The University of Waikato, Hamilton, New Zealand, 157 pp.

Sturgeon, C.J., 2013. Assessing dissolved organic carbon export from Kopuatai bog, New Zealand, The University of Waikato, Hamilton, New Zealand, 156 pp.

Thamm, A.G., Grundling, P. and Mazus, H., 1996. Holocene and recent peat growth rates on the Zululand coastal plain. Journal of African Earth Sciences, 23(1): 119-124.

Thompson, M.A., Campbell, D.I. and Spronken-Smith, R.A., 1999. Evaporation from natural and modified raised peat bogs in New Zealand. Agricultural and Forest Meteorology, 95(2): 85-98.

Thornburrow, B., 2005. Fluxes of CO_2 and water vapour at Opuatia wetland, The University of Waikato, Hamilton, New Zealand, 96 pp.

van Leeuwen, W.J.D. and Huete, A.R., 1996. Effects of standing litter on the biophysical interpretation of plant canopies with spectral indices. Remote Sensing of Environment, 55(2): 123-138.

Wagstaff, S.J. and Clarkson, B.R., 2012. Systematics and ecology of the Australasian genus Empodisma (Restionaceae) and description of a new species from peatlands in northern New Zealand. PhytoKeys(13): 39-79.

Welsch, M. and Yavitt, J.B., 2003. Early stages of decay of Lythrum salicaria L. and Typha latifolia L. in a standing-dead position. Aquatic Botany, 75(1): 45-57.

Wieder, R.K., Vitt, D. and Benscoter, B., 2006. Peatlands and the Boreal Forest. In: R.K. Wieder and D. Vitt (Editors), Boreal Peatland Ecosystems. Ecological Studies. Springer Berlin Heidelberg, pp. 1-8.

Woods, R. and Rowe, L., 1996. The changing spatial variability of subsurface flow across a hillslope. Journal of Hydrology (NZ), 35(1): 51 - 86.

Zhang, X., Mao, R., Gong, C., Qiao, T. and Song, C., 2014. CO2 evolution from standing litter of the emergent macrophyte Deyeuxia angustifolia in the Sanjiang Plain, Northeast China. Ecological Engineering, 63(0): 45-49.

Zona, D., Oechel, W.C., Richards, J.H., Hastings, S., Kopetz, I., Ikawa, H. and Oberbauer, S., 2011. Light-stress avoidance mechanisms in a Sphagnum-dominated wet coastal Arctic tundra ecosystem in Alaska. Ecology, 92(3): 633-644.

Appendix

Supporting material and raw data is supplied on the attached CD-ROM.